Inhibition of Nitritation and ANAMMOX Processes by Sludge Thermal Hydrolysis

by

Yuan Li

A dissertation submitted in partial satisfaction of the

requirements for the degree of

Doctor of Philosophy

in

Engineering - Civil and Environmental Engineering

in the

Graduate Division

of the

University of California, Berkeley

Committee in charge:

Professor Slav W. Hermanowicz, Chair
Professor Lisa Alvarez-Cohen
Professor Mary K. Firestone

Fall 2019

Abstract

Inhibition of Nitritation and ANAMMOX Processes by Sludge Thermal Hydrolysis

by

Yuan Li

Doctor of Philosophy in Engineering - Civil and Environmental Engineering

University of California, Berkeley

Professor Slav W. Hermanowicz, Chair

With the development of urbanization, the excess amount of reactive nitrogen released to the environment caused many environmental issues. In San Francisco, over 60% of the nitrogen load comes from municipal wastewater treatment plants, which can provoke algal bloom and threaten the ecosystem. Sidestream is the wastewater derived from anaerobic sludge digestion. Due to its high nitrogen concentration, the sidestream needs to be treated separately. One optimized biological nitrogen removal process is the nitritation and ANAMMOX process. Compared to the traditional nitrification and denitrification process, the optimized process requires less aeration, zero-carbon inputs and produces much less sludge. The cost-effective nitritation and ANAMMOX process has been successfully applied for sidestream nitrogen removal. The thermal hydrolysis process (THP) is a pre-treatment process for anaerobic digestion. The pre-treatment can enhance anaerobic digestion efficiency. The wastewater produced with THP pre-treatment is called THP-sidestream (THP-S). However, previous work found that THP-S inhibit the nitritation and ANAMMOX processes. While the rate-limiting step and inhibition mechanisms remained unknown, a two-stage nitritation and ANAMMOX process were built to determine and study the inhibition mechanism of each process. Also, 16s rRNA and metagenome were applied to study the changes in microbial community structures after long-term THP-S treatment, providing biomarkers for tracking process performance.

The Nitritation process was established in the sequencing batch reactors (SBRs). The short-term effects of THP-S on ammonium-oxidizing bacteria (AOB) were evaluated. A higher THP-S percentage resulted in a lower specific ammonium removal rate by AOB. The Luong inhibition model best described the inhibition of AOB by THP-S. Long-term acclimation could not eliminate the negative effects of THP-S on the performance of the nitritation process. The nitrite accumulation percentage reduced by 55% using 100% of THP-S as feed. The AOB concentration decreased by 95% as the total biomass concentration increased. High-F: M-ratio batch tests also indicated that THP-S suppressed the growth of AOB.

ANAMMOX process was established in the membrane bioreactors. The short-term study revealed that the 1/20 diluted THP-S caused a 28% decrease of specific ANAMMOX activity. The MBR achieved a volumetric nitrogen loading rate of 3.64 $kg/(m^3d)$ with undiluted regular sidestream (RS) feed, while the reactor crashed with 70% diluted THP-S as feed. The ratio of produced $NO3^--N$ to consumed $NH_4^+ - N$ also decreased compared with RS feeding. *Candidatus Brocadia* was the dominant ANAMMOX bacteria species with the average abundances of 33.3% (synthetic wastewater), 6.42% (RS) and 2.51% (THP-S). The abundances of metagenome bins for dissimilatory nitrate reduction to ammonium (DNRA) increased in the system with THP-S compared with RS. The reason for the inhibition of ANAMMOX by THPS could be the high content of organic carbon in THP-S, which caused the over-population of heterotrophic bacteria, i.e., DNRA bacteria, leading to ANAMMOX bacteria washout.

To recover the nitritation process treating THP-S, the nitritation process was operated under extended sludge retention time (SRT), longer hydraulic retention time and elevated dissolved oxygen set-points. With the changes in operational strategies, the stable operation of nitritation treating THP-S was achieved. The nitritation pre-treatment can effectively reduce the concentrations of proteins and CODs, especially refractory CODs in both RS and THP-S. The subsequent ANAMMOX process also showed stable performance treating both nitritation pre-treated RS and nitritation pre-treat THP-S. However, rapid ANAMMOX process failure was observed having additional COD added into THP-S feed, implying that the high COD levels in THP-S can inhibit the ANAMMOX process. 16s rRNA sequencing revealed that the abundance of *Nitrosomonas* increased and the abundances of denitrification associated bacteria decreased with the extended SRT and aeration. This finding illustrates that nitritation treating THP-S can benefit from the new operational strategies. Similar bacterial community structures were observed in ANAMMOX RS samples and ANAMMOX THP-S samples. Additionally, ANAMMOX RS samples contained higher abundances of anaerobic digestion associated bacteria, indicating more refractory organics in RS. With extra COD added into influent, the ANAMMOX THP-S samples did not show many differences. The two-stage nitritation/ANAMMOX process can be a solution for treating THP-S.

The single-stage nitritation/ANAMMOX process, which can save operational cost while reducing footprints of the wastewater treatment plant, becomes the new trend in industrial application. Integrated fixed-biofilm activated sludge (IFAS) pilot was applied for the first time treating THP-S. Nitritation/ANAMMOX process was established in the IFAS pilot. Feeding with RS, the IFAS pilot achieved a much higher nitrogen removal rate (NRR) of 3.03 $gN/L/d$ than the SBR pilot with NRR of 0.67 $gN/L/d$. The stable operation was achieved by the IFAS pilot treating THP-S, of which the NRR reached 1.38 $gN/L/d$. On the contrary, significant increases of effluent nitrogen concentrations were observed in the SBR pilot treating THP-S. DNA was extracted from IFAS biofilm samples, IFAS suspension samples, and SBR samples. According to 16s rRNA sequencing, the structures of the bacterial community were quite stable in IFAS biofilm samples despite changing the feed from RS to THP-S. With most ANAMMOX bacteria observed in IFAS biofilm samples and most AOB observed in IFAS suspension samples, the distribution reduced the diffusion limits of

substrates, resulting in higher NRR of IFAS. Also, mutually symbiotic heterotrophic bacteria such as *Limnobacter*, *Bryobacter*, *Truepera* and *Sandaracinus* were detected in the IFAS samples, benefiting the stable operation of nitritation/anammox process. When fed with THP-S, ANAMMOX bacteria was gradually washed out from the SBR pilot with the occurrences of fermentation bacteria such as *Fastidiosipila*, *vandinBC27*, and *Methanosarcina*. The results indicated that IFAS configuration, which promoted the build-up of the robust bacterial ecosystem, would be helpful for establishing stable nitritation/anammox treating THP-S.

This dissertation studied the inhibition of THP-S on separate nitritation and the ANAMMOX process for the first time and demonstrated the inhibition kinetics and inhibition mechanisms of THP-S on both processes. These findings are directly relevant to industrial applications. Recommendations for future research include applying different immobilization techniques on nitritation/ANAMMOX process to avoid washout while receiving better nitrogen removal efficiency, and developing THP-S pre-treatment methods to remove organic contents.

Contents

Contents **i**

List of Figures **iii**

List of Tables **vi**

1 Introduction **1**
1.1 Nitrogen Cycle And The Relevant Environmental Issues 1
1.2 Nitrogen Elimination Processes 3
1.3 Thermal Hydrolysis Pre-treated (THP) Anaerobic Digestion(AD) 28
1.4 Research motivation, objectives and dissertation outline 30

2 Experimental set-ups and basic methods **34**
2.1 Nitritation reactor start-up 34
2.2 ANAMMOX reactor start-up 35
2.3 Regular sidestream (RS) and thermal hydrolysis pre-treated sidestream (THP-S) 38
2.4 Experimental methods 42

3 Inhibition of both metabolic activity and growth of ammonium-oxidizing bacteria by sludge thermal hydrolysis **49**
3.1 Introduction 49
3.2 Details of Experiments 50
3.3 Results 52
3.4 Discussion 58
3.5 Conclusion 59

4 Inhibition of ANAMMOX by sludge thermal hydrolysis and metagenomic insights **61**
4.1 Introduction 61
4.2 Details of Experiments 62
4.3 Results 64
4.4 Conclusion 77

5 The establishment of two-stage nitritation/ANAMMOX process treating thermal hydrolysis pre-treated sidestream **78**
5.1 Introduction 78
5.2 Details of Experiments 79
5.3 Results 80
5.4 Conclusion 93

6 The effects of different reactor configurations on nitritation/ANAMMOX process to treat sidestream **95**
6.1 Introduction 95
6.2 Details of Experiments 96
6.3 Results 97
6.4 Discussion 105
6.5 Conclusions 107

7 Conclusions **113**
7.1 Summary of Major Findings 113
7.2 Recommendations for Future Research 115

Bibliography **116**

List of Figures

1.1 The creation of reactive nitrogen. 2
1.2 Nitrogen discharges to the Bay from municipal wastewater treatment plants. (Figure resources: *https://baykeeper.org/content/ammonia-discharges-san-francisco-bay-municipal-wastewater-treatment-plants*. EBMUD: East Bay Municipal Utility District. SFSE: San Francisco South East Wastewater Treatment Plant. 3
1.3 The diagram of different nitrogen elimination processes. (A) the conventional nitrification-denitrification (CND) process; (B) the short-cut nitrification-denitrification (SCND) process; (C) the autotrophic nitritation/ANAMMOX process; (D) the simultaneous nitritation ANAMMOX and denitrification (SNAD) process; (E) the dissimilatory nitrate reduction to ammonium (DNRA) coupled with autotrophic nitrogen removal process. 32
1.4 The diagram of bacteria distribution on ANITA MOX biomass carriers. 33
1.5 The schematic of THP pre-treatment. 33
1.6 The diagram of the production of THP-S. 33

2.1 The ANAMMOX MBR. 35
2.2 The schema of ANAMMOX MBR. 35
2.3 Start-up of Nitritation SBR with SWW influent. 36
2.4 The ANAMMOX MBR. 37
2.5 The schema of ANAMMOX MBR. 37
2.6 Start-up of the ANAMMOX process with influent substrate concentrations increasing gradually. 39
2.7 The experimental stoichiometric ratios after 270 days of operations. 40
2.8 The evolution of ANAMMOX biomass at day 0 (left) and day 150 (right). . . . 42
2.9 The picture of thermal hydrolysis process. 43
2.10 Molecular weight distributions of RS and THP-S. 44
2.11 EEM fluorescence spectra of RS. 45
2.12 EEM fluorescence spectra of THP-S. 45

3.1 Batch tests of AOB activity with SWW, RS, and THP-S. 53
3.2 THP-S inhibition kinetics on AOB and the kinetic inhibition models. 54
3.3 Long-term performance of the nitritation SBR with a) RS; b) THP-S. 56

3.4 Long-term effects of RS on the activity and community of AOB. a) Weekly changes in the AOB activity and the relevant$NH_4^+ - N$ conversion percentage; b) weekly changes in the abundance of AOB and the relevant MLVSS in the system. Long-term effects of THP-S on AOB activity and community. c) Weekly changes in AOB activity and the relevant $NH_4^+ - N$ conversion percentage; d) weekly changes in the abundance of AOB and the relevant MLVSS in the system. . . . 57
3.5 Plot of the logarithms of NO_x^--N concentrations against time for a) SWW; b) RS; c) THP-S. 59

4.1 The diagram of ANAMMOX MBR fed with RS and THP-S. 64
4.2 a): Ammonium concentration decreased with time with different sidestreams of different dilutions; b): Ammonium removal rate tested with different sidestreams of different dilutions; c): Ammonium concentration decreased with time with different COD concentrations; d): Ammonium removal rate tested with different COD concentrations. 65
4.3 RSAA (relative specific ANAMMOX activity) at different COD concentrations. 66
4.4 Performance of ANAMMOX MBR fed with RS. 67
4.5 The stiochiometric ratios of ANAMMOX MBR fed with RS. 68
4.6 Performance of ANAMMOX MBR fed with THP-S. 69
4.7 The stoichiometric ratios of ANAMMOX MBR fed with THP-S. 70
4.8 Relative abundances of detected phyla in the six samples. The data were visualized via Circos software [221]. 72
4.9 Sequences assignment results at the genus level. 73
4.10 Nitrogen metabolism pathways of 115-*Planctomycetes* genomes. 75
4.11 The complete B12 synthetic pathway found in 115-*Planctomycetes* genomes. . . 76
4.12 The relative nitrogen cycle involving ANAMMOX, DNRA and denitrification. . 77

5.1 The performance of the nitritation SBR treating THP-S with extended SRT and increased aeration. 81
5.2 EEM fluorescence spectra of NRS. 82
5.3 EEM fluorescence spectra of NTHP-S. 82
5.4 The performance of ANAMMOX process treating NRS. 83
5.5 The stiochiometric ratios of ANAMMOX process treating NRS. 84
5.6 The nitrogen removal rate of ANAMMOX process treating NRS and NTHP-S. . 85
5.7 The performance of ANAMMOX process treating NTHP-S. 86
5.8 The stiochiometric ratios of ANAMMOX process treating NTHP-S. 87
5.9 The application of principal coordinates analysis to determine microbial compositional differences among nitritation process samples. 89
5.10 Relative abudances of detected phyla in the nitritation samples 90
5.11 Phylogenetic tree and the relevant sequences assignment results at the genus level of nitritation process. 91

5.12 The application of principal coordinates analysis to determine microbial compositional differences among ANAMMOX process samples. 92
5.13 Phylogenetic tree and the relevant sequences assignment results at the phylum level of ANAMMOX process. 94

6.1 The diagram of **a** SBR pilot. **b** IFAS pilot. 97
6.2 The picture of IFAS pilot. 98
6.3 **a** The performance of the SBR pilot treating RS. **b** The performance of the IFAS pilot treating RS. **c** The evolution of VSS and sNRR of the two systems. **d** The sCOD RE of the two systems. 100
6.4 The performance of the SBR pilot and the IFAS pilot treating THP-S. 108
6.5 Phylogenetic tree of 16s rRNA gene sequences. The tree illustrates the relationships of the 9 samples collected in this study using Bay-Curtis distances with NJ analysis. The scale bar represents 10 % sequence divergence. 109
6.6 Relative abundances of each major phylum. The figure only shows the phlum with relative abundaces $> 0.5\%$ 110
6.7 Relative abundances of bacterial community composition detected in different samples at genus levels showing in a heatmap. Titles for rows are genus names, and title for columns are sample information. The left side of the graph is the genus clustering tree, and the top is the sample clustering tree. 111
6.8 Absolute abudances of nitrogen cycle related bacterial communities detected in different samples. 112

List of Tables

1.1 The comparison of energy demands among the CND process, SCND process, and nitritation/ANAMMOX process. . . . 6
1.2 The biodiversity of AnAOB. . . . 9
1.3 The fast start-up of ANAMMOX process using different seeding sludges. . . . 13
1.4 The start-up of ANAMMOX process using various gel entrapment materials. . . 16
1.5 The application of nitritation/ANAMMOX process treating various wastewater. 27

2.1 Composition of SWW. . . . 37
2.2 The correlations between the increase of $(NH_4)_2SO_4$ concentration and the decrease of $KHCO_3$ concentration in SWW. . . . 38
2.3 Wastewater quality of RS and THP-S. . . . 41
2.4 Concentrations of metals of RS and THP-S. . . . 41
2.5 Physical and chemical analysis methods. . . . 44

3.1 Kinetic inhibition model and the relevant fitting values. . . . 54
3.2 Effective maximum specific growth rate of AOB in SWW, RS, and THP-S. . . . 58

4.1 Number of sequence and estimated diversity indices. . . . 70
4.2 Summary of bin-genome reconstruction from metagenomes. . . . 71
4.3 Abundances of metagenome bins in the six samples. . . . 74

5.1 The average concentrations of RS and THP-S parameters after nitritation treatment. . . . 82
5.2 Number of sequence and estimated diversity indices of nitritation process and the subsequence ANAMMOX process. . . . 88

6.1 The performance of the SBR pilot and the IFAS pilot treating RS and THP-S. . 101
6.2 Sampling information and comparison of alpha diversity indexes amonge all the DNA samples. . . . 103

Acknowledgments

I want to express my sincere gratitude to all the people who have helped me to finish this dissertation. Foremost, I would like to thank Professor Slav W. Hermanowicz, my Ph.D. advisor, for bringing me to the field of environmental engineering, guiding me through my research and giving me countless intellectual and personal inspirations. I would like to thank my preliminary and qualifying exam committee members, Professor Lisa Alvarez-Cohen, Professor Mary K. Firestone, Professor David Sedlak, Professor Baoxia Mi, and Professor Celine Pallud. Your extensive knowledge and insights have brought inspiration to this work. I would also like to thank Professor Siqing Xia from Tongji University. Thank you for kindly sharing lab resources and academic opinions. The work in this dissertation was made possible by the funding support from Tsinghua Berkeley Shenzhen Institution.

I am very grateful for having two co-workers to work with during the doctoral program, Dr. Zaoli Gu and Dr. Yifeng Yang, who have helped me to set up the reactors and collaborated with me to complete the research. I can not forget the days and nights we worked together to repair the reactors and to solve all kinds of puzzles. This work can not be accomplished without your support and efforts. I would like to thank my awesome student interns, Yangge Xu, Yihong Ding, Shuanger Li, Olivia Dai, Jungmin Lee, Connor Shingai, Hillary Buntara, and Fillarry Susanto. Thank you for being so consistent and responsible for maintaining reactors and analyzing effluent qualities.

I feel honoured to have my great colleagues at Berkeley, who have provided me with both academic advice and moral support: Negassi Hadgu, Vivek Rao, Henry Kagey, Jennifer Lawrence, Ned Antell, Shan Yi, Ke Yu, Mohan Sun, Joe Charbonnet, Linden Schneider, Sarick Matzen, Siva Rama Satyam Bandaru, Xiaochen Tang, Yilin Tian, Ivy Tao, Minghui Zhang, Yutong Liang, Jin Zhao and Jianqiao Li. Their academic support and friendship have not only helped me grow as a researcher but also made me become a better and happier person. I also feel very lucky for the collaboration with Domenec Jolis and David Graham from San Francisco Public Utilities Commission. Their practical expertise has enlightened me and helped me to solve many research problems.

Last but not least, I would like to dedicate this dissertation to my family members: My loving parents, Dr. Xiaolong Li and Qinghua Liu, who has taught me to pursue my dream no matter what and raised me in the best way possible. They have traveled countless times between China and USA just to take care of me; and my husband Dr. Chenguang Xi, thank you for taking care of everything in my life and thank you for loving me through ups and downs. Your unreserved love has brought endless happiness to my life. I can not wait to spend the rest of life with you!

Chapter 1

Introduction

1.1 Nitrogen Cycle And The Relevant Environmental Issues

Starting from the 20th century, the significant increase of the world population was strongly correlated to the consumption of nitrogen fertilizer [1, 2]. As one of the minor constituents of all living creatures, the importance of nitrogen is crucial. Serving as a protein resource and nucleic acid component, nitrogen is an essential component of cell tissues and genetic materials. Also, as one of the most commonly yield-limiting nutrients in agriculture, nitrogen is essential for global food security [2, 3]. However, the majority of nitrogen exists as nonreactive gaseous nitrogen (N_2), making up approximately 78% of the atmosphere. The strong triple bond between the two nitrogen atoms makes the gas extremely inert and not readily available to plants or animals [4]. Reactive nitrogen, which includes organic nitrogen-containing compounds, inorganic reduced form of nitrogen such as ammonia (NH_3) and ammonium (NH_4^+), and inorganic nitrogen oxides (NO_X), can be readily used to sustain life.

The natural creation of reactive nitrogen from N_2 occurs primarily by two processes: lightning and biological nitrogen fixation (BNF). In BNF, N_2 is converted to reactive nitrogen by a limited number of bacteria and legume−bacteria symbioses such as legume−Rhizobium [5]. In prehuman times, reactive nitrogen was barely accumulated in environmental reservoirs, as nitrogen fixation was almost equal to nitrogen elimination processes. The increase in human activities in recent decades break this balance. The widespread cultivation of legumes, rice, and other crops increases reactive nitrogen creation through BNF. Fossil fuel combustion converts both atmospheric N_2 and fossil nitrogen to reactive NO_X [5, 6]. Additionally, synthetic ammonia fertilizer was invented in the early 20th century by Fritz Haber and Carl Bosch (Figure 1.1). In the Haber-Bosch process, ammonia can be synthesized by reacting dinitrogen gas with hydrogen gas under high temperature and pressure with the presence of an iron catalyst. The synthesis of ammonia fertilizer boosts agricultural production and meets human protein needs. More than one-third of protein nourishing humankind origi-

nates from ammonia fertilizer [2]. Unfortunately, nitrogen use efficiency is relatively low. The accumulation and loss of nitrogen from agriculture would release to the environment and cause many environmental issues [7, 8].

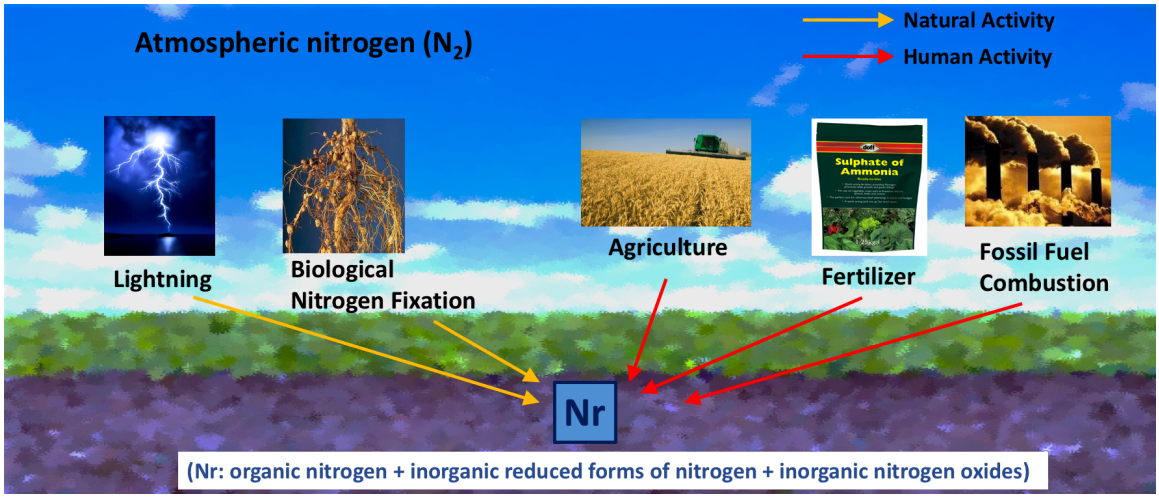


Figure 1.1: The creation of reactive nitrogen.

The large influx of reactive nitrogen to the environment leads to deleterious consequences. Soil acidification is a result of reactive nitrogen accumulation. The emission of NO_X into the atmosphere causes ozone depletion and greenhouse gas warming [9]. Additionally, nitrogen fertilizer run-off and the drainage of large amounts of N-rich organic waste into rivers and estuaries result in water eutrophication with side effects of aquatic habitat compression. Worse, the concentrated level of nitrogen such as free ammonium (FA) is toxic to aquatic life.

Wastewater management is essential for regulating water eutrophication, as wastewater contains a concentrated level of reactive nitrogen and is discharged into reservoirs. In the San Francisco Bay area, municipal sewage treatment plants are estimated to contribute over 60 % of the nitrogen load to San Francisco Bay (Figure 1.2). It was reported that the daily ammonia load to the Bay from all local municipal wastewater treatment plants was approximately 40,000 kg[10]. The massive amount of nitrogen discharged to the coastal waters can provoke excessive algal blooms, leading to the hypoxic dead zone in the water system [10]. In 2014, Nutrient Watershed Permit was established by the San Francisco Bay Regional Water Quality Control Board for nutrient discharges to the Bay from 34 outfalls for treated municipal wastewater. The Permit contains effluent monitoring requirements but does not contain effluent limits. However, the Permit states a potential compliance strategy for regulating effluent nutrient limits in future permits. So, stringent regulation of nutrient effluent is a possibility in the Bay areas [11].

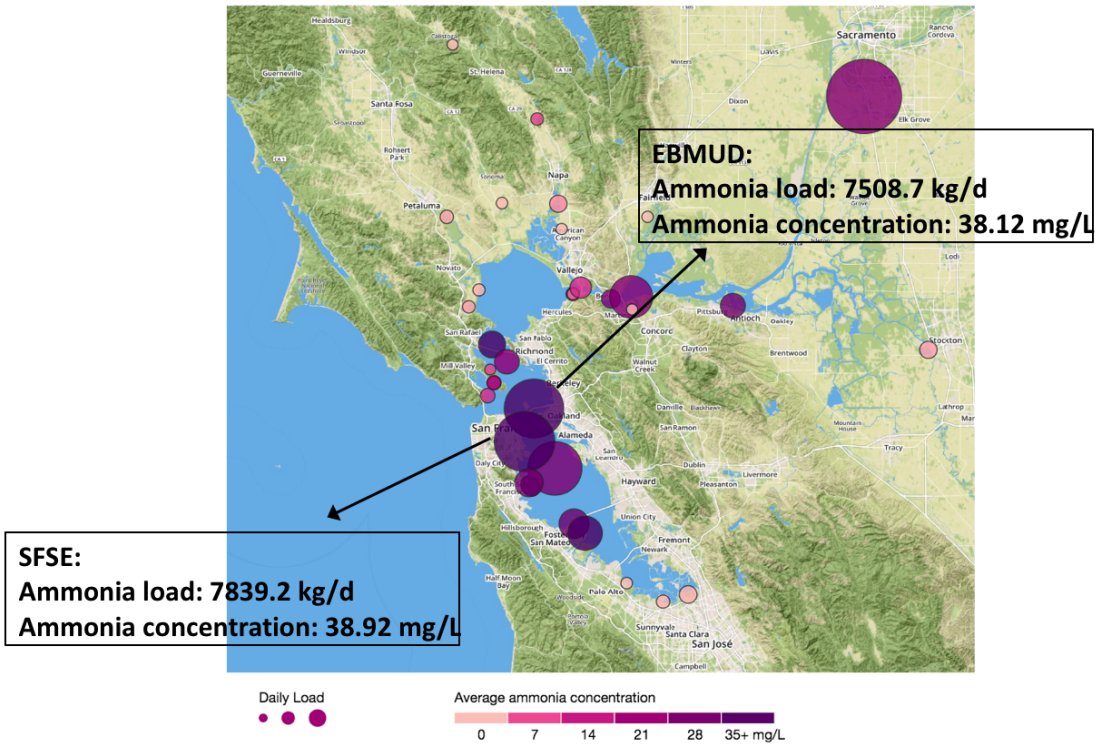


Figure 1.2: Nitrogen discharges to the Bay from municipal wastewater treatment plants. (Figure resources: *https://baykeeper.org/content/ammonia-discharges-san-francisco-bay-municipal-wastewater-treatment-plants*. EBMUD: East Bay Municipal Utility District. SFSE: San Francisco South East Wastewater Treatment Plant.

Wastewater treatment is a series of energy consuming processes, which accounts for about 3% of electrical energy consumption in USA society. In a typical municipal wastewater treatment plant with activated sludge process, $0.6kW \cdot h$ of electricity is required for treating 1 ton of wastewater [12]. Among all the processes, aeration will take about half of the electrical energy [12]. Developing energy-efficient processes can decrease energy usage while achieving nutrient removal in wastewater treatment. At the same time, wastewater is also a potential energy resource. Anaerobic digestion treating sludge produces methane, which can be applied for electricity generation.

1.2 Nitrogen Elimination Processes

1.2.1 Conventional Nitrification-Denitrification (CND) Process

One of the most commonly applied nitrogen elimination process in conventional wastewater treatment plant is a two-step process, involving a nitrification process followed by a deni-

trification process. Nitrification is a chemolithoautotrophic process, in which ammonium is oxidized to nitrate under aerobic condition. Two sequential oxidative stages achieve complete nitrification. In the first stage, ammonium is oxidized to nitrite by ammonium-oxidizing bacteria (AOB). Second, nitrite is converted into nitrate by nitrite-oxidizing bacteria (NOB) (Figure 1.3). Although each stage is carried out by different bacterial genera, both bacteria use oxygen as the electron acceptor and inorganic carbon as the carbon source. Genetic analysis revealed that AOBs are closely related to beta and gamma subdivision of the *Proteobacteria*. The most commonly recognized AOBs include *Nitrosomonas*, *Nitrosopira* and *Nitrosococcus* [13–15]. The ammonium oxidation is regulated by two enzymes: ammonia monooxygenase (AMO) and hydroxylamine oxidoreductase (HAO). *amoA* gene, which encodes subunit A of AMO, is widely used as a molecular marker to study the diversity and ecology of AOB [16, 17]. NOBs are phylogenetically diverse, occurring in several subdivisions of the class *Proteobacteria*. For example, the most well-studied member of this group of organisms is *Nitrobacter*, which is closely related to alpha subdivision of the *Proteobacteria* [13, 14, 18]. Equations for synthesis and oxidation of ammonium oxidation, nitrite oxidation, and the overall nitrification are in Eqs. (1.1)-(1.3) [13, 16]:

$$0.51NH_4^+ + 0.7O_2 + 1.01HCO_3^- \rightarrow 0.01C_5H_7O_2N + 0.5NO_2^- + 0.53H_2O + 0.96H_2CO_3 \quad (1.1)$$

$$0.5NO_2^- + 0.00125NH_4^+ + 0.24O_2 + 0.005H_2CO_3 + 0.00125HCO_3^- \rightarrow 0.00125C_5H_7O_2N + 0.5NO_3^- + 0.00375H_2O \quad (1.2)$$

$$NH_4^+ + 1.83O_2 + 1.98HCO_3^- \rightarrow 0.021C_5H_7O_2N + 0.98NO_3^- + 1.04H_2O + 1.88H_2CO_3 \quad (1.3)$$

As the second stage, the heterotrophic denitrification process is commonly coupled with nitrification process for nitrogen removal from wastewater system. In denitrification process, oxidized nitrogen compounds are used as terminal electron acceptors and are finally reduced to nitrogen gas by a group of heterotrophic bacteria under anoxic condition (nitrate is first reduced to nitrite, which is then reduced to nitrogen gas). Instead of inorganic carbon, organic carbon (such as methanol, acetate, glucose, ethanol) is required by the denitrification process as the carbon source, and organic carbon or hydrogen gas or elemental sulfur is required as the electron donor. Denitrifying bacteria are common among the Gram-negative alpha and beta subdivisions of the class *Proteobacteria*. The genus of bacteria includes *Pseudomonas*, *Thiobacillus*, *Paracoccus* and *Alcaligenes*. An example of the synthesis and reduction of the denitrification process using methanol as an electron donor is presented in Eq (1.4) [13, 19].

$$NO_3^- + 1.08CH_3OH + 0.24H_2CO_3 \rightarrow 0.056C_5H_7O_2N + 0.47N_2 + 1.68H_2O + HCO_3^- \quad (1.4)$$

The operation of the conventional nitrification-denitrification (CND) process is highly energy-intensive. As an aerobic biological process, the oxygen consumption ratio of the

nitrification process is 4.18 mg O_2/mg NH_4^+, resulting in high energy consumption through aeration. Furthermore, extra carbon inputs are always required for most wastewater with low chemical oxygen demand (COD)/N ratio, as 2 g to 9 g of COD are needed for reducing 1 g of N in the denitrification process [13, 20]. From Eq (1.3) and Eq (1.4), yields for the complete process is 0.61 mg cells/mg NH_4^+. As a result, a large amount of excess energy is needed for treating biomass sludge produced by the nitrification and denitrification process.

1.2.2 Short-Cut Nitrification-Denitrification (SCND) Process

Both nitrification and denitrification processes have nitrite as an intermediate. To reduce energy consumption, short-cut nitrification-denitrification (SCND) process has been developed and applied. In the SCND process, ammonium is aerobically oxidized into nitrite by AOB (this process is also called nitritation), and then nitrite is anoxically reduced to nitrogen gas by denitrifying bacteria (Figure 1.3). Compared to the complete nitrification-denitrification process, the application of the SCND process has many economic benefits. Without nitrite oxidation and nitrate reduction, SCND process can save 25% of oxygen input in nitrification and more than 40% of COD demand in denitrification. Also, SCND process has only about 78% biomass yield of the complete process. In addition, the presence of nitrite allows 63% higher denitrification rates than the reduction of nitrate [21–23]. Eq (1.5) represents the nitrite reduction of denitrification process using methanol as carbon source [13].

$$NO_2^- + 0.53CH_3OH + 0.67H_2CO_3 \rightarrow 0.04C_5H_7O_2N + 0.48N_2 + 1.23H_2O + HCO_3^- \quad (1.5)$$

The successful establishment of the SCND process requires the elimination of nitrite oxidation by suppressing NOB growth. Several operating parameters can be regulated to achieve nitritation process. NOBs have been found to be more sensitive to FA and free nitrous acid (FNA) than AOBs, so the different tolerance levels to FA and FNA by AOB and NOB are significant contributors to eliminate nitrite oxidation [24]. As a result, high inputs of ammonium concentration can be applied with pH control. Similarly, controlling dissolved oxygen (DO) at a lower level is another way of getting nitrite accumulation. At high temperature, AOB has a superior growth rate to NOB, so the temperature should be controlled at a higher level with a shorter solids retention time (SRT) to wash out NOB [25]. According to the stoichiometric equation, the alkalinity to ammonium molar ratio should be controlled to achieve NOB removal.

1.2.3 Autotrophic Nitritation/ANAMMOX Process

Even though the SCND process is a much more energy-efficient process than the CND process, the SCND process still requires many inputs for extra organic carbon, aeration, and sludge treatment. In the mid-1990s, a novel biological process, termed anaerobic ammonium oxidation (ANAMMOX), was discovered, in which ammonium is converted to nitrogen gas

mg per mg of N	CND Process	SCND Process	Nitritation/ANAMMOX Process
Oxygen consumption	4.1829	3.1373	1.8353
COD input (as methanol)	2.4192	1.1877	0
Sludge production	0.6125	0.4748	0.1564

Table 1.1: The comparison of energy demands among the CND process, SCND process, and nitritation/ANAMMOX process.

under anoxic conditions using nitrite as the electron acceptor. A chemolithoautotrophic nitrogen removal process, ANAMMOX uses inorganic carbon as carbon source [26, 27]. These specialties of the ANAMMOX process make it a promising way of saving energy during wastewater nitrogen removal.

Unlike ammonium, nitrite is not common in wastewater. Therefore, nitritation process is required as a prerequisite step of ANAMMOX process. In the nitritation/ANAMMOX process, about half of the ammonium will be oxidized into nitrite, and then the remaining ammonium will be combined with nitrite to generate nitrogen gas (Figre 1.3). From the environmental and economic perspectives, nitritation/ANAMMOX process has many advantages over the SCND process. As only about half of ammonium will be oxidized into nitrite, nitritation process can save about 40% of oxygen demand. Both nitritation and ANAMMOX processes are chemolithoautotrophic bacteria; therefore, this process requires zero organic carbon input. Also, due to the slow growth rate of ANAMMOX bacteria (AnAOB), this process produces much less sludge: the doubling time of AnAOB is about two weeks [28, 29], decreasing energy demand for sludge treatment. The comparison of energy demands among the CND process, SCND process, and nitritation/ANAMMOX process is shown in Table 1.1.

Unfortunately, the extremely slow growth of AnAOB hinders the application of nitritation/ANAMMOX process, leading to a much longer start-up period for the ANAMMOX process. Moreover, inhibitors present in wastewater can negatively affect the performance of the nitritation/ANAMMOX process. Significant effort has been made on the study of the establishment of nitritation/ANAMMOX process. The following sections discuss previous studies on nitritation/ANAMMOX process with an emphasis on the characteristics of ANAMMOX process, start-up of ANAMMOX process, inhibitors of nitritation/ANAMMOX process and the application of nitritation/ANAMMOX process.

1.2.3.1 ANAMMOX Process

It was believed that the oxidation of ammonium required oxygen and a mixed-function oxygenase. Because of this, the anaerobic oxidation of ammonium was thought to be infeasible. In 1977, Austrian chemist Broda predicted the existence of two groups of chemosynthetic bacteria that could oxidize ammonium to nitrogen gas in the absence of oxygen based on thermodynamic calculations [30]. Later on, in 1995, a fascinating discovery was observed in

a denitrifying fluidized bed reactor pilot. The finding revealed that ammonium disappeared at the expense of nitrate with the increasing of nitrogen gas, this process was then named ANAMMOX [27]. Later on, the process was studied by isotope experiments, in which ^{15}N-labeled ammonium was added into the pilot plant, and the nitrogen conversion was tracked, confirming nitrite was the actual electron acceptor [31]. In 1998, the stoichiometric equation for the ANAMMOX process was achieved by mass balance calculation. Besides nitrogen gas, the ANAMMOX process also produced nitrate as another product. The overall nitrogen balance gave a ratio of ammonium consumption to nitrite consumption to nitrate production of 1:1.32:0.26 [32]. The overall equation is shown in Eq (1.6).

$$NH_4^+ + 1.32NO_2^- + 0.066HCO_3^- + 0.13H^+ \rightarrow 0.066CH_2O_{0.5}N_{0.15} + 1.02N_2 + 2.03H_2O + 0.26NO_3^- \quad (1.6)$$

The bacteria responsible for the ANAMMOX process are called ANAMMOX bacteria (AnAOB). Scanning electron microscopy (SEM) and gene analysis proved that AnAOB occupies a deep branching group within phylum *Planctomycetes*. Same as other members of *Planctomycetes*, AnAOB also contains complex membrane-bound subcellular compartments [33]. From the outermost to the innermost, the cytoplasm of AnAOB is divided into three compartments: paryphoplasm, riboplasm, and anammoxosome. The paryphoplasm is defined on its outer side by the cytoplasmic membrane and cell wall, and intracytoplasmic membrane on its inner side. Similar to other *Planctomycetes* members, the cell wall of AnAOB lacks peptidoglycan [34]. Because of this, AnAOB is neither Gram-positive nor Gram-negative [35]. The intracytoplasmic membrane surrounds the riboplasm. Similar to the standard cytoplasmic compartments of other bacteria, riboplasm is the site where transcription and translation processes are assumed to take place [36]. The innermost compartment, anammoxosome, is unique for AnAOB. The membrane surrounding anammoxosome incorporates a lipid bilayer composed of one type of ladderane lipid. This unusual lipid structure is built from concatenated cyclobutane rings, which form a molecule ladder. Moreover, the tightly-packed molecule ladders make the membrane less permeable; therefore, confine ANAMMOX intermediates. [28, 33]. It is believed that the anammoxosome is where all catabolic processes and ATP synthesis happen. Several cytochrome c proteins catalyze the catabolic reactions of AnAOB metabolism. First, nitrite is reduced to nitric oxide by nitrite reductase (NirS). Second, nitrite is combined with ammonium to form highly reactive hydrazine by hydrazine synthase (HZS). Finally, hydrazine is oxidized into nitrogen gas by hydrazine dehydrogenase (HDH). Also, because of the high content of cytochrome proteins, AnAOB is red-colored [36, 37]. As mentioned before, another special trait of AnAOB is their slow growth rate, with doubling time ranging from 7 to 20 days, depending on the species, making the culture of AnAOB a challenge [28, 29].

The assumption that AnAOB has a completely chemolithoautotrophic metabolism is not accurate. More studies have shown that AnAOB has a more versatile lifestyle. Small organic molecules such as acetate, formate, and propionate can act as electron donors for AnAOB.

With organic carbon as electron donor and nitrate as electron acceptor, AnAOB can reduce nitrate to ammonium via dissimilatory nitrate and nitrite reduction, following by converting nitrite and ammonium into nitrogen gas through the common ANAMMOX pathway. By using nitrate directly, AnAOB can outcompete other heterotrophic bacteria in the presence of ammonium and can be applied to nitrate concentrated wastewater. Two genera of AnAOB, *Candidatus Brocadia* and *Candidatus Anammoxoglobus*, are capable of oxidizing organic carbon [38–40]. Besides organic carbon, inorganics can also play an important role in ANAMMOX metabolism. Iron and manganese oxides can work as electron acceptors, while formate can play as an electron donor by one genus *Candidatus Kuenenia* [41]. Furthermore, another species *Candidatus Anammoxoglobus sulfate* is able to achieve nitrogen removal with sulfate reduction. Using ammonium sulfate as the sole substrate, ammonium and sulfate were successfully removed from the system with nitrogen gas and solid sulfur as the terminal products [42]. The discoveries of the versatile metabolism of AnAOB enable the application of ANAMMOX process on more diverse wastewater.

So far, 23 AnAOB species have been successfully identified. These species are divided into six *Candidatus* genera. AnAOB have been widely detected in various man-made and natural ecosystem, such as wastewater treatment system [27], marine sediments [43], fresh water system [44], petroleum reservior [45], suboxic zone of Black Sea [46], subtropical mangrove sediment [47], hot springs [48], and etc. It was reported that only members of genus *Candidatus Scalindua* of AnAOB were found in marine envrionment, whereas AnAOB in freshwater system were mainly identified as *Candidatus Brocadia*, *Candidatus Kuenenia* and *Candidatus Scalindua* [49]. The ubiquity of AnAOB makes ANAMMOX process play an indespensible role in the nitrogen cycle. It is reported that up to 50% of nitrogen turnover in the marine evironment is due to AnAOB [50]. The details of AnAOB are tabulated in Table 1.2.

1.2.3.2 Start-up of ANAMMOX Process

Despite the high nitrogen removal rate (NRR) and economic advantages of ANAMMOX process, the extremely slow growth rate of AnAOB makes the application of ANAMMOX process very difficult. Start-up periods of ANAMMOX process ranged from months to years. In order to shorten the start-up period, many useful strategies were proposed such as optimizations of operating conditions, inoculation of high-quality seeds, improvements of biomass retention by applying immobilization techniques [69, 70]. The following paragraphs discuss the operating conditions, seeding sludge and immobilization techniques in detail.

- **Operating Conditions**

  Temperature is a crucial parameter for regulating ANAMMOX process performance in the wastewater treatment plant. It can not only affect the activity of AnAOB but can also determine the concentrations of FA and FNA together with pH and substrate concentrations. The higher the temperature, the smaller the concentrations of FA and FNA. In the natural environment, AnAOB exists in all kinds of extreme environments

Genus	Species	Treated water type	Source of seeds	Ref.
Brocadia (B)	*Ca.*[1] *B anammoxidans*	Wastewater	-	[51]
	Ca. B sinica	Synthetic wastewater	Mixed inoculation	[52]
	Ca. B fulgida	Synthetic wastewater w/acetate	Activated sludge	[53]
	Ca. B brasiliensis	Synthetic wastewater	Activated sludge	[54]
	Ca. B sapporoensis	Synthetic wastewater	Bioreactor	[55]
	Ca. B caroliniensis	Sludge liquor	-	[56]
	Ca. B sp.40	Synthetic wastewater	Brewery sludge	[57]
Kuenenia (K)	*Ca. K stuttgartiensis*	Sludge liquor	-	[58]
Jenttenia (J)	*Ca. J asiatica*	Synthetic wastewater	River sediments	[59]
	Ca. J caeni	Synthetic wastewater	Activated sludge	[60]
Anammoximicrobium	*Ca. Anammoximicrobium moscowii*	Sludge liquor	River sediments	[61]
Anammoxoglobus	*Ca. Anammoxoglobus propionicus*	Synthetic wastewater w/propionate	-	[62]
	Ca. Anammoxoglobus sulfate	Synthetic wastewater w/sulfate	Bioreactor	[42]
Salindua (S)	*Ca. S zhenghei*	Sea water	Marine sediments	[63]
	Ca. S richardsii	Sea water	Sea suboxic zone	[64]
	Ca. S brodae	Landfill leachate	-	[65]
	Ca. S wagneri	Landfill leachate	-	[65]
	Ca. S sorokinii	Sea water	Sea suboxic zone	[46]
	Ca. S arabica	Sea water	Sea suboxic zone	[66]
	Ca. S profunda	Sea water	Marine sediments	[67]
	Ca. S marina	Sea water	Marine sediments	[68]
	Ca. S japonica	Sea water	Bay sediments	[67]
	Ca. S sinooilfield	Oilfield production water	Petroleum reservior	[45]

Table 1.2: The biodiversity of AnAOB.

[1] *Candidatus*

with temperatures ranging from as high as 80°C to as low as -5°C [49]. For this reason, AnAOB enriched from different resources have different optimal temperatures. For example, AnAOB enriched from Japan marine sediments had an optimal temperature of 25°C [71], while AnAOB enriched from Arctic marine sediments had an optimal temperature of 12°C [72]. However, in the wastewater treatment system, the optimal temperatures of most AnAOB species are between 30°C and 40°C [49, 60, 73]. An irreversible inhibition on AnAOB activity was observed at the temperature higher than 45°C, resulting in orange color in the liquid phase, which is probably due to biomass lysis. On the other hand, lower temperatures also decrease AnAOB activity. It was reported that in a fixed bed reactor the nitrogen NRR was 11.5 $kgNm^{-3}d^{-1}$ at 37°C, while the NRR decreased to 8.1 $kgNm^{-3}d^{-1}$ at 20-22 °C [74]. Even though the ANAMMOX process was successfully operated at 18°C after long-term adaptation, nitrite accumulation was observed, and the process stability was lost at 15°C [75]. Lower temperature also decrease AnAOB growth rate. By lowering temperature from 29°C to 12.5°C, the doubling time of AnAOB increased from 18 to 79 days [76]. Further study suggested that the variation of temperature can affect AnAOB cell structure, and therefore result in activity decrease and loss. Segregation of cytochrome c was a cause of AnAOB activity loss at high-temperature [75]. The concentration of the extracellular polymeric substance (EPS) decreased with the increase of temperature. Moreover, the special ladderane membrane of anammoxosome was also affected by temperature [77]. As a result, a safe high temperature in the range of 30°C to 40°C is recommended to quickly start-up ANAMMOX process.

pH control is essential during process operation, as AnAOB is sensitive to pH changes. In wastewater treatment, the optimal pH used for AnAOB activity and growth was in the range of 6.7-8.3 [51]. pH changes along with temperature are associated with the concentration of substrate inhibitors, FA and FNA. FA concentration increases with the increase of pH and decreases with the decrease of pH, while FNA concentration decreases with the increase of pH and increases with the decrease of pH. Therefore, a neutral pH is required to prevent FA and FNA inhibitions [78]. In addition to the increase of substrate inhibitors, unavailability of trace elements by a high pH can also cause AnAOB activity loss [73]. Furthermore, according to the stoichiometric equation of ANAMMOX process, H^+ is consumed with pH increasing during the reaction. Without pH control, the continuous increase in pH will eventually lead to ANAMMOX process inhibition. As a result, constant pH control is essential for the stable operation of the ANAMMOX process. Several strategies can be applied to achieve this goal, such as balancing the system with CO_2 gas, dosing with HCl solution and using a slightly acidic influent [49, 73].

Because ANAMMOX is an anaerobic process, dissolved oxygen (DO) should be depleted for its stable operation. According to the redox ladder, oxygen is a much more favorable electron acceptor than nitrite. In the presence of oxygen, nitrite will not be used as the electron acceptor, leading to the decrease of AnAOB activity. It was

reported that AnAOB activity was completely inhibited by DO at 0.04 mg/L, and the inhibition was reversible at 0.16 mg/L [79]. Later on, NRR of 2.0 $kgNm^{-3}d^{-1}$ was achieved on start-up ANAMMOX process on day 91 with DO concentration at 0.30 mg/L, suggesting there is no need to deoxygenate ANAMMOX influent. It was believed that the anaerobic microzones inside granules and aggregates prevented AnAOB from DO, and enable ANAMMOX reaction to occur [69]. Also, the coexistence of aerobic bacteria in the system, especially aerobic nitrifiers, can help to deplete DO.

Substrate concentrations in influent water should also be controlled to prevent AnAOB inhibition. The application of substrates at concentrations lower than the inhibition threshold is safe for operating the ANAMMOX process. However, having substrate concentrations that are a too low can result in substrate limitation and affect AnAOB growth during the start-up period [80]. Therefore, a lower substrate concentrations and a higher nitrogen loading rate (NLR) can be used to solve this problem. With careful monitoring of the effluent, NLR should be gradually increased by controlling hydraulic retention time (HRT) to meet the demands of ANAMMOX process [69, 81, 82]. The influent ammonium to nitrite ratio is another critical parameter for achieving fast ANAMMOX process start-up. Since AnAOB is more sensitive to FNA, nitrite should be supplied as a limiting factor. By having higher influent ammonium to nitrite ratio, the lower FNA inhibition was demonstrated by the lower influent nitrite concentration, leading to the higher ANAMMOX ammonium removal rate [81]. In addition, COD/N ratio in influent water should also be considered for the ANAMMOX process start-up. With a high COD/N ratio, AnAOB will be outcompeted by heterotrophic denitrifying bacteria, resulting in the decrease of ammonium removal. However, a lower COD concentration can promote total NRR via heterotrophic denitrification without negative effects on AnAOB activity. It was reported that a COD/N mass ratio threshold for ANAMMOX inhibition was 3.1, as ammonium removal dropped to 80 % at this ratio[60, 83].

The red-colored AnAOB is composed of a set of heme c proteins, such as HZS and HDH. Making up 30% of AnAOB protein, the synthesis of these heme c proteins requires chelating ferrous irons to generate the active regions of the heme proteins [28, 84]. As part of the electron transferring chain, this iron switches between reduced (ferrous) and oxidized (ferric) oxidation states [85]. AnAOB can benefit from the appropriate increase of ferrous iron concentration in influent water. It was proposed that AnAOB can synthesize more heme c proteins and accelerate AnAOB growth with ferrous iron increasing from 0.03 to 0.12 mM [86]. Also, increased ferrous iron dosing to 0.09 mM can help to shorten the start-up period of ANAMMOX process [84].

- **Seeding sludge**

  Selecting proper seeding sludge is crucial for the successful and rapid start-up of ANAMMOX process. Several types of seeding sludge, including conventional activated sludge [87], nitritation sludge [69], denitrifying sludge [88], methanogenic anaer-

obic granules [89], ANAMMOX biomass [90], mature granular ANAMMOX sludge [91] and the mixed sludge [89, 92, 93], have been applied for ANAMMOX start-up and enrichment. Among all these seeding sludge, using mature granular ANAMMOX as seed ended up with the fastest start-up time, of which ANAMMOX process was successfully established in an up-flow anaerobic sludge blanket reactor within two weeks [91]. However, many areas have limited access to mature granular ANAMMOX sludge. Therefore, having appropriate conventional seeding sludge for start-up ANAMMOX process is very important.

The granular aggregates have a higher settling velocity than suspended biomass, thus, improving biomass retention and minimizing biomass washout. Also, the formation of granules can have stronger resistance to inhibition, shorten start-up period, achieve better ANAMMOX performance and reduce the infrastructural costs of ANAMMOX process. It is well-known that EPS can promote adhesion phenomena and the formation of biomass granules [37]. Compared with activated sludge, denitrifying sludge contains much higher EPS contents. As a result, a shorter start-up time of 25 days was achieved by seeding with denitrifying sludge [92]. It was reported that using nitritation sludge as inoculum can also save the start-up time. In nitritation system, the ammonium and nitrite concentrations are quite suitable for the growth of AnAOB. Because of this, the start-up time was reduced significantly. Moreover, seeding with anaerobic granular sludge can increase NRR. A good carrier for AnAOB growth, the anaerobic granular sludge is able to accelerate the granulation process of AnAOB, resulting in better biomass retention and higher NRR. However, the application of anaerobic granular sludge as seed, such as methanogenic granules, can cause sludge hydrolysis at the beginning of process start-up [89]. To sum up, the proper seeding sludge should be able to facilitate AnAOB granulation while providing beneficial conditions for AnAOB to accumulate. A recommended order of seeding sludge is ANAMMOX sludge > denitrifying sludge > nitritation sludge > activated sludge > methanogenic anaerobic granules. Table 1.3 shows the seeding sludge used in the fast start-up of ANAMMOX process.

- **Immobilization techniques**

  Another way to improve the ANAMMOX process start-up is to efficiently retain biomass by applying immobilization techniques. The inert porous material is usually applied as the biomass carrier due to its large-specific area, which provides sufficient space for biomass attachment. Acting as nuclei for biofilm development, these carriers enhance sludge aggregation and diminish biomass washout. In 1997, sintered glass beads were used as AnAOB carriers because of their high surface area. Biofilm attachment was shortly observed after the reactor start-up. However, after 60 days of operation, the grown-together beads caused the entrapment of gas and clogging of the bed, leading to activity loss of ANAMMOX process [102]. Using zeolite particles as biomass carriers can effectively promote granulation of AnAOB, resulting in

Recator type	Seed sludge	Carrier	Start-up time(Days)	pH	T[2] (°C)	NRR$_{(max)}$ ($kg/m^3/d$)	NRE[3] (%)	Ref.
UASB[4]	ANAMMOX granule	-	14	7.5-8	37	0.93	99.29	[91]
MSBR[5]	ANAMMOX sludge	Hollow fiber membrane	273	7.8-8.7	35	0.7	73.6	[90]
SBR[6]	Activated sludge	-	49	7.5-8.5	35	-	>90	[87]
UASB	Mixed nitritation sludge with ANAMMOX sludge	-	35	7-8.6	24-30	6.2	-	[69]
UASB	Mixed denitrifying sludge with ANAMMOX sludge	-	25	7-7.5	35	0.7	-	[92]
FBR[7]	Mixed activited sludge with nitrifying sludge	Non-woven ring	39	8±0.2	35±0.2	9.2	89	[93]
UASB	Methanogenic granule	-	83	6.8-7	35±1	11.7	-	[89]
FBR	Activated sludge	Honeycomb-like polypropylene	45	8	35	-	-	[94]
UASB	Activated sludge	Bamboo charcoal	85	7.53-8.55	30±1	-	98	[95]
Biofilm reactor	Denitrifying sludge	Non-woven material	-	-	-	0.041	60±6.3	[96]
UFCR[8]	ANAMMOX sludge	PE sponge strip	<56	7.6-8.2	35±1	3.6	>85	[97]
SBR	ANAMMOX sludge	Zeolite particles	-	7-8	33	-	-	[98]
UFCR	ANAMMOX sludge	PE sponge	<30	7-8	36	7.6	90	[99]
DHS[9]	Activated sludge	Sponge material	-	8	30-35	2.27	95	[100]
Biofilm reactor	Denitrifying sludge	Non-woven fabric sheet	<50	7-7.5	37	26	-	[81]
Hybrid reactor	ANAMMOX sludge	Non-woven fabric	38	-	35	6.6	>70	[101]

Table 1.3: The fast start-up of ANAMMOX process using different seeding sludges.

[2] *Temperature*
[3] *Total Nitrogen Removal Efficiency*
[4] *Upflow Anaerobic Sludge Blanket*
[5] *Membrane Sequencing Batch Reactor*
[6] *Sequencing Batch Reactor*
[7] *Fixed Bed Reactor*
[8] *Upflow Column Reactor*
[9] *Down-flow hanging sponge reactor*

the successful ANAMMOX process build up with the specific ANAMMOX activity (SAA) of 0.5 $gN/gvolatilesuspendedsolids(VSS)/day$. Also, the cation exchange capacity (CEC) of zeolite enables ammonium ion adsorption and provides substrates for AnAOB growth. On the other hand, the vigorous mixing required by the high-density zeolite particles leads to high shear stress between zeolite particles, causing adverse effects on biomass attachment [98]. The submerged hollow fiber membrane module is another option. Despite the cost of membranes and operation due to membrane fouling and energy consumption by pumping, the biomass in the membrane system tended to grow in suspension, which suffered a lighter diffusion problem compare with granular biomass [90]. Simultaneously, the light weighted porous polyethylene (PE) sponge carrier [97, 99] and non-woven carrier [93] have been applied for stable immobilization of AnAOB. The outstanding adsorption ability of PE sponge carrier ensured the sufficient biomass volume in the reactor. By using PE sponge carrier, the ANAMMOX process achieved a stable NRR of 7.6 $kg/m^3/day$ [99]. The non-woven carrier is also a suitable material for ANAMMOX start-up, a high-rate ANAMMOX biofilm reactor filled with non-woven sheets was established with a super high NRR of 26 $kg/m^3/day$ [81]. Charcoal is one of the most suitable biomass carriers. With the microporous structure and great CEC, the usage of charcoal can prevent oxygen penetration, absorb ammonium ions and create an optimal environment for AnAOB growth. Among all kinds of charcoal, bamboo charcoal stands out due to its more magnificent microporous structure and higher adsorption efficiency. With a maximum adsorption capacity for ammonium of 0.85 $mgNH_4^+/g$, the application of bamboo charcoal can shorten the start-up time from 117 days to 85 days [95]. With shorter start-up time and higher NRR, volcanic rock was reported to be a better biomass carrier compared to charcoal. It was believed that the coarse surface and hydrophilic nature of volcanic rock made it more accessible for the attachment of AnAOB, while the trace elements of volcanic rock also facilitate AnAOB growth [103]. To sum up, a suitable biomass carrier for ANAMMOX start-up should have: i) good adsorption ability, high CEC; ii)a microporous structure to prevent oxygen penetration and iii) large surface area to facilitate AnAOB attachment.

Except for biomass carriers, gel entrapment is also widely applied for biomass immobilization. Gel entrapment techniques have many advantages over biomass carriers. First of all, gel beads have higher diffusivity than biomass granules, leading to higher NRR. It was reported that ANAMMOX gel beads had higher activity than aggregated biomass granules [104]. The thick biofilm formed on the carriers makes the substrate less diffusive to the inner biomass. The previous study demonstrated that the inner biomass of ANAMMOX granules was not metabolically active, as ANAMMOX activity was only found in the outer layers of biomass [105]. However, ANAMMOX activity was evenly observed throughout the gel beads, which was due to improved substrate diffusion [105]. Second, much less sludge is required to achieve ANAMMOX start-up by gel entrapment. Within 35 days of operation, ANAMMOX reactor with gel beads achieved NRR of 10.8 $kg/m^3/day$ by inoculating 0.33 $gVSS/L$ of seed sludge, whereas

the reactor with granular biomass achieved NRR of $3.5 kg/m^3/day$ by inoculating 2.5 $gVSS/L$ of seed sludge [104]. Also, the gel entrapment technique is more time efficient. The formation of granules is affected by several factors, such as the presence of EPS, shear stress and ionic strength [105]. As natural aggregation needs a long term stabilization period, the application of gel entrapment can save more time for process start-up. Fourth, the gel entrapment facilitates the solid-liquid separation and higher stability of biomass retention. Unlike membranes, which suffer from membrane fouling issues, the use of gel entrapment can avoid this problem and reduce operation cost. Finally, biomass immobilized by gel entrapment can be more resistant to toxic substances in the environment. For example, with gel entrapment, AnAOB is more tolerant of nitrite inhibition. AnAOB activity decreased by 50 % when exposing to nitrite concentration of 350 mgN/L, whereas the gel entrapped AnAOB activity only decreased 37 % when the nitrite concentration was 430 mgN/L, and the activity was not completely lost until exposing to nitrite concentration of 750 mgN/L [106].

In order to ensure the long-term stable operation of the ANAMMOX process, the selection of gel immobilization material is crucial. A suitable gel immobilization material needs to be insoluble in wastewater, non-biodegradable, good in mechanical stability and diffusivity [107]. Several synthetic polymeric gel materials have been proven to be suitable immobilization material, such as polyvinyl alcohol (PVA), sodium alginate (SA), a mixture of PVA and SA, and polyethylene glycol (PEG) [60]. Usually, the biomass was firstly immobilized by these gel material, which was then polymerized by adding solidifying solution such as 2% $CaCl_2$. A summary of the start-up of ANAMMOX reactors using various gel immobilization materials is shown in Table 1.4.

The first step of my research is to establish a robust ANAMMOX process. According to the literature, the ANAMMOX process should be operated under the anoxic condition at a temperature between 30°C to 40°C. As higher temperature can promote AnAOB growth, a higher temperature should be applied. To prevent substrate inhibitions, pH should be carefully controlled. Another strategy to prevent substrate inhibitions is to start up the process with lower substrate concentrations and higher NLRs. Ferrous iron, as an essential element of the functional enzymes in AnAOB, should be applied to facilitate AnAOB enrichment.

Biomass granulation is one of the most commonly applied strategies to achieve rapid ANAMMOX process start-up. Besides ANAMMOX sludge, seeding sludge including denitrifying sludge and anaerobic granular sludge can shorten the start-up time of ANAMMOX process by accelerating biomass granulation. However, the application of anaerobic granular sludge can cause sludge hydrolysis at the early start-up phase, and is not highly recommended. Nitritation sludge, providing suitable substrate condition for the ANAMMOX process, is another good seeding option.

Due to the slow growth rate of AnAOB, it is important to efficiently retain biomass in the system. Immobilization techniques can shorten the start-up time of the ANAMMOX process by diminishing biomass washout. Biomass carriers, such as zeolite particles, PE sponge, non-woven carriers, charcoal, and volcanic rock, can act as nuclei for biofilm devel-

Recator type	Seed sludge	Seed concentration ($gVSS/L$)	Immobilization material	Start-up time (Days)	Agitation speed (rpm)	Packing volume (%)	NRR $_{(max)}$ ($kg/m^3/d$)	Ref.
CSTR[10]	Activated sludge	9	7.5% PVA+1%SA	93	400	18.5	0.62	[105]
CSTR	ANAMMOX sludge	0.85	7.5% PVA+1%SA	39	400	18.5	1.34	[105]
UFCR	ANAMMOX sludge	0.33	3% PVA+1%SA	35	-	70	10.8	[104]
CSTR	Activated sludge	3	7.5% PVA+1%SA	42	1000	30	1.12	[108]
CSTR	ANAMMOX sludge	1.79	10% PVA	30	100	20	0.5	[109]
SBR	ANAMMOX sludge	0.7	3% PVA+1%SA	60	80	40	0.58	[110]
CSTR	ANAMMOX sludge	0.72	10% PEG	67	80	30	3.7	[111]
CSTR	ANAMMOX sludge	0.176	15% PEG	65	60-70	20	5.4	[112]
UFCR	ANAMMOX sludge	1	3% PVA+1%SA	35	-	70	8.03	[113]
CSTR	ANAMMOX sludge	3.8	7.5% PVA+1%SA	30	100	30	8.2	[114]

Table 1.4: The start-up of ANAMMOX process using various gel entrapment materials.

[10] *Continously Stirred Tank Reactor*

opment, and therefore, retain biomass in the system. Among all the biomass carriers, bamboo charcoal stands out because of its high CEC and microporous structure. Volcanic rock is another good option, as it is rich in trace elements which can facilitate AnAOB growth. Submerged hollow fiber membrane module can also work efficiently to retain biomass. Different from other biomass carriers, biomass in the membrane system tends to grow in suspension, which has fewer substrate diffusion problems than biomass aggregates and granular biomass. However, membrane application is often accompanied by fouling issues. Also, the usage of pumping with membrane costs additional energy. Gel entrapment is also a widely applied immobilization technique. With lower mass transfer limitations than biomass granules, gel entrapment application can achieve higher NRR with less biomass seeded. On the other hand, AnAOB will be inevitably exposed to oxygen during the gel entrapment preparation, decreasing AnAOB activity. Based on all these findings, a robust ANAMMOX enrichment system was designed, and more details will be discussed in Chapter 2.

1.2.3.3 The Inhibitors of Nitritation/ANAMMOX Process

Both nitritation and ANAMMOX processes can be affected by several types of inhibitors, including substrates, organic matters, metals, and other common wastewater constituents. In order to establish a robust and stable operation of nitritation/ANAMMOX process, it is important to understand the inhibitors and their limiting thresholds of these inhibitors for each process. The following paragraphs illustrate the inhibitors of nitration and ANAMMOX process.

- **The inhibitors of nitritation process**

  AMO, the enzyme responsible for oxidizing ammonium to hydroxylamine, is most commonly identified as the target enzyme for nitritation inhibitors. Similar to methane monooxygenase, AMO can not only catalyze the oxidation of N-H bond of ammonia but can also catalyze the oxidation of aryl C-H, alkyl C-H, C=C, and C-O-C. For example, AMO can oxidize CO and CH_4 to CO_2 [115]. In this way, the oxidation of ammonium can be inhibited due to the fact that other chemicals will compete with ammonium for AMO and oxygen. Dimethylsulfide and dimethyl disulfide were found to be substrates for AMO. After incubated with *Nitrosomonas europaea* for 10 minutes, 30% of 0.5 μmol dimethylsulfide and 60% of 0.5 μmol dimethyl disulfide were consumed. By treating the cells with acetylene, a specific inhibitor of AMO, the consumption of dimethylsulfide and dimethyl disulfide were prevented, which means AMO was the active site for dimethylsulfide and dimethyl disulfide [116]. The broad substrate range of AMO inhibited the catabolic oxidation of ammonium. A list of alternative AMO substrates was reported by McCarty [117]. Another group of AMO inhibitor is mechanism-based inhibitors. AMO is a Cu-containing monooxygenase enzyme. With the formation of highly reactive products by the mechanism-based inhibitors, Cu within the active site of AMO was bound by the reactive products, generating Cu-chelating complex and resulting in AMO inhibition. The mechanism-

based inhibitors of AMO include carbon disulfide (CS_2), acetylene, calcium carbide (CaC_2), allylsulfide, etc.

Volatile fatty acids (VFAs) are the most common products generated by the anaerobic digestion treatment process, such as acetic acid, propionic acid, and butyric acid. The inhibition of VFA on the nitritation process has been reported. The performance of nitritation process was evaluated with the presence of total organic carbon (TOC) of 32 mg/L for each VFA. AOB activity reduction was barely observed in the presence of acetic acid, while 20% of AOB activity inhibition was achieved when butyric acid was applied. More batch experiments indicated that a non-competitive model with an inhibition constant of 685 mg/L can describe the nitritation performance reduction with the increase of acetic acid concentration. It was concluded that VFA inhibited AOB activity due to kinetic limitations, and the inhibition on nitritation increased with an increase of VFA molecular weight [118].

Metals, which have been found in significant concentrations in various wastewaters, have been postulated as a cause for ammonia oxidation inhibition. Many heavy metals can inhibit AOB activity, including nickel (Ni), copper (Cu), cadmium (Cd), lead (Pd) and zinc (Zn). It was believed that free metal cations but not the total analytical metal concentrations were the cause of inhibition, as adding a strong chelating agent ethylenediaminetetraacetic acid (EDTA) can reduce the deleterious effects [119, 120]. Previous studies reported that Cu metal ion had stronger inhibition on nitritation process than Zn metal ion. With 0.08 mg/L of Cu and Zn, the ammonium oxidation rate was reduced by 50% and 12%, respectively [121]. In another study, a 50% decrease of AOB activity was observed when exposing to 173 mg/L of Cu ion or 8.3 mg/L of Cd ion [122]. Also, at least 94% of ammonium oxidation inhibition was detected with Ni concentration increased to 250 mg/L. And 16.9 mg/L of Pb resulted in 67% inhibition on the nitritation process [123]. All these data indicated that AOB is sensitive to metals, which may affect the respiration of bacteria leading to activity and growth inhibition [124].

FA and FNA are substrate and product inhibitors of the nitritation process. Ammonium, which is the major substrate of nitritation process, will be in solution as the forms of ammonium ion and the unionized free ammonia. The equilibrium equation between ammonium and FA is $NH_3+H_2O=NH_4^+ + OH^-$. Similar with ammonium, as the major product of nitritation process, nitrite is correlated with FNA, where the equilibrium equation is $HNO_2=NO_2^- + H^+$. The concentrations of FA and FNA can be calculated through a relationship between pH and the concentrations of total ammonia and nitrite nitrogen Eqs. (1.7) (1.8), respectively [78]. K_a is the ionization constant of the nitrous acid equalibrium equation and varies with temperature. $K_a = \exp^{-\frac{2300}{273+T^\circ C}}$. K_b is the ionization constant of ammonia equilibrium equation. $K_b = \exp^{\frac{6344}{273+T^\circ C}} * K_w$.

K_w is the ionization constant of water. Both K_b and K_w vary with temperature.

$$FA \text{ as } NH_3 \left(\frac{mg}{L}\right) = \frac{17}{14} \times \frac{\text{total ammonia as}(\frac{mg}{L}) \times 10^{pH}}{K_b/K_w + 10^{pH}} \tag{1.7}$$

$$FNA \text{ as } HNO_2 \left(\frac{mg}{L}\right) = \frac{46}{14} \times \frac{NO_2 - N(\frac{mg}{L})}{K_a \times 10^{pH}} \tag{1.8}$$

A study on *Nitrosomonas* culture illustrated that FNA inhibited both the growth capability and the energy generation capacity of *Nitrosomonas*. While the growth capability was completely inhibited at around 0.4 mg FNA-N $/L$, only 50% inhibition of the energy generation capacity was observed at around 0.63 mg FNA-N $/L$. However, FA had no effect on both the growth and the energy generation of Nitrosomonas with the concentration up to 16.0 mg/L [125, 126]. The inhibition of AOB by FA was observed at a higher FA concentration of 300 mg/L [127]. Because AOB is more tolerant to FA than FNA, a decrease of pH which will increase the FNA concentration should be avoided.

- **The inhibitors of ANAMMOX process**

  Similar to the nitritation process, ANAMMOX process can also be inhibited by FA and FNA. The mechanism of FA inhibition has been well studied [4, 73]. FA rather than ammonium can diffuse easily across the cell membrane. Due to the equilibrium equation between ammonium and FA, the formation of FA is associated with the increase of pH. With the increase of FA in solution, the concentration gradient between intracellular and extracellular spaces will drive the diffusion of FA across the cell membrane. The FA in the cell changes the intracellular pH, and this may cause cell death in the worst case [4]. For ANAMMOX process, the lowest FA toxicity threshold concentration was 1.7 $mgNL^{-1}$ at the reactor start-up period [128]. A much higher tolerant level can be achieved by long-term adaptation. In a study of ANAMMOX biofilm reactors, FA concentrations of 57-187 mgL^{-1} caused inhibition on ANAMMOX process [129]. Similar to AOB, AnAOB is more sensitive to FNA inhibition. In the short-term study, 50% of specific ANAMMOX activity (SAA) loss (IC_{50}) was detected at 11 μg FNA-N$/L$. In the long- term study, a decrease of operation efficiency was found with the FNA concentration range between 0.7 μg/L and 1.5 μg/L [130]. Based on the analysis and conclusion of different research results and operating conditions, it was believed that an influent nitrite concentration of 280 mg/L should be considered as the warning value of ANAMMOX process [73]. Different toxicity thresholds of FA and FNA were reported, which was probably due to the differences in operating conditions. Generally, long-term adaptation can enable AnAOB to stand with higher concentrations of FA and FNA.

  Non-toxic organic matter can also reduce ANAMMOX process performance due to the changes in bacterial community structure. The high organic concentration can stimulate the growth of fast-growing heterotrophic bacteria, such as denitrifying bacteria,

which would compete for nitrogen substrates with AnAOB. Therefore, AnAOB was outcompeted by heterotrophic bacteria, leading to the reduction of ANAMMOX process. Moreover, due to the versatile metabolic pathways of AnAOB, organic carbon instead of ammonium can be used as the electron donor by AnAOB, thus, results in the decrease of ANAMMOX nitrogen removal efficiency (NRE) [67]. More details of the ANAMMOX versatile metabolism was discussed in the previous section.

Toxic organic matter such as alcohol and aldehydes are inhibitors of ANAMMOX process. Methanol, a common intermediate product of anaerobic digestion, was proved to be an irreversible anammox inhibitor. It was reported that the activities of AnAOB were reduced to 70% and 51% at methanol concentrations of 1.7mM and 3.3mM, respectively [131]. However, another study reported that the activity of AnAOB was completely lost by the addition of 0.5mM of methanol [132]. The mechanism of methanol inhibition was ultimately found to be formaldehyde inhibition. Methanol may be converted to formaldehyde intracellularly via the ANAMMOX enzyme HZS. The produced formaldehyde destroys the enzyme activity by irreversibly cross-linking the peptide chains, and therefore, the anammox activity is destroyed [131]. Apart from methanol, ethanol can also inhibit ANAMMOX activity. Research found that 2mM of ethanol can reduce the AnAOB activity to 70%. The inhibition mechanism is most likely also due to the enzyme HZS, which converts ethanol to its corresponding acetaldehyde, and acetaldehyde directly inhibits the anammox reaction.

Phenol is another group of toxic organic matter, which is rarely present in municipal wastewater but can be detected in some industrial wastewater, such as coke-ovens wastewater. It was found that with 50 mg/L of phenol added into the ANAMMOX influent, the AnAOB activity was impaired. However, after phenol was removed from the feed, the ammonia-oxidizing activity recovered. Also, AnAOB was found to be able to slowly adapt to phenol. With the increase of phenol feed from 50 mg/L to 550 mg/L, the ammonia-oxidizing activity was still observed and even increased [133]. All these pieces of evidence proved that even though phenol had an adverse effect on ANAMMOX, the AnAOB activity was enhanced by acclimation to phenol.

Phosphate is a common inorganic inhibitor of the ANAMMOX process, its inhibitory effects have been widely studied. Previous study reported that granular AnAOB had a higher tolerance to phosphate than suspended biomass. In a gas-lift bioreactor, where granular AnAOB was observed, IC_{50} value of phosphate inhibition on the ANAMMOX process was 20 mM, which is above the range of phosphate concentration usually found in industrial wastewater [134]. On the other hand, complete inhibition of the suspended AnAOB was observed by exposing to 5 mM phosphate [88]. As a result, biomass granulation and aggregation can improve the tolerance of ANAMMOX to phosphate.

Sulfide inhibition was also tested because sulfate reduction takes place quite often during anaerobic digestion. The toxicity of sulfide is often associated with hydrogen sulfide

(H_2S). Sulfide can cause AnAOB activity inhibition at very low concentrations. In one study, H_2S also showed serious inhibition on the anammox activity with IC_{50} values of 0.03 and 0.11 mM for suspended biomass and granular biomass, respectively. With the concentration of 0.32 mM, H_2S can completely inhibit the activity of ANAMMOX suspended biomass [135]. Long-term acclimation can diminish the sulfide inhibition on the ANAMMOX process. After acclimation of 18 days, the NRR of ANAMMOX only decreased by 17.2% at sulfide level of 40 mg/L[136]. It was proven that sulfide inhibition is associated with the heme centers of cytochrome oxidase of AnAOB. The presence of sulfide can affect the activity of cytochrome oxidase by binding and reducing heme iron in cytochrome c, leading to disruption of AnAOB metabolism [135, 137].

High salinity results in high osmotic pressure and causes microorganisms to become plasmolyzed, dormant and even die. First discovered in the anoxic marine environment, AnAOB has a high tolerance to salinity and can adapt to higher salts concentration by acclimation [73]. According to long-term acclimation, the salinity inhibition on ANAMMOX was reduced from 67.5% to 43.1 % [136]. Different AnAOB genera have different tolerant levels to salinity. For example, the IC_{50} of NaCl on genus *Candidatus Brocadia* was 93±4 mM, and the AnAOB activity was completely inhibited with NaCl concentration increased to 200mM and higher [135]. Another genus, *Candidatus Kuenenia*, has been shown to be relatively tolerant of high salinity. NaCl concentration as high as 150 mM did not affect *Candidatus Kuenenia* activity, while KCl and Na_2SO_4 affect the AnAOB activity only at concentrations higher than 100 and 50 mM, respectively [134]. *Candidatus Scalindua* is another AnAOB genus with high tolerance to salinity. The AnAOB retained active at salts (90% NaCl and 10% KCl) concentration up to 0.5M ($30g/L$) [138].

As significant components of many enzymes and co-enzymes, the addition of some metals to the culture medium as trace elements are recommended for cultivating AnAOB [51]. While stimulating the metabolism of microorganisms, the excessive concentrations of hardly biodegradable metals can accumulate in organisms and cause biological toxicity. In 1995, while proving that ANAMMOX is a biologically mediated process, van de Graaf et al. found out that 1 $mmol/L$ of $HgCl_2$ can fully inhibit AnAOB activity [31]. Later on, more metals were proven to be inhibitors of ANAMMOX process. The inhibitory effects of Cu and Zn on AnAOB activity were studied by batch tests, and the study revealed that the IC_{50} of Cu and Zn were 1.9 and 3.9 mg/L, respectively [139]. Different heavy metals have different toxicity threshold concentrations to the ANAMMOX process. It was reported that Zn^{2+}, Cu^{2+} and Cd^{2+} were highly toxic to AnAOB with the IC_{50} values of approximately 4.2, 7.6 and 11.2 mg/L, respectively. $Ni^{2+}$was moderately toxic to AnAOB with the IC_{50} of approximately 48.6 mg/L. Pb^{2+} and Mo^{2+} were slightly toxic to AnAOB that Mo^{2+} was not inhibitory at concentration up to 22.7 mg/L and 75 mg/L of Pb^{2+} only caused 32% inhibition [140]. Despite being a weak inhibitor of ANAMMOX process, Mo was the most influential inhibitor.

Another study reported that the inhibitory effect of Mo on AnAOB was irreversible, whereas the Ni, Cu, Co, and Zn are all reversible inhibitor on ANAMMOX process [141]. A severe decrease of AnAOB metabolic activity was observed with the joint effects of Cu and Zn at 3 mg/L. A potent inhibitor of the electron transfer chain, excessive concentration of Zn^{2+} can lower the electron flux via the catabolic and anabolic pathways. Also, Zn^{2+} can displace the essential divalent cations existing in enzymes, causing loss of protein functionality. Different from the inhibitory mechanisms of Zn^{2+}, Cu^{2+} can chelate with sulfhydryl groups, disrupt heme c and protein bonds, leading to metabolic disorder and cytoplasmic membrane rupture. The damage of cell membrane caused by Cu^{2+} may facilitate the adsorption of Zn^{2+}, resulting in a more severe inhibitory effect on the ANAMMOX process by the joint effect. As with AOB, the toxicity of metals on AnAOB is associated with free cations instead of total analytical metals. The abundant functional groups in EPS are able to form organometallic complexes with multivalent cations, thus, preventing metals from damaging the cells [142]. Therefore, the increase of EPS level can help to defend the heavy metal inhibitions.

Antibiotics are widely used to prevent infections and treat diseases. Antibiotics were detected in wastewaters from pharmaceutical plants, swine plants [142] and anaerobic digesters. Several works have been published about the inhibitory effects of antibiotics on the ANAMMOX process. With 200 mg/l of chloramphenicol and 800 mg/l of ampicillin added into the ANAMMOX process, the AnAOB activity in the batch tests was inhibited by 68% and 71%, respectively [31]. In a long-term SBR, continuous feeding with chloramphenicol of 20 mg/L decreased the NRR of ANAMMOX process by 25%. Similar effects were also observed by continuously feeding with $50mg/L$ of tetracycline hydrochloride. Moreover, the presence of chloramphenicol in the feeding led to the disrupture of biomass granule [143]. The IC_{50}s of oxytetracycline (OTC) and sulfathiazole on AnAOB were also evaluated. By exposing to OTC and sulfathiazole for 24h, the IC_{50}s were 650 and 1100 mg/L, respectively [139]. Furthermore, the joint effect of 0.04 $kg/m^3/day$ of Cu and OTC retarded the growth rate of AnAOB by 47.6%. As a broad-spectrum antibiotic belongs to the tetracycline class, OTC interferes the attachment of transfer RNA by binding with 30S ribosomal subunit, preventing subsequent amino acid elongation and protein synthesis [142].

The inhibitors of nitritation/ANAMMOX process can be roughly classified into three categories: 1) FA and FNA inhibitors; 2) Enzyme-associated inhibitors; 3) non-toxic organic matter inhibitors. FA and FNA are common inhibitors for both nitritation and ANAMMOX processes. Also, both AOB and AnAOB are more tolerant to FA than FNA. The concentrations of FA and FNA can be regulated by pH control. A group of enzyme-associated inhibitors of AOB is AMO substrates, which compete with ammonium for AMO and oxygen, leading to a decrease of ammonium oxidation. Another group of enzyme-associated inhibitors of AOB works on the Cu ion in the active site of AMO by creating Cu-chelating complex, resulting in AMO inhibition. Free metal ions, rather than total analytical metals, are inhibitors of both AOB and AnAOB. By displacing the essential metal ions in enzymes,

these free metal ions inhibit nitritation and ANAMMOX processes by disrupting enzyme functions. Sulfide inhibition is also associated with the high dependence of ANAMMOX process on heme proteins. Moreover, alcohol and aldehydes inhibitions work on functional enzyme HZS in the ANAMMOX process. Non-toxic organic matters have different inhibition mechanisms on AOB and AnAOB. VFAs are non-competitive inhibitors of AOB, while the non-toxic organics affect ANAMMOX process performance by enriching heterotrophic bacteria, which will compete for nitrogen substrates with AnAOB. Other inhibitors also include phenol, salinity, phosphate, and antibiotics. One way to eliminate inhibition is to promote biomass granulation. With granular biomass, AnAOB became more tolerant of phosphate. Moreover, higher EPS produced during biomass granulation can chelate metals, and therefore eliminate metal inhibitions. Long-term adaptation can also alleviate several types of inhibition such as FA and FNA inhibitions, salinity inhibition, phenol inhibition, and etc. To prevent non-organic matter inhibitions, higher and longer aeration should be applied during the nitritation process in order to enrich heterotrophic bacteria, which can consume the organics in the system.

1.2.3.4 The Application of Nitritation/ANAMMOX Process

The nitritation/ANAMMOX process has been applied to various types of wastewaters, such as landfill leachate, swine digester liquor, refinery wastewater, etc [144–146]. Since the start-up of first full-scale ANAMMOX reactor at Rotterdam in 2007, 114 reported full-scale ANAMMOX reactors had been installed worldwide by 2015, with 88 of full-scale reactors constructed in Europe [60, 80, 147]. The volume capacities of the reactors have been increased from 70 m^3 to more than 142,000 m^3 [60, 147]. As the prerequisite step of ANAMMOX process, the nitritation process requires oxic condition, which is different from the anoxic condition required by the ANAMMOX process. As a result, the two-stage SHARON-ANAMMOX process has been widely applied. With the development of automatic controls in recent years, the establishment of single-stage systems became the mainstream. The single-stage nitritation/ANAMMOX process can save operational cost while reducing the footprints of the wastewater treatment plant. Also, with continuous consumption of nitrite, the one-stage system avoids the potentially toxic feed for the second step. The single-stage system implementation includes SBR, granular sludge processes and biofilm reactors. A summary of the application of nitritation/ANAMMOX process on various wastewater nitrogen removal is listed in Table 1.5.

SHARON-ANAMMOX Process

SHARON is an abbreviation of single reactor system for high activity ammonium removal over nitrite. As a two-stage process, the SHARON-ANAMMOX process is usually composed of a CSTR for nitritation process and an SBR for the ANAMMOX process. Being operated in the CSTR, the SHARON process is responsible for converting part of ammonium into nitrite by AOB and providing suitable influent for the subsequent ANAMMOX process.

During the operation of the SHARON process, partial ammonium oxidation is achieved

by running the system as a chemostat. Without biomass retention, the SRT is equal to HRT. By controlling the system under relatively high temperature and short SRT, the fast-growing AOB is selected over NOB, restricting nitrite oxidation and leading to nitrite accumulation. The ammonium/nitrite ratio in the effluent of the SHARON process can be mediated by controlling pH. Nitritation is an acid-producing process. Ammonium oxidation can be enhanced by increasing pH in the system, which results in the decrease of ammonium concentration in the effluent. In 2001, the SHARON-ANAMMOX process was successfully applied to the nitrogen removal of sludge recycle liquor. The SHARON process was operated in a 10-L CSTR with HRT of 1 day. 53% of ammonium conversion was achieved in the SHARON effluent with no nitrate detected. The following ANAMMOX process was operated as a granular SBR process. With the NLR of 1.2 $kg/m^3/day$, the NRE of the process reached 80% [148]. In 2002, a pilot-scale SHARON-ANAMMOX process was established for treating ammonium-rich digester supernatant. With 58% of ammonium conversion achieved in the SHARON process, the NRR of the system was 2.4 $kg/m^3/day$ with more than 90% of nitrogen removal [26]. Following the SHARON process, the first full-scale ANAMMOX reactor was built up treating sludge digestate in 2007 [80].

One-Stage SBR

SBR is the most commonly applied reactor type for establishing the one-stage nitritation/ANAMMOX process. The pH-controlled deammonification system (DEMON) is one of the most popular SBR technologies [147]. Intermittent aeration was applied based on pH controls within a very tight interval of 0.01. During aeration, aerobic ammonium oxidation occurred with the production of H^+, which reduced the pH to the lower set-point and shut down oxygen input. With the depletion of DO, AnAOB can oxidize ammonium using the accumulated nitrite as electron acceptor under anoxic condition. While recovering alkalinity in the system and driving pH to the upper set-point, aeration was switched back on. Also, to prevent the presence of NOB, DO was controlled around $0.3mg/L$. The full-scale DEMON was firstly implemented on rejection water nitrogen removal at Strass, Austria. After the operation of the system for 2.5 years, the DEMON has reached the nitrogen removal capacity of 300 kg/day. The intermittent aeration can reduce compressed air demand from 109 m^3/kgN to 29 m^3/kgN [149]. AOB grows 10 times faster than AnAOB. In order to balance the biomass composition and shorten DEMON start-up time, a cyclone was installed to control selected SRT. AnAOB aggregates have a higher density than other AOB and NOB flocs. According to the different densities, AnAOB was retained in the system by recycling underflow from the cyclone, while NOB was washed out by wasting overflow [150].

Continuous aeration was also applied to one-stage SBR. By controlling DO level lower than 0.1 mg/L, simultaneous nitritation and ANAMMOX processes can happen. The SBR cycle was controlled via the ammonium sensor. The ammonium set-point controlled the feed rate, resulting in variable cycle length. Continuous aeration has many advantages over intermittent aeration: 1) the operation of continuous aeration is much simpler; 2) better monitoring of the process resulted in higher performance; 3) simultaneous nitrite formation and depletion leading to less nitrite accumulation. It was concluded that intermittent aer-

ation was preferred for the start-up stage of the process with low activity sludge, whereas continuous aeration should be applied for normal operation [147, 151].

One-Stage Granular Sludge Processes

Granular biomass, is easily retained in the reactor and has higher settling velocity than suspended biomass. Also, granular biomass has higher tolerance to errors, such as high nitrite concentrations, incoming solids, and COD. A decrease of suspended AnAOB activity was observed when exposed to nitrite concentration of 4.8 mg/L [152]. With granular AnAOB, nitrite concentration up to 42 mg/L didn't cause inhibition. It was reported that the granular biomass had at least six times higher tolerant level to nitrite toxicity than suspended biomass. Moreover, granular biomass with higher densities can be easily separated from the incoming solids and biomass flocs growing based on the incoming COD, which can be washed out from the system. Full-scale one-stage granular sludge nitritation/ANAMMOX process was established for nitrogen removal of potato wastewater and reject water in Olburgen sewage treatment plant. After 3-year's operation, the maximum NLR reached 1.5 $kg/m^3/day$ with ammonium removal efficiency of 91% on average [153]. The upflow granular sludge bed reactor was applied on the implementation of completely autotrophic nitrogen removal over nitrite (CANON) process. During CANON process, limited oxygen was supplied to achieve balanced interaction between AOB and AnAOB [154, 155]. The excellent settleability of granular biomass enabled higher biomass retention and improved system performance. By treating with anaerobic sludge liquid, NRE of the upflow granular sludge bed reactor was 94% at HRT of 7 days [156].

One-Stage Biofilm Reactor

Oxygen-limited autotrophic nitrification-denitrification (OLAND) biofilm reactor was successfully applied on nitrogen removal of high ammonium concentration wastewater. Consisting of AOB and AnAOB biofilms for autotrophic nitrogen removal, OLAND process was operated in a rotating biological contactor (RBC) treating digested black water. After the adaption period, a stable NRR of 0.7 $kg/m^3/day$ was reached. Fluorescent *in situ* hybridization was performed to study the morphology of AOB and AnAOB. During the treatment period, AnAOB were housed in spherical microcolonies, while AOB was composed of scattered, ungrouped cells as well as typical spherical microcolonies in distances. Lower substrate concentrations in deeper biofilm were thought to be the reason for the dispersed AOB cells [157]. As less substrate was accessible in deeper biofilm, AOB cells preferred to grow in distance to access more substrates. In another study, an RBC was operated under OLAND condition for treating high-salinity wastewater. A NRE of 84% was achieved at NLR of 0.725 $kg/m^3/day$ with salt concentration of 30 g/L. It was believed that AnAOB had higher tolerances of salts when encapsulated in thick biofilms [158].

Moving-bed biofilm reactor (MBBR) was also used for the nitritation/ANAMMOX process. In 2010, the first full-scale ANITA MOX plant was started up for nitrogen removal of sidestream in Malmö, Sweden. Within the startup of 4 months, the ammonium removal rate reached 1.2 $kg/m^3/day$ with 90% of ammonium removal. ANITA MOX process was

a one-stage MBBR process, where nitritation and ANAMMOX took place simultaneously. Limited oxygen was provided, resulting in oxygen mass transfer limitation and creating aerobic and anoxic zones of the biofilm. Nitritation process took place in the outer aerobic layer of the biofilm. While converting partial ammonium into nitrite, nitritation process in the outer layer also prevented oxygen diffusing into the anoxic layer. ANAMMOX process took place in the inner anoxic biofilm layer (Figure 1.4). The remaining ammonium and produced nitrite from the outer layer diffused into the inner anoxic layer and provided substrates for the ANAMMOX process. Pre-colonized carriers were used to accelerate the start-up time of the ANITA MOX process; also, the carriers provided large surface area for developing the biofilm. Together with the carriers, the presence of retention grids in ANITA MOX process avoided any loss of biomass [159]. The performance of biofilm reactors can be further improved by integrated fixed-biofilm activated sludge (IFAS) configuration. By incorporating a settler in the MBBR system, the IFAS configuration can achieve 2 to 2.5 times higher NRR. The system performance can benefit from the suspended sludge retained from the effluents, which can be enriched under lower DO and substrate levels due to less mass transfer limitations [160].

1.2.4 Simultaneous Nitritation ANAMMOX AND Denitrification (SNAD) Process

Despite the energy-saving and cost-effective benefits of the autotrophic nitritation/ANAMMOX process, the process also has a few drawbacks: 1) With the consumption of ammonium and nitrite, the ANAMMOX process produces 11% of nitrogen as nitrate in the effluent, indicating that ANAMMOX process can only remove up to 90% of influent nitrogen; 2)NOB, which competes with AnAOB for nitrite substrate, needs to be restrained from the system, requiring complicated operational controls; 3) The organics present in wastewater can inhibit the growth and activity of AnAOB, affecting NRR of the system (discussed in 1.2.3.2: operating conditions, and 1.2.3.3: the inhibitors of ANAMMOX process). Recently, the simultaneous nitritation ANAMMOX and denitrification (SNAD) process has been successfully applied to the nitrogen removal of low COD/N ratio wastewater. The addition of the denitrification process can not only convert produced nitrate into nitrogen gas but can also reduce nitrate into nitrite, which can support the AnAOB activity (Figure 1.3). Moreover, the denitrification process is able to use organic carbon as the electron donor, alleviating the inhibition of organic carbon on ANAMMOX. The application of SNAD process can facilitate simultaneous nitrogen and organic carbon removal [162, 163]. Mature landfill leachate with low COD/N ratio of 1 (g/g) was treated by SNAD running an SBR. Intermittent aeration was applied to build up the balanced bacterial community of the system. The long-term result showed that the SNAD process led to a lower ratio of produced nitrate than the nitritation/ANAMMOX process. Also, a COD removal efficiency of 77.8% was achieved with a high TN removal efficiency of 99.31%, of which 74.5% of nitrogen removal was based on ANAMMOX and 18.3% or nitrogen removal was from denitrification [163]. In another study,

Process name	Reactor type	Location	Treated wastewater	Reactor volume (m^3)	NLR ($kg/m^3/day$)	NRR ($kg/m^3/day$)	Energy demand (Kwh/Kg_N)	Ref.
One-stage process								
DEMON	SBR	Austria	Sidestream	500	0.68	0.6	0.79	[149]
DEMON	SBR	Switzerland	Sidestream	2×1400	-	0.5	1.11	[151]
OLAND	RBC	Belgium	SWW with high salinity	0.05	0.73	-	-	[158]
CANON	Granular sludge reactor	Netherlands	Potata WW[11] +reject WW	600	2.08	-	1.86	[153]
ANITA MOX	MBBR	Sweden	Sidestream	200	0.83	0.63	1.45-1.75	[159]
IFAS	MBBR	Sweden	Sidestream	50	-	2-2.5	-	[160]
Two-stage process								
SHARON-ANAMMOX	Granular sludge reactor	Netherlands	Sidestream	1500+70	-	9.5	4.17	[80]
SHARON-ANAMMOX	UASB	Japan	Semiconductor WW	3600+58	-	3		[161]
CIRCOX-ANAMMOX	-	Netherlands	Tannery	150+75	-	1.7-1.9	-	[147]

Table 1.5: The application of nitritation/ANAMMOX process treating various wastewater.

[11] *Wastewater*

SNAD biofilm reactor was established by feeding with SWW and extra COD. The TN removal efficiency reached 90% with the influent COD/N ratio of 2.57. With limited COD supplied, the denitrification process would stop consuming nitrite after using up COD, and the nitrite generated by nitritation would be mainly used by ANAMMOX process [164].

1.2.5 Dissimilatory Nitrate Reduction To Ammonium (DNRA) Coupled With Autotrophic Nitrogen Removal Process

The dissimilatory nitrate reduction to ammonium pathway, another major pathway in the nitrogen cycle, usually starts with nitrate reduction to nitrite, then ammonium, though it may also begin with nitrite [165] (Figure 1.3). By using organic carbon as the electron donor, the DNRA pathway is governed by groups of heterotrophic bacteria as well as some ANAMMOX species, such as *Candidatus Anammoxoglobus propionicus* and *Candidatus Brocadia fulgida*. With the presence of organic matters, these ANAMMOX species are able to accomplish partial DNRA (convert nitrate into nitrite) or full DNRA [39]. The coexistence of DNRA and ANAMMOX have been discovered in many oxygen minimum natural systems, including marine sediments, lakes, wetland and coastal ecosystem [166–168]. As DNRA can generate more energy per unit nitrate reduced than the denitrification process, DNRA can outcompete the denitrification process, especially under nitrate limiting conditions [165]. It was reported that DNRA dominated benthic nitrate reduction in tropical estuaries [169]. Efficient in both nitrate reduction and ammonium production, DNRA can sustain the ANAMMOX process. DNRA coupled with ANAMMOX reached a high NRR for municipal wastewater treatment. According to Gibbs free energy calculations, partial DNRA by AnAOB was favored over heterotrophic DNRA and denitrification under organic carbon limiting condition. Also, with the presence of external ammonium, partial DNRA was preferred as more energy can be generated. As a result, the joint implementation of partial DNRA and ANAMMOX process by AnAOB was a promising and energy favored approach for nitrogen removal [170].

1.3 Thermal Hydrolysis Pre-treated (THP) Anaerobic Digestion(AD)

Anaerobic digestion (AD), a process that leads to overall gasification of organic waste to methane and carbon dioxide, has been widely applied for biological sludge treatment [171]. Governed by groups of microbes in absence of oxygen, AD is usually composed of four steps: 1) Hydrolysis, where the complex organic matter such as polymers, carbohydrates, proteins, and lipids are broken down into smaller parts; 2) The hydrolyzed compounds are further digested into VFAs, alcohol, ammonia, hydrogen and carbon dioxide via acidogenesis by acidogenic bacteria; 3) During the next step, acetogenesis, the simple molecules produced by acidogenesis are further digested into acetic acids, carbon dioxide and hydrogen; 4) The final step is methanogenesis, where methane is generated via either reduction of acetic acid by

acetoclastic methanogenesis or reduction of carbon dioxide by hydrogenotrophic methanogenesis. By treating with AD, the biosolids collected from primary and secondary clarifiers can be reduced up to 50%. Also, the produced biogas such as methane from AD is an energy resource. In most cases, the produced biogas is transferred into a combined heat and power installation for the simultaneous generation of electricity and heat. It was reported that 1 kg of organic dry solids of sewage sludge could produce 0.59 m^3 of methane [172]. By 2011, the U.S. Environmental Protection Agency (EPA) estimated that 544 of 16 000 municipal wastewater treatment plants were employed with AD, while only 106 of them utilized produced biogas to generate electricity and heat. It was believed that if the biogas produced from all of the 544 treatment plants were used for energy generation, that would be equivalent to removing emissions of approximately 430 000 cars [12]. For the digestion of particulate substrates, hydrolysis is the rate-limiting step [173–175]. To accelerate the hydrolysis step by enhancing solubilization of complex particulate matter and the breakage of flocs, thermal hydrolysis process (THP), an enhancing pre-treatment step of AD, has been applied worldwide since 1995 [176]. With high temperature and high pressure, THP helps to disintegrate sludge cells and make sludge become more digestible. During THP pre-treatment, the thickened sludge is firstly pumped into the pulper which is preheated to 97 °C. The increase in temperature and mixing decreases the viscosity of the sludge. From the pulper, the pre-heated material is pumped into the reactor. Steam is injected directly into the reactor until the required operating pressure (6 bar) and temperature (165 -170°C) are reached. Under the high temperature and pressure, cell walls are destroyed and proteins are made accessible for biological degradation, while complex carbohydrates and protein substrates are hydrolyzed to signal monomers of saccharides, amino acids, and lipids, which undergo decarboxylation and produce acetic acid [177]. Finally, the hydrolyzed material is added into a flash tank to cool down before it is pumped into the anaerobic digester(Figure 1.5). THP pre-treatment would aid the disintegration of sludge cells and improve the digestibility of the sludge. By increasing AD efficiency, the gas production and cake dewaterability are promoted, resulting in higher biosolid quality and reduce the cost of transportation. The increased biogas production can largely compensate the surplus energetic expense for bringing the sludge to the hydrolysis temperature and pressure. The residual heat can also aid in maintaining the digester's temperature and conserve energy. Also, the increased temperature and pressure allow doubling of dry solids loading and save footprints for wastewater treatment plant [178–180].

In wastewater treatment plants with AD, the supernatant of anaerobically digested sludge, named sidestream, is usually recycled back into the mainstream without treatment, increasing the nitrogen loading to the treatment train by as much as 30% [181]. Separate treatment of the sidestream, which contains a high concentration of ammonium (>1000 mgN/L), would significantly reduce the nitrogen load of mainstream and improve nitrogen elimination. Because of the low COD/N ratio of sidestream, the applications of nitritation/ANAMMOX process on sidestream nitrogen removal have been reported by many studies (Table 1.5). Due to higher AD efficiency, increased dry solids loading, enhanced digestion, the sidestream produced with THP pre-treatment (THP-S) (Figure1.6) contains higher

concentrations of ammonium and COD than the sidestream produced without THP pretreatment (RS). Still having low COD/N ratio, the application of nitritation/ANAMMOX process on THP-S nitrogen removal is an attractive option. In 2014, the Blue Plains wastewater treatment plant in Washington, DC started the operation THP for solids pretreatment prior to mesophilic AD in combination with the nitritation/ANAMMOX process using the DEMON configuration to remove nitrogen from the sidestream. Nitrogen conversion rates decreased significantly, pointing to inhibitory effects of THP-S on nitritation/ANAMMOX process [178, 182].

1.4 Research motivation, objectives and dissertation outline

Previous studies reported that the observed inhibition of nitritation/ANAMMOX process by THP-S can be ameliorated by 1) enhanced biomass adaptation which lower the influent load; 2) 1 to 1 dilution of the feed [178, 182]. Without identifying the specific inhibitor, Figdore et al. emphasized that biological activity limitations had the highest correlation with inert soluble COD [178]. In 2016, Zhang et al. found the inhibition can be overcome by increasing DO and aeration time [182]. They concluded that the nitritation process but not the Anammox process was inhibited by THP-S [178, 182]. However, the conclusion had several knowledge gaps. First, the nitritation/ANAMMOX process has previously been performed in the one-stage DEMON process. With this approach, it is difficult to distinguish inhibition kinetics specific to each process, and thus, these inhibitions on each process kinetic mechanisms remain unknown. Second, Zhang et al. used only 50-70% (vol/vol ratio) of THP-S, and therefore the effect of using pure THP-S still needs to be elucidated. Third, despite short-term inhibition of nitritation/ANAMMOX process by THP-S, a long term adaptation of the microbial community to THP-S was possible. The timeline and specific community shifts associated with the adaptation must be understood.

The research in this dissertation has been motivated by the opportunities to clarify the rate-limiting step of the nitritation/ANAMMOX process treating THP-S, with the goal of providing feasible solutions to overcome the inhibition and to successfully apply nitritation/ANAMMOX process on THP-S nitrogen removal. More specifically, the research aims to:

1. study the inhibitory effects of THP-S on the independent nitritation process with both short-term and long-term tests (Chapter 3);

2. study the inhibitory effects of THP-S on the independent ANAMMOX process with both short-term and long-term tests (Chapter 4);

3. establish two-stage nitritation/ANAMMOX process to overcome THP-S inhibition by applying different operational strategies for nitritation process (Chapter 5);

4. evaluate the applications of different one-stage nitritation/ANAMMOX configurations treating THP-S via process performance analysis and the study of bacterial community structures (Chapter 6).

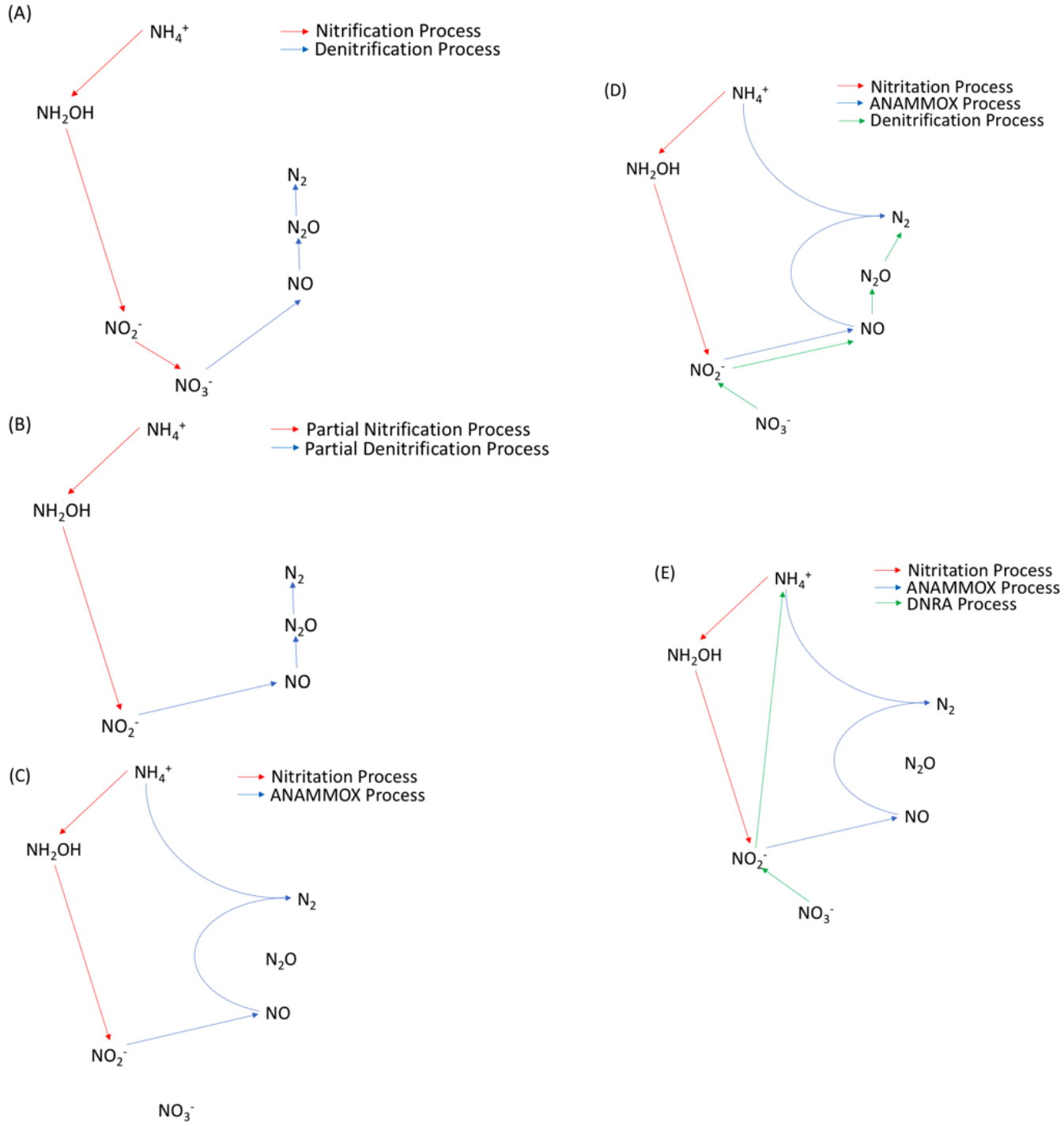


Figure 1.3: The diagram of different nitrogen elimination processes. (A) the conventional nitrification-denitrification (CND) process; (B) the short-cut nitrification-denitrification (SCND) process; (C) the autotrophic nitritation/ANAMMOX process; (D) the simultaneous nitritation ANAMMOX and denitrification (SNAD) process; (E) the dissimilatory nitrate reduction to ammonium (DNRA) coupled with autotrophic nitrogen removal process.

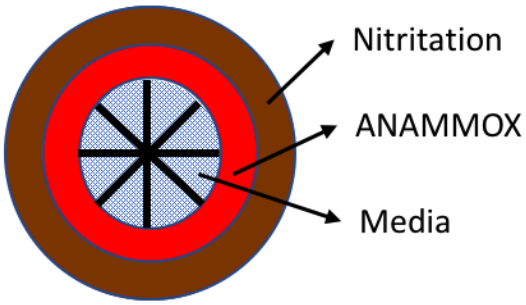


Figure 1.4: The diagram of bacteria distribution on ANITA MOX biomass carriers.

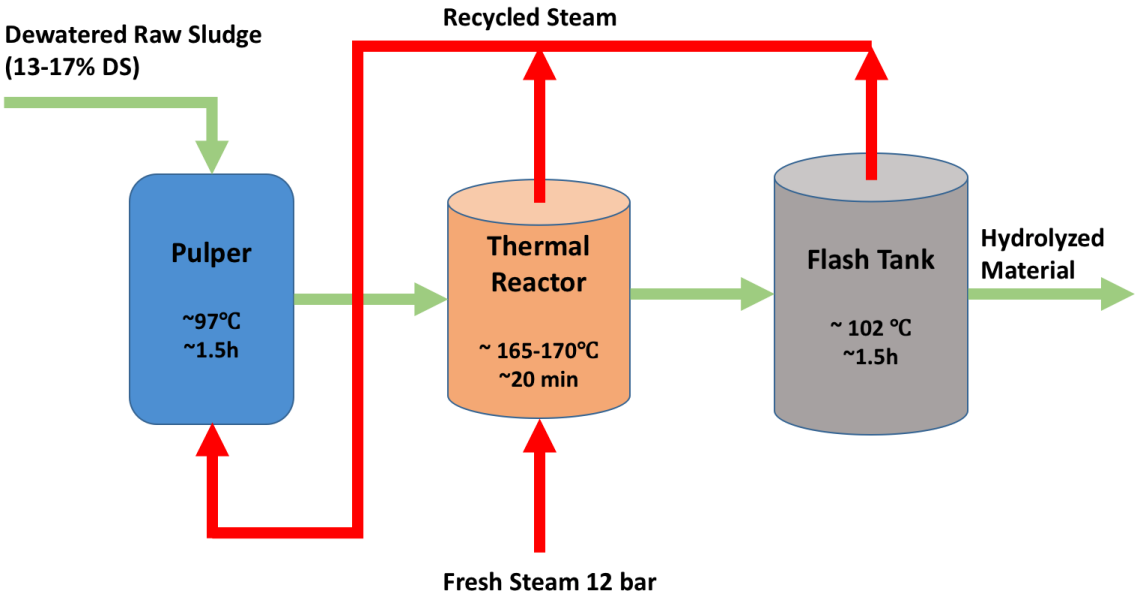


Figure 1.5: The schematic of THP pre-treatment.

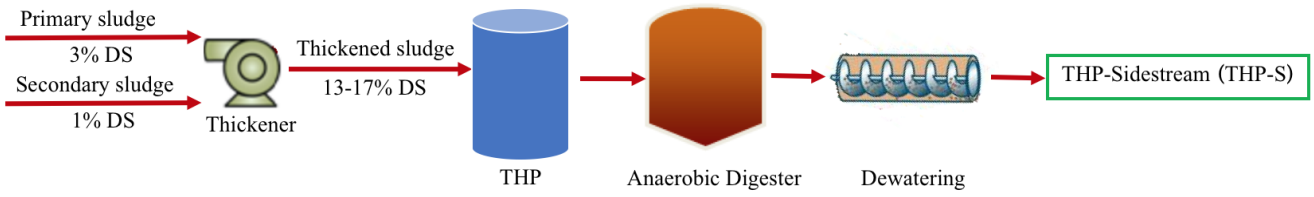


Figure 1.6: The diagram of the production of THP-S.

Chapter 2

Experimental set-ups and basic methods

2.1 Nitritation reactor start-up

Nitritation process was established in a 5 L sequencing batch reactor (SBR) (New Brunswick BioFlo 115, Eppendorf, Germany). The process was automatically controlled by a Programmable Logic Controller (PLC) according to the setpoints and equipped with sensors that monitored the real-time data of pH, dissolved oxygen(DO), water level, agitation, temperature and feed rate. Complete mixture was achieved with a mechanical stirrer, and aeration was carried out using air diffusers at the bottom of the rector 2.2. The reactor was heat jacketed, and the temperature was maintained at 37°C by a thermometer. pH was kept around 7.5 through the addition of sodium hydroxide (5N). DO was controlled at a set-point of 0.5 mg/L by mixing and aeration. The reactor was operated with 2 h per cycle, consisting of 90 min feeding under aeration, 20 min settling and 10 min drawing. The reactor was inoculated with 3 L sludge from a nitritation/ANAMMOX pilot at SFPUC Southeast Wastewater Treatment Plant in San Francisco, California, USA. The seed mixture contained the initial biomass concentration of 5.5 g volatile suspended solids (VSS)/L. The biomass was washed 3 times with 1 × PBS at 3000 g for 5 min under 4°C before inoculation. Synthetic wastewater (SWW) was used to establish the nitritation process with a solid retention time (SRT) of 8 days and hydraulic retention time (HRT) of 0.5 days. The compositions of SWW were based on previous studies [154] with $(NH_4)_2SO_4$ as ammonia source. $NaHCO_3$ was added to the influent to make the N/C ratio of 1.

Figure 1a represents the evolution of influent NH_4^+-N concentration and the concentrations of effluent nitrogen compounds. In order to achieve nitritation process and to allow AOB being the dominant species in the system, the nitritation SBR was established with SWW. Progressive biomass acclimation to high nitrogen strength wastewater was gained by gradually increasing influent NH_4^+-N concentration from 280 mg/L to almost 2000 mg/L. The accumulation of NO_2^--N increased along with the stepwise increase of influent NH_4^+-N



Figure 2.1: The ANAMMOX MBR.

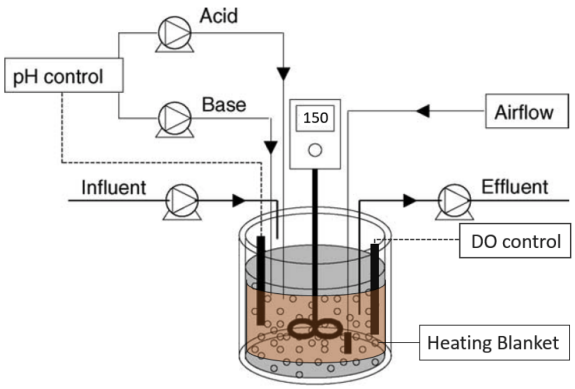


Figure 2.2: The schema of ANAMMOX MBR.

concentration. At day 40, the influent NH_4^+-N concentration was increased to approximately 2000 mg/L with high concentrations of NO_2^--N and negligible amounts of NO_3^--N accumulated, indicating that nitritation process was successfully established and AOB was the dominant species in the system. To investigate the long-term stability of the system, the reactor was operated under high influent NH_4^+-N concentration with nitrogen loading rate (NLR) of about 4 $gN/L/d$. During the 100 days of stable operation, the average conversion efficiencies of NH_4^+-N to NO_2^--N and NH_4^+-N to NO_3^--N were 67% and $< 3\%$, respectively (Figure 2.3). It was clear that nitritation process can treat high nitrogen strength wastewater and produce appropriate influent for the subsequent ANAMMOX process after long-term acclimation.

2.2 ANAMMOX reactor start-up

The ANAMMOX process was started up in a 3 L continuous flow membrane bioreactor (MBR). Hollow fiber membranes with the pore size of 0.22 μm were applied to retain biomass for having shorter HRT than SRT. The reactor was inoculated with 1 L of ANAMMOX biomass collecting from the pilot-scale nitritation/ANAMMOX reactor at Southeast Wastewater Treatment Plant with 5000 mg/L of VSS. Before inoculation, the biomass was washed 3 times with 1 $\times$ PBS at 3000 g for 5 min under 4°C. The temperature of the reactor was controlled at 37°C by recirculating heated water in the water bath with a heating pump. Substrate inhibition should be carefully avoided at the start-up of the ANAMMOX process. Previous studies reported that free ammonia (NH_3, FA, 38 mg/L) and free nitrous acid (HNO_2, FNA, 11$\mu g/L$) caused ANAMMOX bacteria (AnAOB) activity loss [73, 130]. To avoid substrate inhibition, the influent ammonium-N concentration was gradually increased

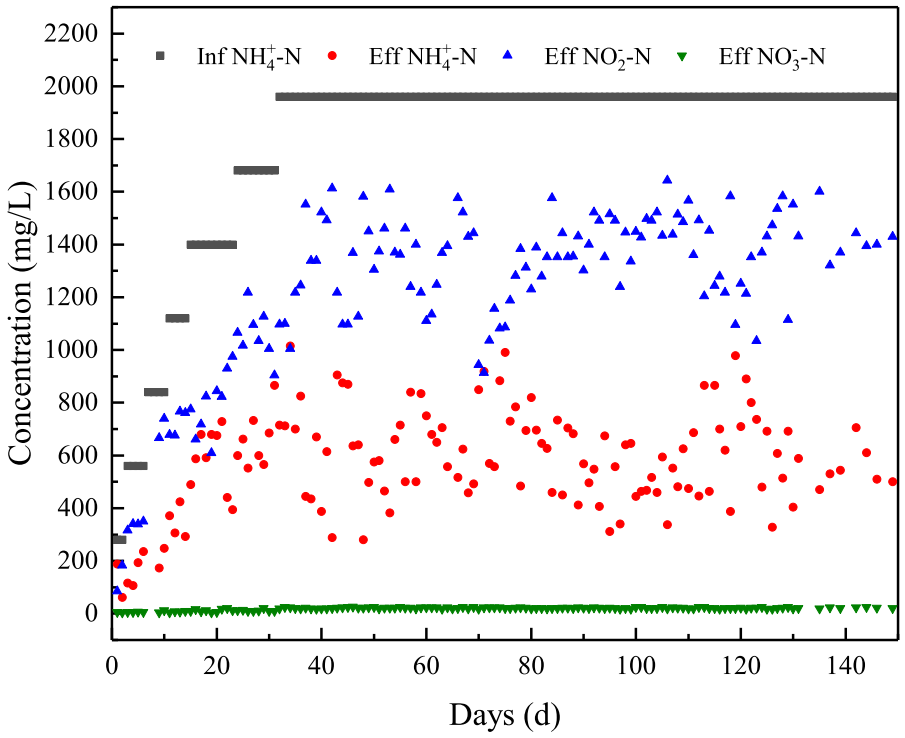


Figure 2.3: Start-up of Nitritation SBR with SWW influent.

from 210 mg/L to over 2000 mg/L. Nitrite was fed with the nitrite-N/ammonium-N molar ratio in the range of 1-1.2, having nitrite as the limiting substrate to avoid FNA inhibition. Also, pH was adjusted in the range of 6.8-7.1 to control FA and FNA concentrations using carbon dioxide (CO_2) gas and bicarbonate. DO was another critical operational parameter for the ANAMMOX process, with inhibition reported even when DO was $< 2\%$ [25]. To create an anoxic environment for ANAMMOX bacteria (AnAOB) growth, an argon (Ar)/CO_2 mix (95%/5%, respectively) was continuously bubbled into the reactor system (Figure 2.5). Vigorous mixing was continuously provided to the system by aeration and magnetic stirring. Also, the turbulence created by aeration can alleviate membrane fouling. The HRT was controlled by an effluent pump, and a level sensor was used to control the influent pump. The biggest challenge of membrane application is fouling issue.

To enrich AnAOB, synthetic SWW was applied. $(NH_4)_2SO_4$ and $NaNO_2$ were used as the nitrogen source, electron donor and electron acceptor, and $KHCO_3$ was used as carbon source. 10 mL/L of 100 $\times$ salts solution, 1 mL/L of 1000 $\times$ trace metal ions solution



Figure 2.4: The ANAMMOX MBR.

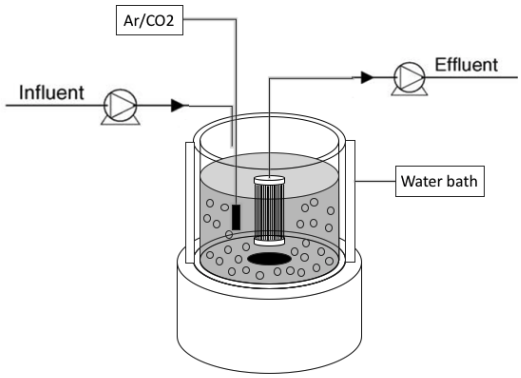


Figure 2.5: The schema of ANAMMOX MBR.

Compound	Unit	Concentration
$(NH_4)_2SO_4$	g/L	0.33-11.89
$NaNO_2$	g/L	0.35-12.42
$KHCO_3$	g/L	0-1
KH_2PO_4	mg/L	27.2
$MgCl_2{\cdot}6H_2O$	mg/L	247
$CaCl_2{\cdot}2H_2O$	mg/L	180
$FeCl_2{\cdot}4H_2O$	mg/L	17.89

Table 2.1: Composition of SWW[1].

and 1 mL/L of 1000 $\times$ ferrous iron solution were added to provide macronutrients and micronutrients for AnAOB. The compostion of the trace metal ions solution was described by Van de Graff et al. [88]. To make the ferrous iron solution, oxygen-free water was prepared by heating deionized (DI) water to boiling point. Then, $FeCl_2{\cdot}4H_2O$ was added with Ar continuously bubbling into the solution to avoid oxygen. Moreover, the pH of the solution was adjusted to be < 3 to prevent the oxidation of ferrous iron. With protons being taken during the ANAMMOX process, the dosage of bicarbonate decreased with the increase of influent nitrogen concentrations in order to control pH around the neutral level (Table 2.2). Ar was constantly bubbled during the preparation of SWW to creat an anoxic condition. The final concentrations of each compound in SWW were listed in Table 2.1.

After about 230 days of enrichment, the ANAMMOX process was successfully established in the MBR with a maximum influent total nitrogen (TN) concentration of 5292 mgN/L.

[1]The concentrations of trace metal ions are not included

$(NH_4)_2SO_4$ concentration (g/L)	$KHCO_3$ concentration (g/L)
0.33	1
0.66	0.8
1.32	0.7
2.64	0.6
3.96	0.5
5.28	0.42
6.6	0.34-0.37
7.93	0.3
9.25	0.2
10.57	0.1
11.89	0

Table 2.2: The correlations between the increase of $(NH_4)_2SO_4$ concentration and the decrease of $KHCO_3$ concentration in SWW.

The volumetric NLR reached 4.12 $gN/L/d$, and the maximum specific nitrogen removal rate reached 0.7 $gN/L/gVSS$. Thourghout the enrichment, the concentration of nitrite in the reactor remained below 20 mgN/L, and more than 90 % of nitrogen removel efficiency (NRE) was achieved (Figure 2.6). The average measured stiochiometric ratios of consumed NO_2^--N/ consumed NH_4^+-N and the produced NO_3^--N/ consumed NH_4^+-N were 1.18 and 0.16 (Figure 2.7), which were lower than the theoretical values of 1.32 and 0.26. The difference between the measured and theoretical values indicated the formation of ammonium or reduction of nitrate, which coule be done by the presence of denitrification and dissimilatory nitrate to ammonium (DNRA). Also, the color of the biomass changed from greyish balck to red, which was due to the increase in cytochrome content (Figure 2.8) [88].

2.3 Regular sidestream (RS) and thermal hydrolysis pre-treated sidestream (THP-S)

Both RS and THP-S were obtained from Southeast Wastewater Treatment Plant. The THP-S was obtained after dewatering anaerobically digested sludge pre-treated with thermal hydrolysis pre-treatment process (THP). During THP, thickened sludge with the total solid (TS) concentration of 13-17 % was introduced to the process at the temperature of 165 °C for 30 min. The THP was followed by mesophilic anaerobic digestion (36 ± 1 °C) [179] at 15-20 days SRT. The picture of THP is shown in Figure **??**. The sludge was dewatered using dewatering polymer (Solenis Praestal 859BS) followed by gravity drainage through a belt filter cloth on a screen (125 μm). RS was obtained from full-scale anaerobic digestion (AD) without THP. The AD was operated at a TS concentration of 2-3 % at 35 °C with

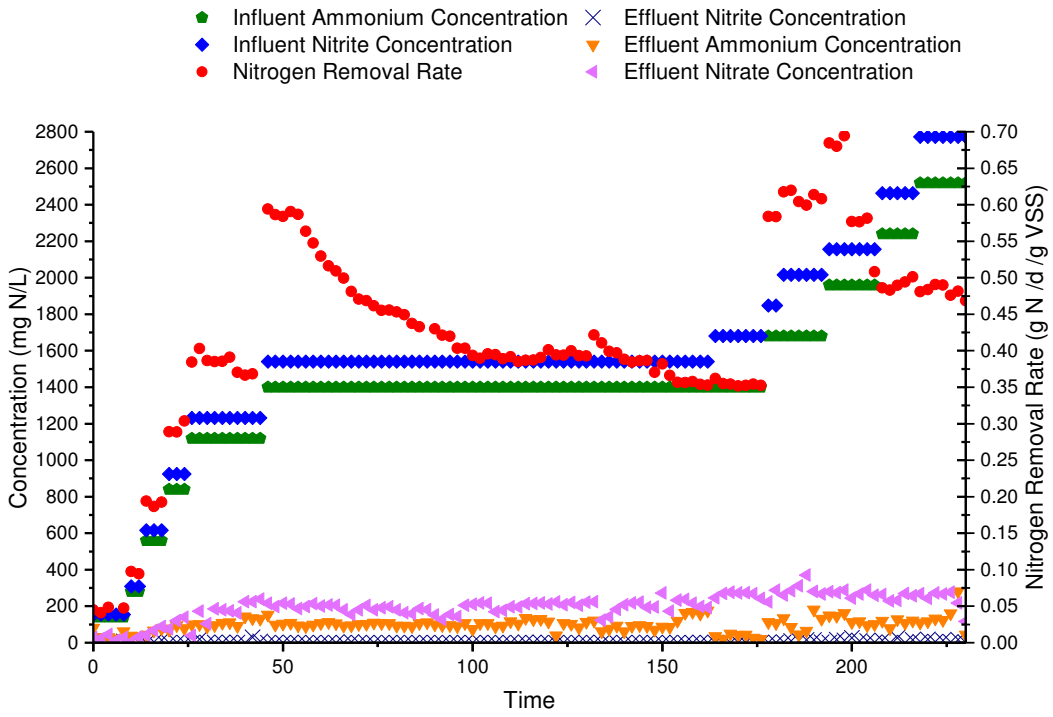


Figure 2.6: Start-up of the ANAMMOX process with influent substrate concentrations increasing gradually.

an SRT of 12-15 days. The sludge was dewatered by adding dewatering polymer (Solenis Praestal 859BS) coupled with centrifuging. The sidestreams were sealed in a plastic drum for storage at 4 °C after been transported from the wastewater treatment plant. Compared with RS, THP-S contained much higher concentrations of NH_4^+-N and chemical oxygen demand (COD). The different dewatering technologies were not linked to the different characteristics of the sidestreams, as equivalent solid capture can be achieved by belt filter press and centrifuge [142, 183]. As a result, the differences of characteristics of sidestreams were the results of different digestion technologies (with/without THP). The characteristics of RS and THP-S were listed in Table 2.3.

According to gel filtration chromatography, the molecular weight distribution of RS was in the range of 4000-447000 Da, while the molecular weight distribution of THP-S was in the range of 2000-100000 Da (Figure 2.10). The weight average molecular weights (MW_w) of RS and THP-S were 48806 Da and 30675 Da, respectively. Three-dimensional EEM fluorescence spectroscopy was carried out to identify the dissolved organic matters properties of RS and THP-S. As shown in Figure 2.11 and Figure 2.12, three peaks for RS can be clearly identified from the EEM fluorescence spectra, while only one peak was identified for THP-S.

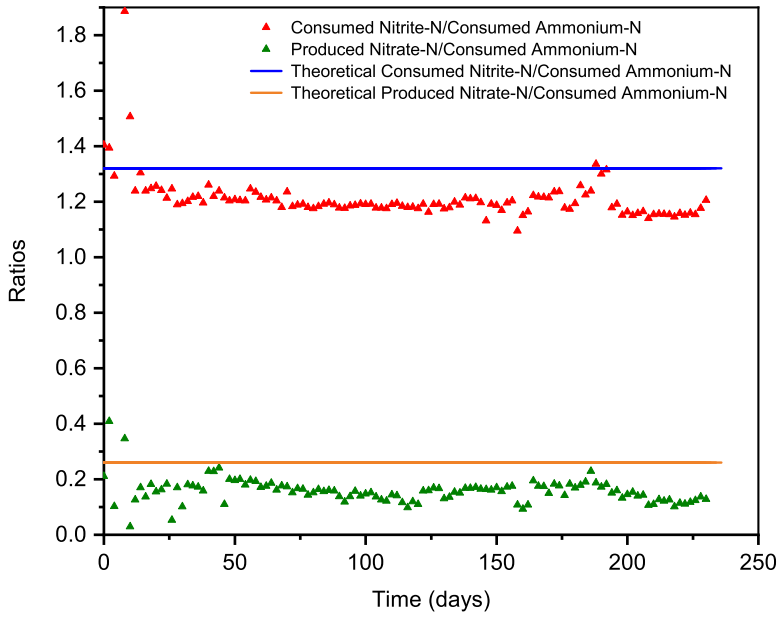


Figure 2.7: The experimental stoichiometric ratios after 270 days of operations.

Peak A was detected in both RS and THP-S, with the excitation/emission (EX/EM) of 400-425/425-450 nm, this peak represented humic acid-like substances, which mostly came from microorganism exudates and were refractory. Peak B was observed at the EX/EM of 320-360/420-460 nm, which was also reported as the humic acid-like peak. Peak C located at the EX/EM of 245-255/450-470 nm was related to fulvic acid-like substances, which was hard to be biodegradable [184, 185]. The lower MW_w and less recalcitrant substances of THP-S indicated that THP effectively improved the biodegradation efficiency of anaerobic digestion, resulting in a higher content of readily biodegradable organic matters. Futhure analysis revealed that THP-S contained higher concentrations of protein and polysaccharides. Similar concentrations of metals were detected in RS and THP-S. The higher concentration of iron in THP-S was caused by overdosing iron-containing coagulants during dewatering (Table 2.4). Acetic acid was the primary volatile fatty acid (VFA) in both RS and THP-S.

Parameters	**Unit**	**RS**	**THP-S**
pH	-	8.0 ± 0.2	8.1 ± 0.2
NH_4^+-N	mg/L	1430 ± 55	1865 ± 325
NO_2^--N	mg/L	< 1	< 0.5
NO_3^--N	mg/L	< 0.5	< 0.5
TP	mg/L	82 ± 7	88 ± 9
Alkalinity as $CaCO_3$	mg/L	3260 ± 230	5600 ± 580
COD (total)	mg/L	696 ± 146	2675 ± 615
COD (soluble)	mg/L	483 ± 137	2046 ± 226
TOC	mg/L	22.9 ± 32.9	851.7 ± 95.3
COD(total)/N	$gCOD/gN$	1.23 ± 0.3	1.5 ± 0.25
COD(soluble)/N	$gCOD/gN$	0.79± 0.21	1.3 ± 0.14
Alkalinity/N molar ratio	-	0.95 ± 0.13	0.6 ± 0.3
Protein	mg/L	241.9 ± 16.9	657.5 ± 47.1
Polysaccharide	mg/L	8.7 ± 1.2	191.3 ± 16.3
MW_w	Da	48806	30675

Table 2.3: Wastewater quality of RS and THP-S.

Metals	**Unit**	**RS**	**THP-S**
Cadmium, Cd	$\mu g/L$	0.56	1.23
Calcium, Ca	mg/L	16.4	16.0
Cobalt, Co	$\mu g/L$	13.8	20.3
Copper, Cu	$\mu g/L$	31.2	30.1
Iron, Fe	mg/L	3.6	107.0
Magnesium, Mg	mg/L	10.1	19.0
Manganese, Mn	$\mu g/L$	58.1	94.8
Molybdenum, Mo	$\mu g/L$	13.8	15.1
Nickel, Ni	$\mu g/L$	16.6	12.8
Potassium, K	mg/L	222	312
Sodium, Na	mg/L	359	253
Zinc, Zn	$\mu g/L$	57	39.3

Table 2.4: Concentrations of metals of RS and THP-S.

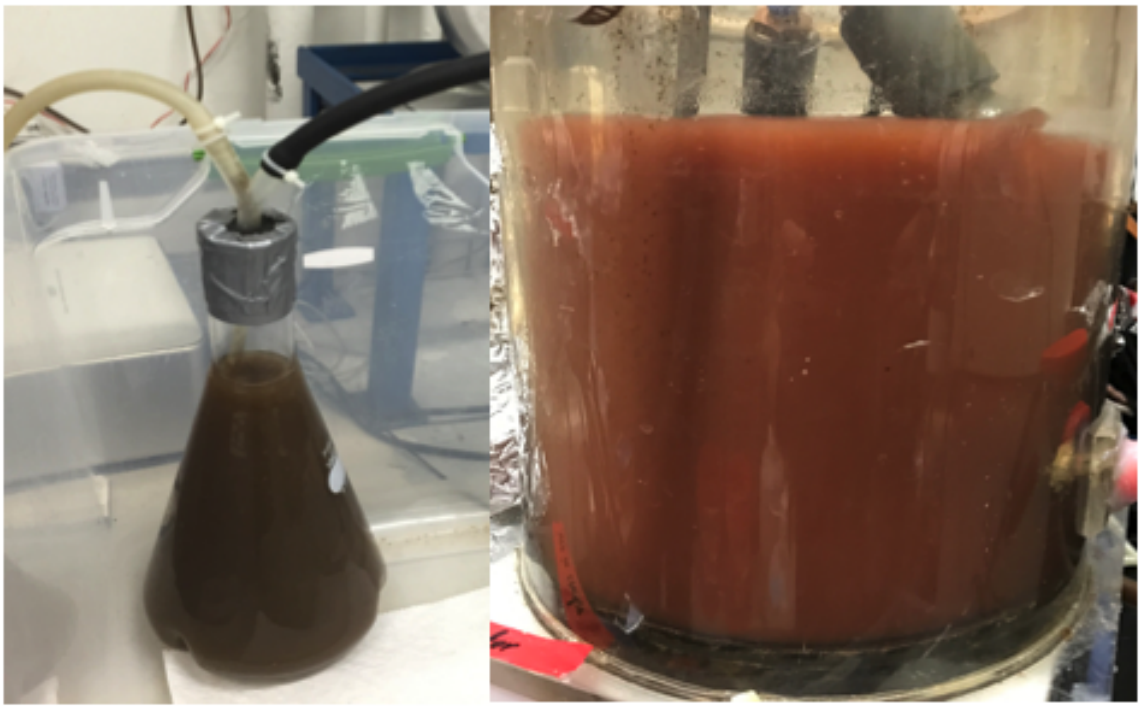


Figure 2.8: The evolution of ANAMMOX biomass at day 0 (left) and day 150 (right).

2.4 Experimental methods

2.4.1 Analytical methods

2.4.1.1 Physical and chemical analysis

NH_4^+-N, NO_2^--N, NO_3^--N and COD were detected using commercial test kits (Hach, USA). The analysis was performed on a designated spectrophotometer (DR2400, Hach, USA). A positive interference of NO_3^--N measurement by Hach was reported at NO_2^- concentration greater than 12 mg/L. As a result, NO_3^--N was also analyzed by an ion chromatograph (ICS). The alkalinity was determined by titrating the sample with sulfuric acid using a digital titrator (AL-DT, Hach, USA). Suspended solids (SS) and VSS was measured according to US standard methods 2540D/E. The concentrations of polysaccharide and protein were measured by the phenol-sulfuric acid method and the Branford method, respectively (Table 2.5).

2.4.1.2 ICS analysis

NH_4^+-N was analyzed on an ICS (ICS-1100, Thermo Scientific, USA) with a Dionex IonPac CS16 IC Column (Dionex, USA). 30 mM methanesulfonic acid was applied as the eluent



Figure 2.9: The picture of thermal hydrolysis process.

solution with the electrolytic suppressor current of 88 mA. Another ICS (ICS-1100, Thermo Scientific, USA) with a Dionex IonPac AS23 IC Column (Dionex, USA) was used for NO_2^--N and NO_3^--N analysis. Carbonate solution with 8 mM of Na_2CO_3 and 1 mM of $NaHCO_3$ were prepared as eluent. The electrolytic suppressor current was set at 25 mA for the analysis of anions. The eluent flow rates for both cation and anion analysis were 1 mL/min.

Before analysis, both columns needed to be washed by eluent for at least 20 mins to achieve a reliable baseline. NH_4^+, NO_2^- and NO_3^- standards were prepared in the range of 0.8-39 mg/L, 0.3-30.5 mg/L and 0.4-22.6 mg/L, respectively. The collected water samples were filtered through 0.45 μm membrane filters and diluted with milli-Q water.

2.4.1.3 Gel filtration chromatography analysis

The molecular weight distributions were studied using a gel filtration chromatography analyzer (GFC, LC-10ATVP, Shimadzu, Japan) with a G4000SW gel filtration column (Tosoh,

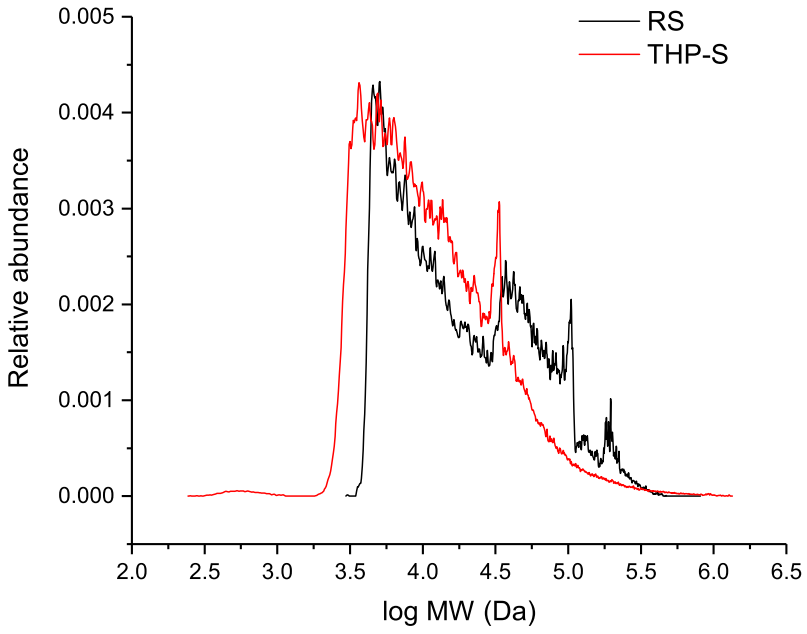


Figure 2.10: Molecular weight distributions of RS and THP-S.

Parameters	**Methods**
pH	HQ40d (Hach, USA), SGD SG98 (Mettler Toledo, USA)
DO	HQ40d (Hach, USA), SGD SG98 (Mettler Toledo, USA)
NH_4^+-N	Salicylate method 10031 (Hach, USA), ICS
NO_2^--N	Diazotization method 10019 (Hach, USA), ICS
NO_3^--N	Chromotropic acid method 10020 (Hach, USA), ICS
TP	Molybdovanadate method 8114 (Hach, USA)
Alkalinity	Tritation (AL-DT, Hach, USA), SM2320B
COD (total)	Digestion method 8000 (Hach, USA), SM5220C
COD (soluble)	Digestion method 8000 (Hach, USA), SM5220D
TOC	TOC-VCPN(Shimadzu, Japan)
Protein	Branford method
Polysaccharide	Phenol-sulfuric acid method
SS	SM2540D
VSS	SM2540E

Table 2.5: Physical and chemical analysis methods.

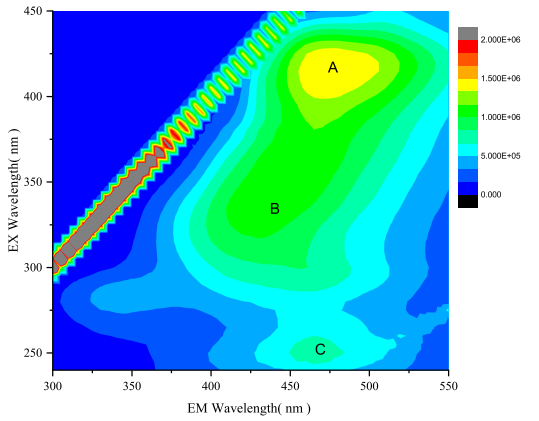


Figure 2.11: EEM fluorescence spectra of RS.

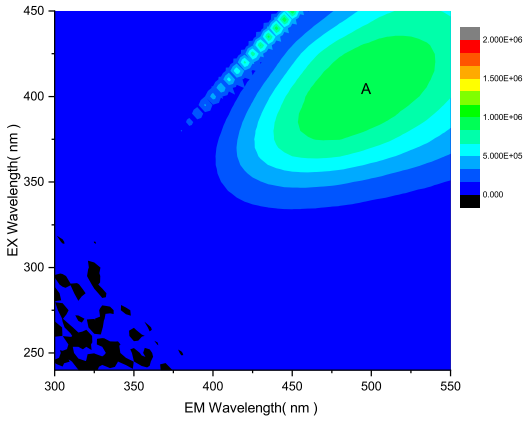


Figure 2.12: EEM fluorescence spectra of THP-S.

Japan). Polyoxyethylene with the molecular weight of 1,215,000 Da, 124,700 Da, 11,849 Da, and 620 Da was applied for establishing the standard curve. The collected water samples were filtered through 0.45 μm membrane filters before analysis.

2.4.1.4 Three-dimensional EEM fluorescence spectroscopy analysis

Three-dimensional fluorescence EEM measurements were conducted using an F-4500FL luminescence spectrometry (Hitachi, Japan) and processed by the software Origin 8.0 (OriginLab, USA). The spectrometer used a xenon excitation source, and the excitation and emission silts were maintained at 10 nm with the scanning speed of 1200 nm/min. To obtain fluorescence EEMs, excitation wavelengths were incrementally increased from 240 nm to 450 nm at 5 nm increments by varing the emission spectra from 300 nm to 550 nm at 5 nm sampling intervals. Distilled water was applied as the blank EEM spectrum samples to ensure the quality of the scanned samples.

2.4.2 DNA extraction and qPCR

Three replicates of 2-mL of biomass mixed liquor were collected on a regular basis. To separate attached biomass from the carriers, the collected carriers were placed into sterile tubes, added with 20 mL of 1 $\times$ PBS and vortexed at maximum speed for 1 min [186]. About 0.2 mg of biomass pellet was gained after centrifuging at 13,000 g for 10 min at 4C. The biomass pellet was washed with 1PBS for 3 times before DNA extraction. PowerSoil DNA Isolation Kit (MO-BIO, USA) was used for DNA extraction by following the manufacturers instruction. DNA concentration and purity were determined by NanoDrop micro-spectrophotometry (ND-1000, Thermo Fisher, USA). DNA samples were stored at -20$^{\circ}C$.

qPCR assay was performed to quantify ammonium oxidizing bacteria (AOB) concentrations by detecting the functional gene *amoA*. Primers amoA-1F (5′-GGGGTTTCTACTGGTGGT-3′) and amoA-2R (5′-CCCCTCKGSAAAGCCTTCTTC-3′) [187] were applied. qPCR assay contained two parts: the establishment of standard curve and real-time PCR.

- The establishment of standard curve

  The standard curve, which can be generated with serial dilutions of a known copy number of the target gene, showed the relationship between *amoA* copy number and threshold cycle (Ct) value. *amoA* gene was amplified by using primers amoA-1F and amoA-2R (Applied Biosystem GeneAmp 9700, USA). The PCR was conducted in a 20 μL reaction mixture that consisted of 1 μL of template DNA, 10 μL of 2 × Taq Plus Master Mix, 0.8 μL of 5 μM forward and back primers, and 7.4 μL of ddH_2O. The PCR protocol for *amoA* amplification was as follows: pre-heating at 95 $°C$ for 5 min, and then 35 cycles of denaturation at 95 $°C$ for 30 s, annealing at 55 $°C$ for 30 s and extension at 72 $°C$ for 1 min. The PCR product was cloned into vector pMD18-T (2692 bp). The constructed plasmid DNA was then introduced into competent cells (DH5α-T1 E.coli, Invitrogen, USA) by the heat shock method. Lysogeny broth(LB) containing antibiotics (100 $\mu g/mL$ of Ampicillin, 0.5 mM of IPTG and 80 $\mu g/mL$ of X-GAL) was added. E.coli was incubated under 37 $°C$ overnight. Colonies were selected according to blue and white spot screening. DNA was extracted from the selected colonies, and the successfully constructed plasmid was confirmed by Sanger sequencing and BLAST. The copy number can be calculated by Eq (2.1), where N was the copy number in $copies/\mu L$, C was the plasmid DNA concentration in $ng/\mu L$ and M was the length of the plasmid in base pair (bp). The standard curve was finally established by doing serial dilutions of the constructed plasmid with the target sequence. Three replicates were prepared for each dilution time.

$$N = \frac{C \times 10^{-9}}{M \times 660} \times 6.02 \times 10^{23} \tag{2.1}$$

- Real-time PCR

  qPCR was performed in a 20 μL reaction mixture that consisted of 2 μL of template DNA, 16.5 μL of 2× AceQ SYBR Green qPCR Master Mix, and 0.8 μL of 5 μM forward and back primers. Three replicates were prepared for each sample. The qPCR protocol for amoA quantification was as follows: denaturation at 95 $°C$ for 5s, annealing at 55 $°C$ for 30s and extension at 72 $°C$ for 40s. The protocol was repeated for 40 cycles. The reactions were carried out in an ABI7500 fast real-time PCR system (Applied Biosystem, USA). Based on the relationship between the copy number of the target gene and Ct value on the standard curve, the gene copy numbers of the samples can be achieved. The cell number of AOB was calculated by the copy number of *amoA* with an average of 2.1 *amoA* genes per AOB cell [188].

2.4.3 Illumia MiSeq 16S rRNA sequencing

Next-generation sequencing (NGS) libraries were prepared for paired-end 300 bp in MiSeq V3 platform (Illumina, USA) at GENEWIZ, Inc. (Suzhou, China) and the California Institue for Quantitative Biosciences (QB3) (California, USA). MetaVx^{TM} library preparation kit (GENEWIZ, USA) was applied. 30-50 ng of DNA template was used to generate amplicons. Forward primers containing the sequence "CCTACGGRRBGCASCAGKVRVGAAT" and reverse primers containing the sequence "GGACTACNVGGGTWTCTAATCC", which aimed at V3 and V4 hypervariable regions of the bacterial and archaeal 16 S rRNA gene, were used for generating amplicons. Moreover, 16S rRNA gene were also amplified using primers 515FB (GTGYCAGCMGCCGCGGTAA) and 806RB (GGACTACNVGGGTWTCTAAT), which was modified from the 515F-806R primer pair [189] and targeted the V4 region of bacterial 16S rRNA gene [190]. The PCR amplification was conducted in a 50 μL reaction system using Platinum Hot Start PCR Master Mix (Thermo Fisher, USA). Reaction conditions were (1) 94 $^{\circ}C$ for 3 min, (2) 94 $^{\circ}C$ for 45 s, (3) 50 $^{\circ}C$ for 60 s, (4) 72 $^{\circ}C$ for 90 s, repeat steps (2)-(4) 30 times and 72 $^{\circ}C$ for 10 min. Additionally, indexed adapters were added to the end of 16S rDNA amplicons for downstream NGS sequencing. Agilent 2100 Bioanalyzer (Agilent Technologies, USA) and Qubit 2.0 Fluorometer (Invitrogen, USA) were used to validate and quantify the DNA libraries. DNA libraries were multiplexed and loaded on an Illumina MiSeq instrument following manufacturers instructions (Illumina, USA), and image analysis and base calling were conducted by the MiSeq Control Software (MCS) embedded in the MiSeq instrument.

The 16S rRNA data was analyzed by QIIME data analysis package. The forward and reverse reads were assembled and assigned to samples according to the barcode. The reads which contained less than 200 bp in length, one or more ambiguous base ('N') and with the mean quality score less than 20 were removed for quality control. The detected chimeric sequences by UCHIME algorithm were removed. Also, the barcode and primer sequence were removed. The filtered sequences were grouped into operational taxonomic units (OTUs) using the clustering program VSEARCH (1.9.6) against Silva 123 database based on the similarity threshold of 97 %. The Ribosomal Database Program (RDP) classifier was applied to assign the taxonomic category to all OTUs at 80 % confidence level. Alpha diversity indexes (ACE, Chao1, Shannon, Simpson and Good's Coverage) and (un) weighted unifrac were calculated and generated using QIIME (1.9.1) software.

2.4.4 Metagenomic analysis

Sequence libraries of 350-bp DNA fragments were prepared and then sequenced by Illumina HiSeq 4000 (paired-end 150 bp). About 10 Gb (giga base pairs) of sequencing data were generated for one sample. Omics raw reads were removed when the ambiguous nucleotides were more than 10% or more than 20% nucleotides had the quality scores of less than 20.

A modified bi-dimension binning process was applied to recover the genomes of dominant species from metagenomic datasets [191]. Contigs grouped by bi-dimension coverage, which

were further clustered by tetranucleotide frequency and paired-end tracking, were extracted from the contig pool as binned genomes. The trimmed paired-end reads were assembled by CLCbio de novo assembly algorithm, using a k-mer of 63 and a minimum contig length of 1k bp. Reads were then individually mapped to scaffolds using CLCbio with a minimum similarity of 95% over 100% of the read length. A genome evaluation software, checkM, was used to evaluate the genome completeness using marker genes [192].

Contigs were submitted to MetaProdigal [193] for the open reading frame (ORF) calling. ORFs were further BLASTx against Kyoto Encyclopedia of Genes and Genomes (KEGG) and NCBI-nr database with an e-value of $1e^5$ for functional annotation. Integration and visualization of KEGG blast results were performed by Pathview [194]. Simultaneously, novel sequences functional prediction was performed by Pfam [195]. Annotation outputs were further manually checked.

Chapter 3

Inhibition of both metabolic activity and growth of ammonium-oxidizing bacteria by sludge thermal hydrolysis

3.1 Introduction

The thermal hydrolysis process (THP) is a promising pre-treatment for the anaerobic digestion (AD). However, the sidestream produced after AD of THP-treated sludge (THP-S) can inhibit the nitritation-ANAMMOX process [178, 182]. Previous work optimized the nitritation-ANAMMOX process with higher dissolved oxygen (DO) set-point and longer aeration time, implying that nitritation process was inhibited by THP-S [182]. To our best knowledge, research on the inhibition of deammonification by THP-S has all been conducted using one-reactor deammonification systems. With this approach, it is difficult to distinguish the specific inhibition kinetics of two processes; therefore, the inhibition kinetic mechanisms of each process remain unknown. The study of inhibition mechanism can provide a reference for process operation and a microbial marker to track process performance. Thus, it is important to also have a good understanding of the inhibition mechanism of nitritation process by THP-S. To study the inhibitory effects of THP-S on an independent nitritation process, sequencing batch reactors (SBRs) were established. The objectives of this study were to 1) identify the inhibitory effects of THP-S on the nitritation process with short-term tests and a long-term study, 2) develop a kinetic microbial inhibition model, 3) investigate the changes in the bacterial community, and 4) determine the inhibition mechanisms by studying the changes in the ammonium-oxidizing bacteria (AOB) growth rate by THP-S.

3.2 Details of Experiments

3.2.1 Long-term nitritation reactor operation with sidestream

The enriched AOB biomass was transferred to two identical 2.5-L SBRs (New Brunswick BioFlo 115, Eppendorf, Germany) treating RS and THP-S respectively. Both of the SBRs were operated under the same conditions as the SBR treating SWW. The sidestream produced directly from AD without THP (RS) or THP-S was gradually introduced to the system with a stepwise increase in the sidestream/synthetic wastewater (SWW) volume ratio. Bicarbonate was added to the influent to create a C: N ratio of 1:1 when the carbon source was limited [25].

3.2.2 AOB inhibition/activity assay

The initial NH_4^+-N removal rates of AOB were analyzed to determine the inhibition of THP-S on AOB activity. Batch tests were conducted using 1 g mixed liquor volatile suspended solids $(MLVSS)/L$ of fresh sludge collected from an SBR treating SWW. To prevent the substrate from affecting AOB activity, $(NH_4)_2SO_4$ was added to the RS to provide it with the same NH_4^+-N concentration as that of THP-S. SWW without nitrogen and carbon sources was used as a dilution buffer, which was used to dilute both RS and THP-S to achieve different initial NH_4^+-N concentrations with different dilution times: 2200 $mgNH_4^+ - N/L$ (no dilution), 1650 $mgNH_4^+ - N/L$ (1.3 times dilution), 1100 $mgNH_4^+ - N/L$ (2 times dilution), 550 $mgNH_4^+ - N/L$ (4 times dilution), 275 $mgNH_4^+ - N/L$ (8 times dilution), 137.5 $mgNH_4^+ - N/L$ (16 times dilution), and 68.75 $mgNH_4^+ - N/L$ (32 times dilution). Batch tests were also conducted using SWW with different initial NH4+-N concentrations as the control group.

To study the inhibition kinetics of THP-S on AOB, batch tests were also conducted with an initial NH_4^+-N concentration of 1100 mg/L by using 1 $gMLVSS/L$ of fresh biomass from the SWW feeding reactor. RS and THP-S were both diluted using the dilution buffer to achieve an initial NH_4^+-N concentration of 1100 mg/L (78% of RS and 50% of THP-S). The diluted RS and THP-S were then mixed in different volume ratios.

To study the long-term effects of THP-S on the AOB community, ex-situ AOB activity tests were conducted while running the long-term reactor with sidestreams. Approximately 1 $gMLVSS/L$ of fresh biomass was collected from both RS/THP-S feeding reactors weekly to perform the batch tests. An initial NH_4^+-N concentration of 550 mg/L was applied for all the ex-situ AOB activity tests.

All batch tests were conducted in 300-mL flasks. The DO was controlled at the saturated level by continuous aeration to ensure that oxygen was not a limiting substrate for the AOB. The temperature was controlled at 37 °C using a water bath. The initial pH of all experiments was controlled at 7.5 by dosing with 5-N HCl and/or 5-N NaOH. The contents of the reactor were mixed by magnetic stirring. During all experiments, samples were taken every 20 min for the first hour, and NH_4^+-N, NO_2^--N, NO_3^--N were measured. The initial ammonium

removal rates (ARR) were calculated based on the consumption of NH_4^+-N. Each test was repeated three times.

3.2.3 Effective maximum specific growth rate estimation

The effective maximum specific growth rate ($\hat{\mu}-b$) was measured according to the exponential increase in NO_x^--N (NO_2^--N+ NO_3^--N) under a high food to mass (F: M) ratio by adopting the model suggested by WERF [196, 197]. The experiments were conducted with fresh sludge collected from the SWW feeding reactor. Three media were prepared for the tests: THP-S, RS with the same substrate level as THP-S, and SWW with the same substrate level as THP-S. To ensure that the carbon source is sufficient, bicarbonate was added to the RS and THP-S. The sludge was agitated by mechanical mixing. A small amount of biomass (approximately 100 $mgMLVSS/L$) was used for the test to create a substrate non-limiting growth environment for the AOB. The temperature was controlled at 37 °C, and DO was controlled at a saturated level. The high NH_4^+-N level of THP-S (approximately 1550 mg/L) resulted in a non-negligible amount of free ammonia (FA), and the potential inhibitor, free nitrous acid (FNA). According to a previous study, FA and FNA inhibit both the anabolic and catabolic processes of AOB. To regulate the levels of FA and FNA, the pH of the tests was precisely controlled within the range of 6.9-7.5. As no inhibition was detected with 16 mg/L of FA, and complete inhibition was observed with 0.4 mg/L of FNA [24], the FA and FNA contents during this test were maintained at approximately 19.5 and 0.2 mg/L, respectively. During the experiment, samples were collected every 3-4 h. NH_4^+-N, NO_2^--N and NO_3^--N were measured. The pH was adjusted according to the concentrations of NH_4^+-N and NO_2^--N. Due to the low product and the substrate concentrations at the beginning and the end of the test, it is impossible to regulate the FNA and FA concentrations to the desired values by adjusting the pH. Therefore, only the data ranging from 400 (or 1150 $mgNH_4^+ - N/L$) to 1100 $mgNO_2^- - N/L$ (or 450 $mgNH_4^+ - N/L$) were used for modeling.

A dual inhibition model was used to correlateNO_x^--N and biomass production [198, 199]:

$$\frac{dS_{NO}}{dt} = -\frac{dS_{NH}}{dt} = \frac{\hat{\mu} X S_{NH}}{Y(K_S\left(1+\left(\frac{S_{FNA}}{K_{I,FNA}}\right)\right) + S_{NH}\left(1+\left(\frac{S_{FNA}}{K_{I,FNA}}\right)+\left(\frac{S_{FA}}{K_{I,FA}}\right)\right))} \tag{3.1}$$

where S_{NO} and S_{NH} are the NO_x^--N and NH_4^+-N concentrations, respectively, $\hat{\mu}$ is the maximum specific growth rate, X is the AOB concentration, Y is the yield coefficient for AOB, K_S is the half-max-rate concentration, S_{FA} and S_{FNA} are the FA and FNA concentrations, respectively, and $K_{I,FA}$ and $K_{I,FNA}$ are the FA and FNA inhibition constants, respectively.

It is assumed that, for a high F:M ratio, the K_S becomes irrelevant because S $\gg K_S$ and the specific growth rate is essentially equal to $\hat{\mu}$. Therefore, the equation can be simplified to:

$$\frac{dS_{NO}}{dt} = \frac{\hat{\mu} X}{Y\left(1+\left(\frac{S_{FNA}}{K_{I,FNA}}\right)+\left(\frac{S_{FA}}{K_{I,FA}}\right)\right)} \tag{3.2}$$

The AOB concentration can be expressed by growth and decay:

$$\frac{dX}{dt} = (\hat{\mu} - b)X \tag{3.3}$$

By integrating equation 3.3, and substituting the result into equation 3.2, the following equation is obtained:

$$\frac{dS_{NO}}{dt} = \frac{\hat{\mu} X_0 e^{(\hat{\mu}-b)t}}{Y\left(1 + \left(\frac{S_{FNA}}{K_{I,FNA}}\right) + \left(\frac{S_{FA}}{K_{I,FA}}\right)\right)} \tag{3.4}$$

where X_0 is the initial AOB biomass concentration. According to the precise pH control, S_{FA} and S_{FNA} are close to constant, and $K_{I,FA}$ and $K_{I,FNA}$ are also constant parameters. Based on a previous study, $K_{I,FA}$ is 3300 μM and $K_{I,FNA}$ is 17 μM [200].

Integrating equation 3.4 yields:

$$S_{NO,t} = \frac{\hat{\mu} X_0}{Y\left(1 + \left(\frac{S_{FNA}}{K_{I,FNA}}\right) + \left(\frac{S_{FA}}{K_{I,FA}}\right)\right)(\hat{\mu} - b)} e^{(\hat{\mu}-b)t} - \frac{\hat{\mu} X_0}{Y\left(1 + \left(\frac{S_{FNA}}{K_{I,FNA}}\right) + \left(\frac{S_{FA}}{K_{I,FA}}\right)\right)(\hat{\mu} - b)} + S_{NO,0} \tag{3.5}$$

where $S_{NO,0}$ is the initial NO_x^--N concentration and $S_{NO,t}$ is the NO_x^--N concentration at any time. With the initial product and biomass concentrations, the second and third terms on the right-hand side of equation 3.5 will be negligible. Taking logarithms then obtains:

$$\ln S_{NO,t} = \ln \frac{\hat{\mu} X_0}{Y\left(1 + \left(\frac{S_{FNA}}{K_{I,FNA}}\right) + \left(\frac{S_{FA}}{K_{I,FA}}\right)\right)(\hat{\mu} - b)} + (\hat{\mu} - b)t \tag{3.6}$$

Consequently, plotting $\ln S_{NO,t}$ against time gives a slope equal to the effective maximum specific growth rate of AOB.

3.3 Results

3.3.1 Short-term tests

Batch tests were conducted to confirm the short-term inhibition of THP-S on AOB (Figure 3.1). Fresh sludge was collected from the nitritation SBR treating SWW. The initial ARRs of the AOB biomass were measured by exposing it to SWW, THP-S, and RS with different concentrations/dilutions. For SWW, the maximum initial ARR was detected when it was exposed to 1100 $mgNH_4^+ - N/L$ and the initial ARR decreased to half of its maximum initial value when exposed to 2200 $mgNH_4^+ - N/L$. This indicates that FA did not inhibit AOB at 52 $mgNH_3/L$ and IC_50 of FA was $105 mgNH_3/L$, which agreed with the previous finding that FA began to inhibit AOB between 10 and 150 $mgNH_3/L$ [25, 78, 198]. The

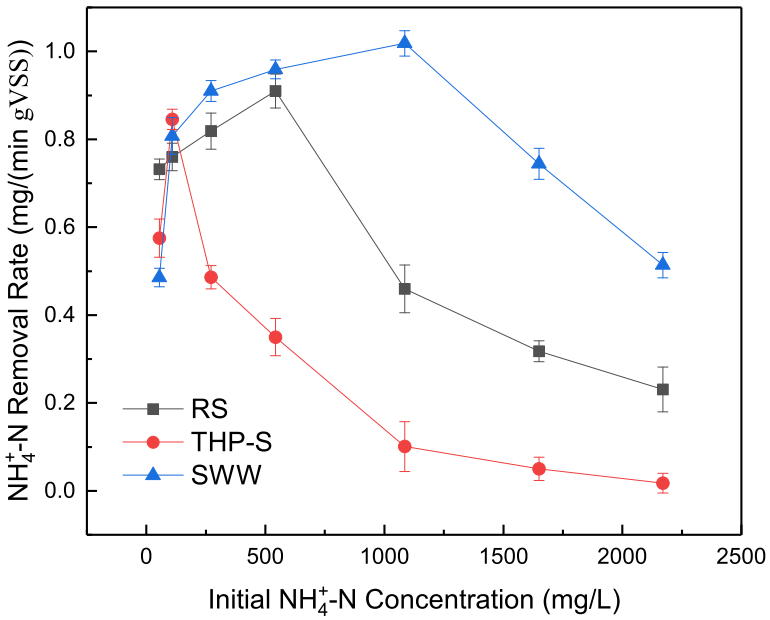


Figure 3.1: Batch tests of AOB activity with SWW, RS, and THP-S.

maximum initial ARR was detected when RS was exposed to 550 $mgNH_4^+ - N/L$ (4 times dilution), and the maximum initial ARR was relatively lower than that for SWW (89 ± 1.5% of SWW maximum initial ARR). A stronger negative effect was observed with THP-S. The maximum initial ARR for THP-S was observed at 137.5 $mgNH_4^+ - N/L$ (16 times dilution), and the maximum initial ARR was 83 3% of that for SWW. As the initial $NH_4^+ - N$ concentration increased and the number of dilutions decreased, the initial ARR for THP-S decreased significantly (10 ± 5% AOB activity remained at 1100 initial $mgNH_4^+ - N/L$). Based on the batch study on SWW, the high initial $NH_4^+ - N$ concentration did not cause inhibition, indicating that specific components of THP-S inhibited the activity of AOB.

To study the inhibition kinetics of THP-S on AOB, batch experiments were conducted to determine the ARR. An initial $NH_4^+ - N$ concentration of 1100 mg/L was used with RS and THP-S mixed in different proportions. The mixed sidestreams were 78% RS, 58.5% RS+12.5% THP-S, 37.5% RS+25% THP-S, 19.5% RS+37.5% THP-S, and 50% THP-S, with average initial ARRs of 0.4594, 0.3934, 0.3416, 0.3031, and 0.2508 $mg/(min \times gVSS)$, respectively. Batch tests without any THP-S were conducted as control tests to assess ARR in the absence of THP-S. Figure 1c shows the adjustment of the kinetic equations with the experimental ARR data obtained by batch tests in the presence of different percentages of THP-S. The inhibition kinetic model, inhibition kinetic coefficients, and the regression

Inhibition model	Equation	Constants	Units	Value
Luong	$\frac{ARR}{ARR_{in absence of THP-S}} = 1 - \left(\frac{Percentage of THP-S^1}{K_{IL}}\right)^n$	K_{IL}	Dimensionless	1.315 ± 0.077
		n	Dimensionless	0.830 ± 0.037

Table 3.1: Kinetic inhibition model and the relevant fitting values.

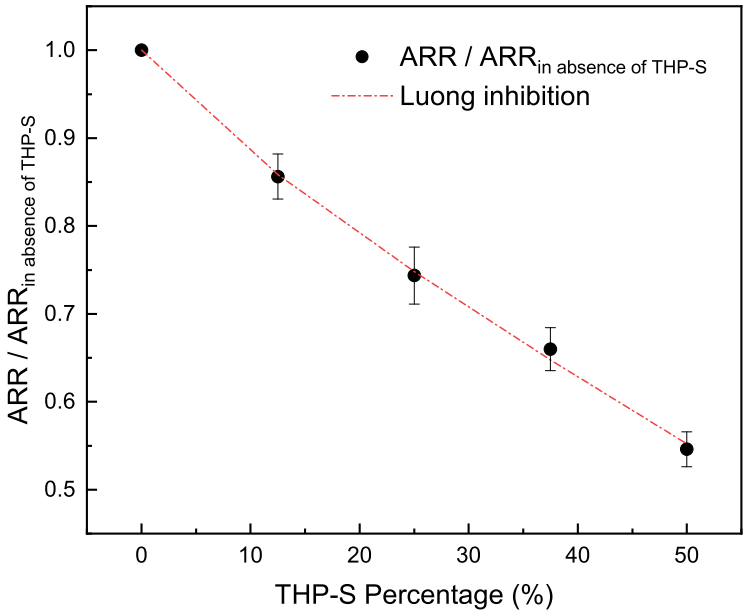


Figure 3.2: THP-S inhibition kinetics on AOB and the kinetic inhibition models.

coefficient (R^2) are shown in Table 3.1, and the Luong inhibition model exhibited the best adjustment (Figure 3.2). The mathmatical model obtained in this study could only be used to describe the relationship between ARRs and percentage of THP-S we got for this study. However, this information can provide reference for predicting the decrease in the AOB activity with the incrase of percentage of THP-S in short-term; therefore, actions can be taken before the total loss of AOB activity.

[1]Percentage of THP-S is calculated as decimal fraction.

3.3.2 The long-term study of THP-S on nitritation process

Figures 3.3a and 3.3b show the nitritation process performance for treating RS and THP-S, respectively. Both RS and THP-S-nitritation SBR systems were successfully established under the same operational conditions with same SWW as the influent. In the RS-nitritation SBR system, as the applied RS/SWW volume ratio gradually increased from 0/100 to 60/40, the conversion efficiency of $NH_4^+ - N$ to $NO_2^- - N$ decreased from 74% to 50%, which was likely due to the incomplete biomass acclimation to the rapid change in the RS/SWW ratio. When the RS/SWW ratio increased to 100/0 and the system had been operated for over three SRTs, more stable nitrite build-up was observed at the average $NH_4^+ - N$ conversion efficiency of 52.76%. The corresponding $NO_2^- - N/\ NH_4^+ - N$ of 1.12 $\pm$ 0.26 was suitable for the subsequent ANAMMOX process. Also, $NO_3^- - N$ production in the system was negligible, indicating that nitritation could be used to treat RS after long-term acclimation. Similarly, the THP-S/SWW volume ratio slowly increased from 0/100 to 100/0 in the THP-S nitritation system. The system operated stably for the first 28 days. However, from day 29, a significant decrease in the accumulation of $NO_2^- - N$ was observed in the system. The decrease in $NO_2^- - N$ in the effluent was not due to NOB conversion, as $NO_3^- - N$ levels remained low in the system. On day 32, the $NH_4^+ - N$ conversion efficiency decreased below 30%, which was likely caused by the inhibitory effects of THP-S on AOB. According to mass balance calculations, the differences were observed between influent nitrogen concentrations and effluent nitrogen concentrations of the THP-S fed nitritation SBR, implying the existence of nitrogen elimination species in the system, possibly denitrifiers. Based on the finding, we can conclude that long-term acclimation could not eliminate the inhibition of THP-S on AOB activity.

3.3.3 Ex-situ AOB activity tests and bacterial community structure study

Figure 3.4a shows the weekly evolution of the activity of the RS-nitritation SBR biomass by measuring ARR ex-situ under optimal conditions. The ARR gradually increased throughout the long-term operation of the RS-nitritation SBR. Although the ARR slightly decreased in week three, which might be due to incomplete biomass acclimation to the rapid increase of RS percentage, the ARR increased by 178.6% in week six. The SBR performance also improved as the $NH_4^+ - N$ conversion percentage increased from 50.5% to 57.1%, and the limited increase in the $NH_4^+ - N$ conversion percentage was due to the limited bicarbonate supply in the influent. To study the changes in the bacterial community structure by feeding RS, the qPCR technique was applied to quantify AOB with amoA as the target gene. Figure 3.4b represents the weekly AOB concentration of the RS nitritation SBR biomass. During long-term operation, the AOB concentration increased from approximately 4.17 E+14 to 1.61 E+15 $cells/gVSS$ as the MLVSS increased throughout the experiment. Compared with week two, 89.5% of the AOB concentration remained in week three; however, as the MLVSS continued to increase over time, the volumetric AOB concentration increased by

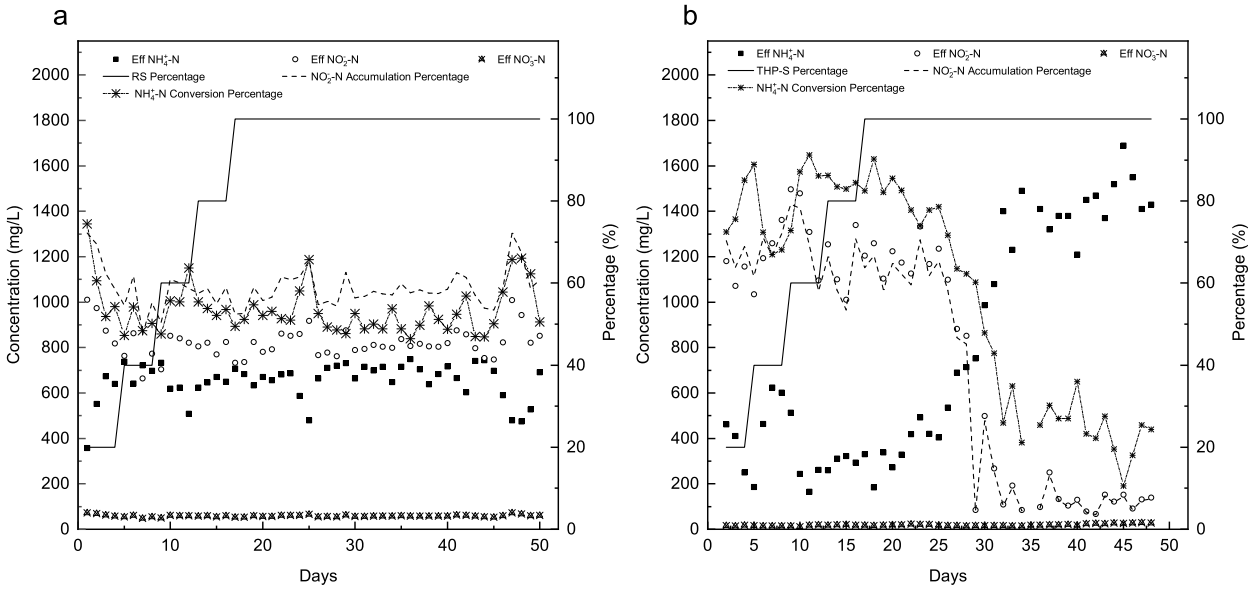


Figure 3.3: Long-term performance of the nitritation SBR with a) RS; b) THP-S.

156%. The clear increase in MLVSS in the system could be due to the growth of AOB together with heterotrophic bacteria caused by the high COD concentration of the RS. To study the effects of THP-S on AOB activity and the relevant changes in the bacterial community, ex-situ batch tests and qPCR were also conducted on the THP-S nitritation SBR biomass. The decrease in ARR began at week three when 100% of THP-S was added to the system, and a sharp decrease in ARR was observed at week four, which resulted in a decrease in the reactor performance of 55% (Figure 3.4c). The average AOB concentration began at 8.00 E+14 $cells/gVSS$. From week three, the AOB concentration began to decrease, and the concentration decreased by 95% at week four. The biomass concentration in the THP-S SBR increased from 3.39 to 6.17 $gVSS/L$ throughout the experiment (Figure 3.4d). The volumetric AOB concentration also decreased by 97.45%, indicating that AOB was outcompeted by other fast-growth bacteria, which most likely include some heterotrophic bacteria. Moreover, the decrease in the activity and abundance of AOB were strongly correlated, indicating that the decrease in the activity of AOB was a result of the decrease in its concentration.

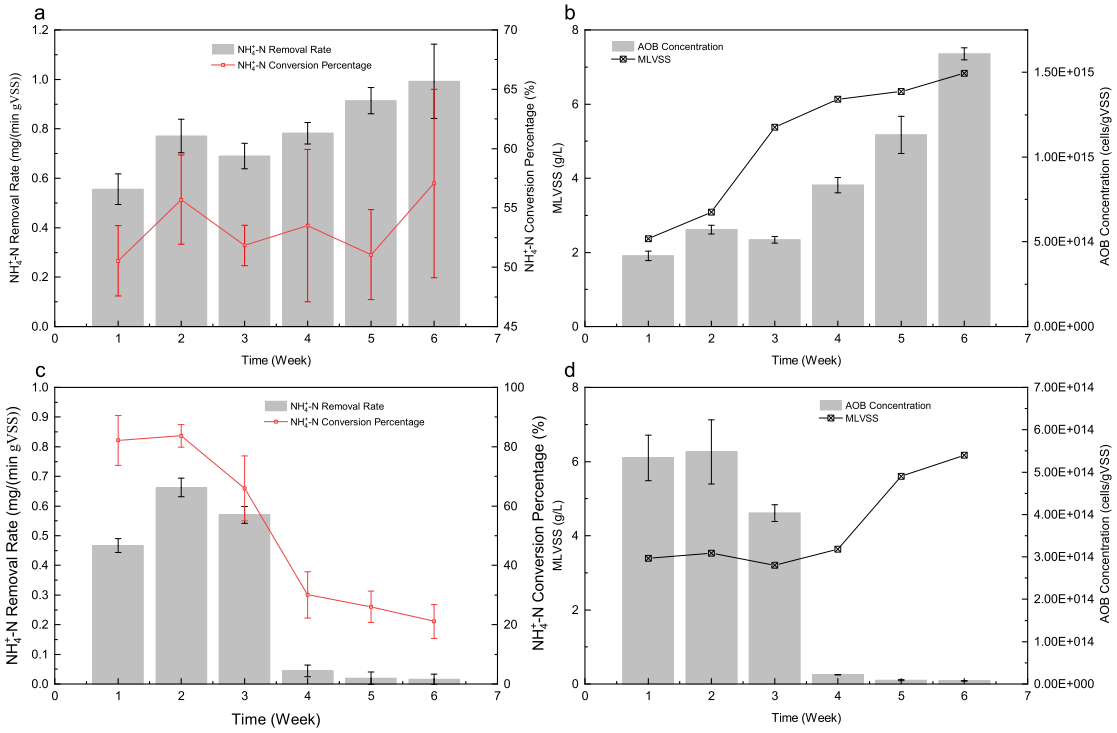


Figure 3.4: Long-term effects of RS on the activity and community of AOB. a) Weekly changes in the AOB activity and the relevant$NH_4^+ - N$ conversion percentage; b) weekly changes in the abundance of AOB and the relevant MLVSS in the system. Long-term effects of THP-S on AOB activity and community. c) Weekly changes in AOB activity and the relevant $NH_4^+ - N$ conversion percentage; d) weekly changes in the abundance of AOB and the relevant MLVSS in the system.

Wastewater	$(\hat{\mu} - b)(d^{-1})$	**Correlation coefficient** R^2
SWW	0.8694	0.9832
RS	0.7742	0.9785
THP-S	0.0684	0.9893

Table 3.2: Effective maximum specific growth rate of AOB in SWW, RS, and THP-S.

3.3.4 Estimation of AOB effective maximum specific growth rate

To study the effects of THP-S on the AOB growth rate, experiments were conducted using high-F: M-ratio batch tests. Typical plots of $\ln NO_3^- - N$ against time are shown in Fig. 4. Linear relationships were obtained for the three types of wastewater. The slope for SWW was determined to be 0.8694 d^{-1} (Figure 3.5a), which is higher than the effective maximum specific growth rate $(\hat{\mu} - b)$ of 0.54 d^{-1} determined by a previous study [201]. The higher $(\hat{\mu} - b)$ discovered in this research might be due to the higher temperature (37 °C) applied during the batch tests, as the optimal temperature for the growth of nitrifiers exceeds 30 °C [202]. Also, the high $NH_4^+ - N$ concentration applied during the establishment of the nitritation process stimulated the domination of fast-growing AOB (r-strategist AOB) [203]. The $(\hat{\mu} - b)$ of AOB in RS was slightly lower than that of SWW (Figure 3.5b). However, the $(\hat{\mu} - b)$ AOB in RS was much higher than the SRT (eight days) applied for the long-term RS-feeding SBR, explaining the clear increase in MLVSS in the system. However, the $(\hat{\mu} - b)$ of AOB in THP-S was less than 10% of that in RS, which required an SRT longer than 14.6 days to prevent biomass washout (Figure 3.5c). The extremely slow growth rate of AOB with THP-S illustrated the reason for the significant decrease in the abundance of AOB in the long-term THP-S-feeding SBR, indicating that AOB growth was significantly suppressed by THP-S and AOB biomass was continuously washed out during long-term operation. $NO_3^- - N$ was barely detected during all experiments, suggesting that NOB was completely inhibited by the high FA and FNA concentrations of the system. The results are summarized in Table 3.2.

3.4 Discussion

THP-S caused a decrease in the AOB activity, and the inhibition could not be eliminated by long-term acclimation. According to the batch tests, lower AOB activity was observed with fewer dilutions of THP-S. Despite the effects of the substrate levels, this finding suggested that THP-S contained a sufficient level of inhibitory compounds to negatively affect AOB activity. The bacterial community study and growth rate kinetics confirmed that THP-S not only inhibited AOB activity but also inhibited their growth. AOB inhibition by THP-S is linked to biodegradable dissolved organic compounds, and the inhibition can be mitigated by treating THP-S through activated carbon adsorption [204]. It was also believed that

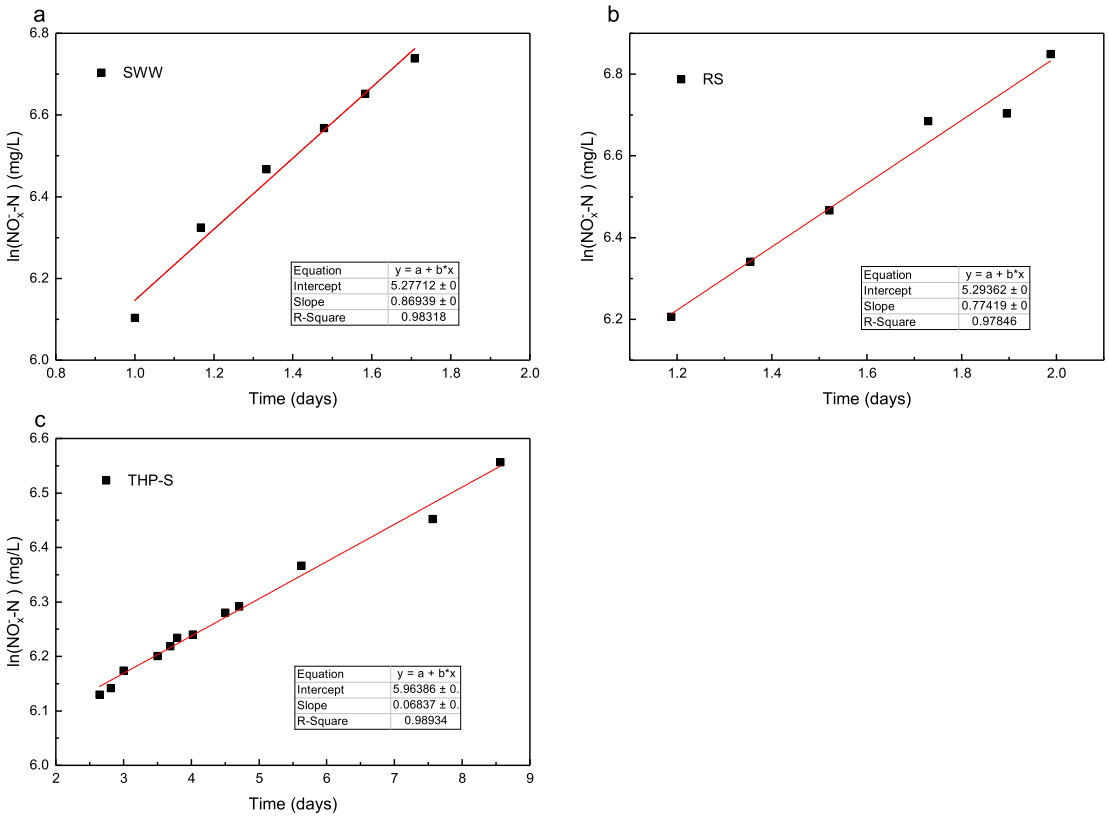


Figure 3.5: Plot of the logarithms of NO_x^--N concentrations against time for a) SWW; b) RS; c) THP-S.

the inhibition of AOB was closely associated with particulate and colloidal organics, as the high level of colloids in the influent might limit the diffusion of substrates and result in a decrease in the activity of AOB [204–206]. Therefore, the development of a robust nitritation process for treating THP-S may benefit from 1) the pre-treatment of THP-S to reduce the concentrations of inhibitors; 2) optimizing the dewatering process to reduce particulate and colloidal organics; 3) extending the SRT of the process to prevent AOB washout. More research needs to be conducted to validate whether the above methods could eliminate the inhibition of THP-S on nitritation in the long-term.

3.5 Conclusion

This study investigated the inhibitory effect of thermal hydrolysis pre-treated sidestream(THP-S) on a separate nitritation process. The activity of AOB was inhibited by THP-S according

to the short-term tests, and the inhibition kinetics fit the Luong inhibition model, which presented a relationship between the decrease in the AOB activity with the percentage of THP-S. The long-term nitritation study with THP-S indicated that long-term acclimation could not prevent the inhibition of AOB activity by the THP-S. Ex-situ AOB activity tests and a study of the bacterial community structure with qPCR indicated a strong correlation between the decrease in the activity and concentration of AOB. The growth kinetics study confirmed that THP-S reduced the AOB effective maximum specific growth rate from 0.77 to 0.068 d^{-1}, which resulted in the washout of AOB from the nitritation process.

Chapter 4

Inhibition of ANAMMOX by sludge thermal hydrolysis and metagenomic insights

4.1 Introduction

Previous studies revealed the sidestream produced with thermal hydrolysis pre-treatment (THP-S) was inhibitory to the one-stage nitritation-ANAMMOX process [178, 182]. Although it is believed that nitritation but not ANAMMOX process was inhibited by THP-S, the effect of THP-S on ANAMMOX process still needs to be elucidated. In previous studies, the ANAMMOX and nitritation processes were operated in one reactor, and it was difficult to distinguish inhibition kinetics specific to each process. Thus, it appears interesting to investigate the specific inhibition of THP-S on a separate ANAMMOX process, which can provide not only a reference for the study of inhibition mechanisms but also a state track to help investigate the microbial evolution with the presence of THP-S. In addition, instead of operating a separate unit for nitritation, which could be intractable to control the nitrite to ammonium ratio in the effluent, providing a relatively precise dosage of nitrite for ANAMMOX might be a practical approach to treat sidestream [207].

Various substrates and chemicals have been found to inhibit the ANAMMOX process, including free ammonia (FA), free nitrous acid (FNA), organic matters, salts, heavy metals, phosphate, and sulfide [73]. Among all inhibitors, the effect of organic matters on the ANAMMOX process was considered to be the key influence of THP-S. Figdore et al. (2011) observed the elimination of inhibition by applying iron precipitants to remove soluble COD [178].

Parts of this chapter are based on the publication: Gu, Zaoli, Yuan Li, Yifeng Yang, Siqing Xia, Slawomir W. Hermanowicz, and Lisa Alvarez-Cohen. "Inhibition of anammox by sludge thermal hydrolysis and metagenomic insights." Bioresource technology 270 (2018): 46-54. Including of this published material has been agreed by all the co-authors.

The mechanism of the effects of COD on the ANAMMOX process could be associated with other heterotrophic pathways in the nitrogen cycle, such as dissimilatory nitrate reduction to ammonium (DNRA) and denitrification. The DNRA pathway is governed by chemoorganoheterotrophic bacteria, which are fast-growing microorganisms and can compete for substrate with ANAMMOX bacteria (AnAOB). DNRA usually starts with nitrate reduction to nitrite, then ammonium, though it may also begin with nitrite [165]. Being more efficient in energy yield compared with denitrification, DNRA pathway was demonstrated to be the dominant pathway of the nitrate/nitrite reduction in the tropical estuarine sediment [169]. The coexistence of DNRA and ANAMMOX has been discovered in marine sediments, lakes, wetland, and coastal ecosystem [166, 167]. The cooperative action between DNRA and ANAMMOX can contribute to enhanced nitrogen removal [170]. However, the occupation of DNRA pathway could out-compete the ANAMMOX process by breaking ammonium to nitrite ratio for ANAMMOX feed, leading to AnAOB washout.

In previous studies, molecular biology approaches were used to reveal microbial community phylogeny, including denaturing gradient gel electrophoresis (DGGE) [208, 209], fluorescence in situ hybridization (FISH) [52, 80]) and sequencing after cloning [94, 210]. However, most of these methods are based on gene amplification, which may cause technical biases [211] and provide limited information about the functional characteristics of cultures [212]. In this study, metagenomic analyses were conducted to reveal community-level functional profiling of the ANAMMOX system.

The objective of this study is to assess the inhibitory effects of thermal hydrolysis process (THP) on the ANAMMOX process. The investigation is based on (a) short-term study on specific ANAMMOX activity; (b) long-term performance of ANAMMOX bioreactor treating RS and THP-S; (c) taxonomic and functional compositions in ANAMMOX communities.

4.2 Details of Experiments

4.2.1 Shock loading assays

A set of shock loading assays were conducted on the 3-L reactor to study the effect of various feed on in situ activity of ANAMMOX microorganisms. Before each test, influent was cut off and $NaNO_2$ was added to lower the concentration of $NH_4^+ - N$ in the reactor to below 0.5 mg/L. Then the reactor was fed with a certain amount of synthetic wastewater with ammonium and nitrite added or sidestream with nitrite added. The $NH_4^+ - N$ and $NO_2^- - N$ consumption rates were examined with both initial concentrations of 100 mg/L. After each shock load which lasted less than 1 hour, the reactor was operated under normal conditions for 3 days to monitor long-term effects of the shock load. Each shock loading assay was repeated for three times.

4.2.2 AnAOB inhibition assay

The short-term responses of the AnAOB to organic stress under the condition of a fixed initial substrate level were performed. Sodium acetate was used as the sole source of organic carbon. Four chemical oxygen demand (COD) concentrations (50, 100, 200 and 500 mg/L) were adopted for test. The initial substrate level was set at 200 $mg-TN/L$ with a $NO_2^- - N$ to $NH_4^+ - N$ ratio of 1. For each experiment, the specific AnAOB activity (SAA = MSCR/VSS, where MSCR is the maximum substrate consumption rate, and VSS is the volatile suspended solids) was recorded to investigate whether the performance of AnAOB was affected by COD addition. The RSAA (relative specific AnAOB activity) was calculated using the equation RSAA = SAA/SAA_{max}, where SAA_{max} is the maximum specific activity among assays.

Four different inhibition models, including non-competitive inhibition kinetic model (Equation 4.1) [213], extended non-competitive inhibition kinetic model (Equation 4.2) and Luong inhibition kinetic model (Equation 4.3) [214], were applied to represent the inhibitory characteristics of COD inhibition on ANAMMOX.

$$RSAA = \frac{K_I}{1 + K_I} \tag{4.1}$$

$$RSAA = \frac{K_I}{I^m + K_I} \tag{4.2}$$

$$RSAA = 1 - (\frac{I}{K_{IL}})^n \tag{4.3}$$

$$\tag{4.4}$$

Where, K_I is the non-competitive inhibition constant, K_{IL} is the Luong inhibition constant, m is the extended constant for non-competitive inhibition, n is the Luong constant, I is the inhibitor concentration.

4.2.3 Reactor operation

Enriched AnAOB was transferred to two identical 1-L submerged MBR reactors treating sidestream without THP pre-treatment (RS) and THP-S respectively. Inert gas with higher CO_2 proportion (90% Ar + 10% CO_2) was selected due to higher alkalinity of the influent. Both RS and THP-S were obtained from a municipal wastewater treatment plant (WWTP) located in Northern California, USA. The sidestream was sealed in a plastic drum for storage at 4 °C after been transported from the WWTP. $NaNO_2$ was added to the influent with a $NO_2^- - N$ to $NH_4^+ - N$ ratio of 1.1. The sidestream to synthetic wastewater (SWW) volume ratio was gradually increased from 0/100 to 100/0 (Figure 4.1). Sludge retention time (SRT) was set at 30 days.

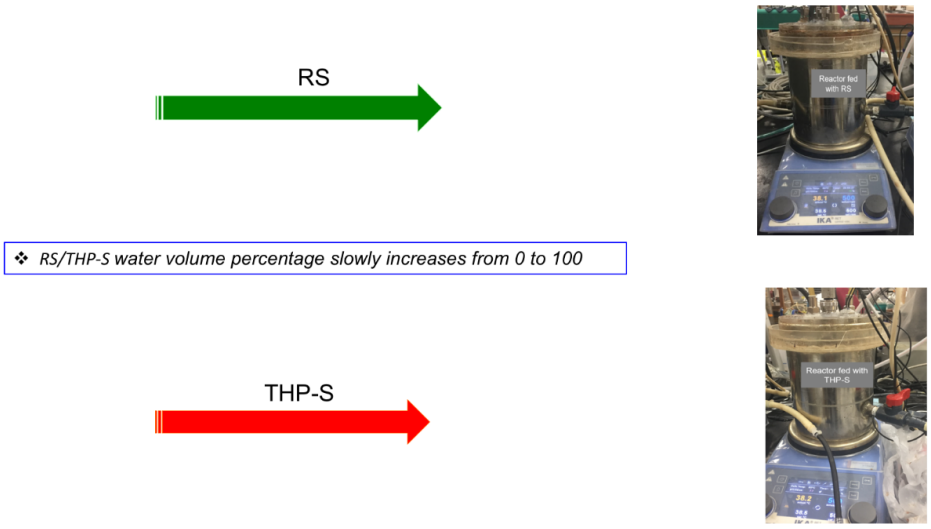


Figure 4.1: The diagram of ANAMMOX MBR fed with RS and THP-S.

4.3 Results

4.3.1 Short-term study

To explore the effect of sidestream on the activity of AnAOB, instantaneous shock load of RS and THP-S was applied. To eliminate the substrate inhibition, three levels of sidestream input (1/20 RS, 1/14 RS, and 1/20 THP-S) were chosen. $(NH_4)_2SO_4$ was added to 1/20 RS so that the initial NH_4^+-N concentration for all input was 100 mg/L. $NaNO_2$ was added with a ratio of NH_4^+-N to$NO_2^- - N$ of 1. The ammonium removal rate (ARR) with the inputs of SWW, 1/20 RS, 1/14 RS and 1/20 THP-S were 26.76, 34.34, 26.04 and 19 $mgN/(h \times VSS)$, respectively. 1/14 RS did not have a notable effect on AnAOB activity, and an increase of ARR was observed under 1/20 RS. 1/20 THP-S caused a decrease of 29% of ARR. A similar trend was observed in short-term AnAOB activity tests by adding different concentrations of COD. With 50 mg/L of COD added, the SAA increased, while the decrease of ARR started from adding 100 mg/L of COD, and the ARR also completely lost with 500 mg/L of COD. The findings implied that the COD in THPS was the inhibitor on AnAOB activity. With the COD/N ratio increased from 0 (SWW), 0.42 (1/20 RS), 0.60 (1/14 RS) to 1.65 (1/20 THPS), the ARR decreased by 29%. The previous study revealed that the ANAMMOX process was inhibited by 20% with the COD/N ratio of 3.1 [215]. On the other hand, it was also reported that a COD/N ratio of 5 didnt affect ANAMMOX performance [216]. The different results might be due to the different testing conditions and the differences between batch tests and continuous flow reactors.

The RSAA at different COD concentrations and the fitting results are shown in Figure 4.3. As shown in the figure, the AnAOB did not show any stress under the shock loading of

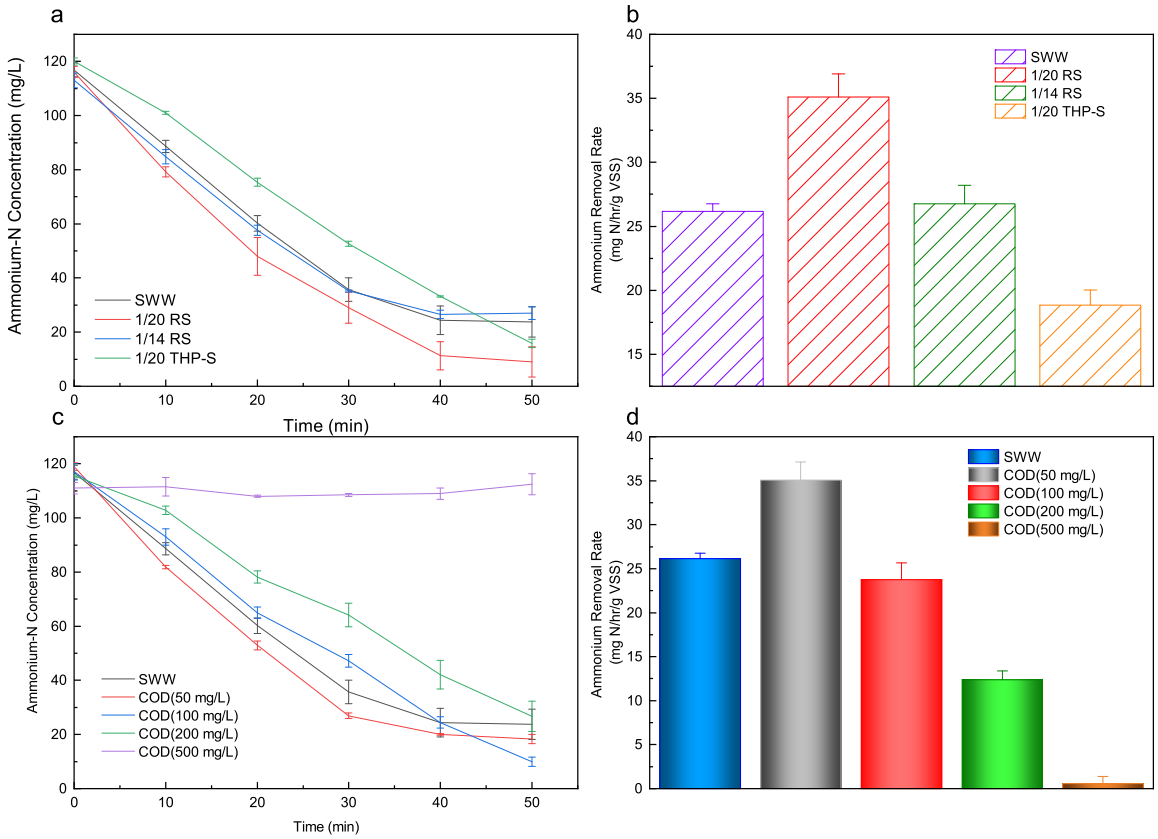


Figure 4.2: a): Ammonium concentration decreased with time with different sidestreams of different dilutions; b): Ammonium removal rate tested with different sidestreams of different dilutions; c): Ammonium concentration decreased with time with different COD concentrations; d): Ammonium removal rate tested with different COD concentrations.

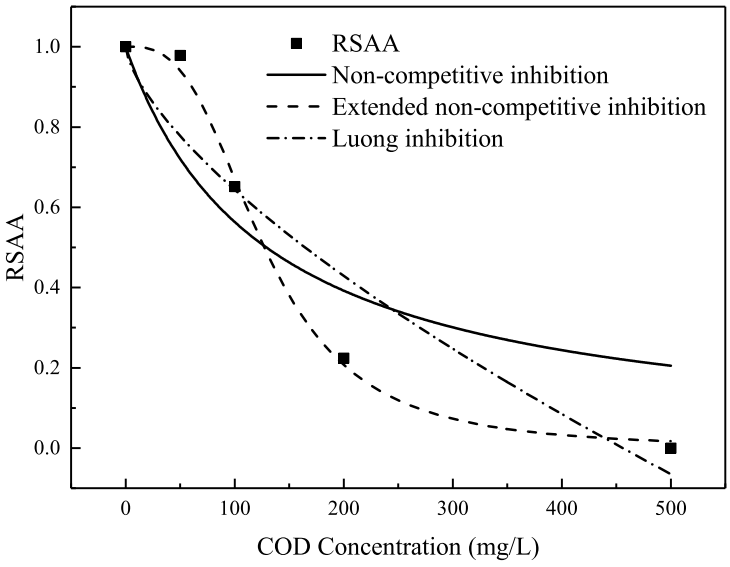


Figure 4.3: RSAA (relative specific ANAMMOX activity) at different COD concentrations.

50 mg/L COD. In fact, in the case of experiments with low COD concentrations, an increase of ANAMMOX performance was observed. This is in accord with previous studies [88, 134], which could be due to the capacity of the AnAOB to carry out organic oxidation simultaneously with anaerobic ammonium oxidation [132]. COD concentrations of 100 mg/L and 200 mg/L resulted in 26 and 74% inhibition percentage. The AnAOB activity completely lost at 500 mg/L of COD. The short-term effects of organic matter on AnAOB activity could be described by the extended non-competitive inhibition kinetic model. The quantitative relationship between the inhibition response and the concentration of COD could be expressed by the following Equation:

$$RSAA = \frac{2.95156 \times 10^6}{I^{3.06099} + 2.95156 \times 10^6} \tag{4.5}$$

4.3.2 The long-term study

Two identical 1-L MBR reactors were inoculated with the same cultivated sludge and operated in parallel. The reactors were fed the diluted RS and THP-S, respectively. The percentage was increased periodically when the reactors reached stable stages. pH was controlled at 7.2 $\pm$ 0.2 by adding hydrochloric acid.

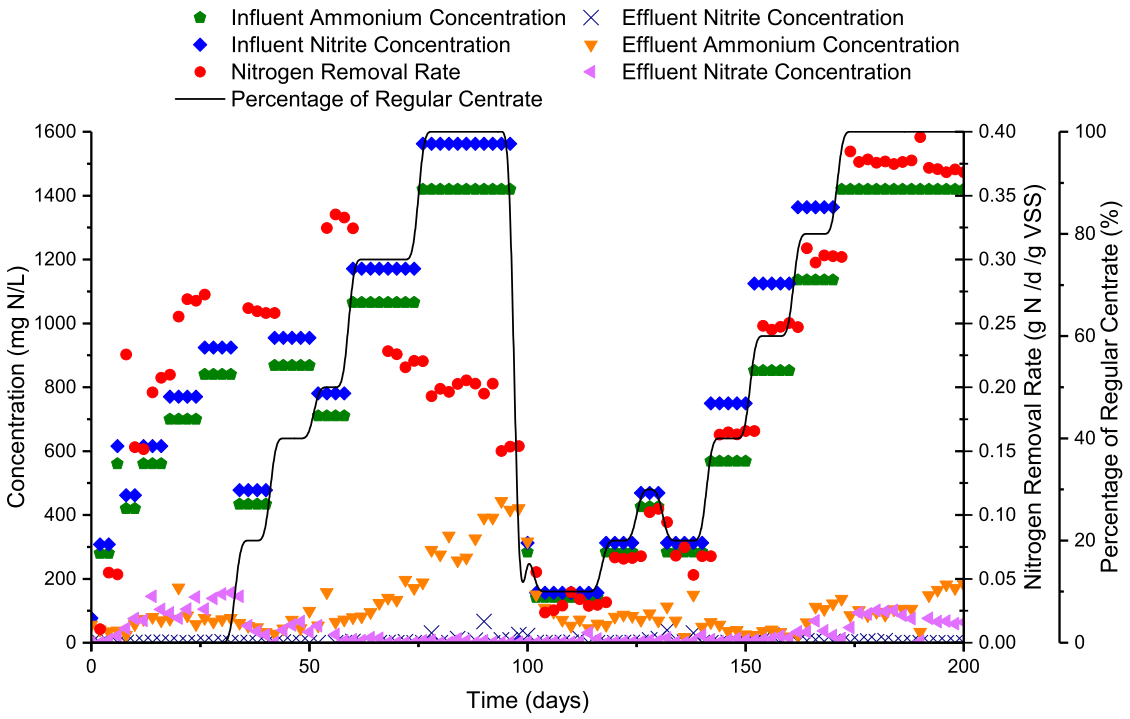


Figure 4.4: Performance of ANAMMOX MBR fed with RS.

The performance of MBRs fed with RS and THP-S is represented in Figure 4.4 and Figure 4.6, respectively. As shown in Figure 4.4, the diluted RS was used beginning from 34 d at an influent concentration of $NH_4^+ - N$ that was diluted to 434 mg/L. The load was increased in steps to undiluted sidestream. The increase of load led to a moderate increase of effluent $NO_2^- - N$ concentration, which was gradually reduced when the system was operated for some time after the load increased. The achieved volumetric nitrogen loading rate was 3.64 $kg/(m^3 \times d)$, and the removal efficiency of TN was above 90% with 100% RS influent feeding. The results suggested that the microorganisms gradually adapted to the RS, and the ANAMMOX process was successful for the undiluted RS. In addition, $NO_3^- - N$ did not massively accumulate, and the ratio of produced $NO_3^- - N$ to consumed $NH_4^+ - N$ was in the range of 0.013 to 0.076 (Figure 4.5) that was much lower than the system with SWW. This indicated the increased presence of DNRA or denitrification in the system fed with RS.

In the meanwhile, the reactor fed with diluted THP-S experienced similar operational phases (Figure 4.6). However, inhibition was observed starting with 70% THP-S feeding. The $NH_4^+ - N$ and $NO_2^- - N$concentration in the effluent increased rapidly and synchronously, which marked the washing-out of biomass. The maximum volumetric nitrogen loading rate was 3.40$kg/(m^3 \times d)$, lower than that of RS. Also, the ratio of produced $NO_3^- - N$ to consumed

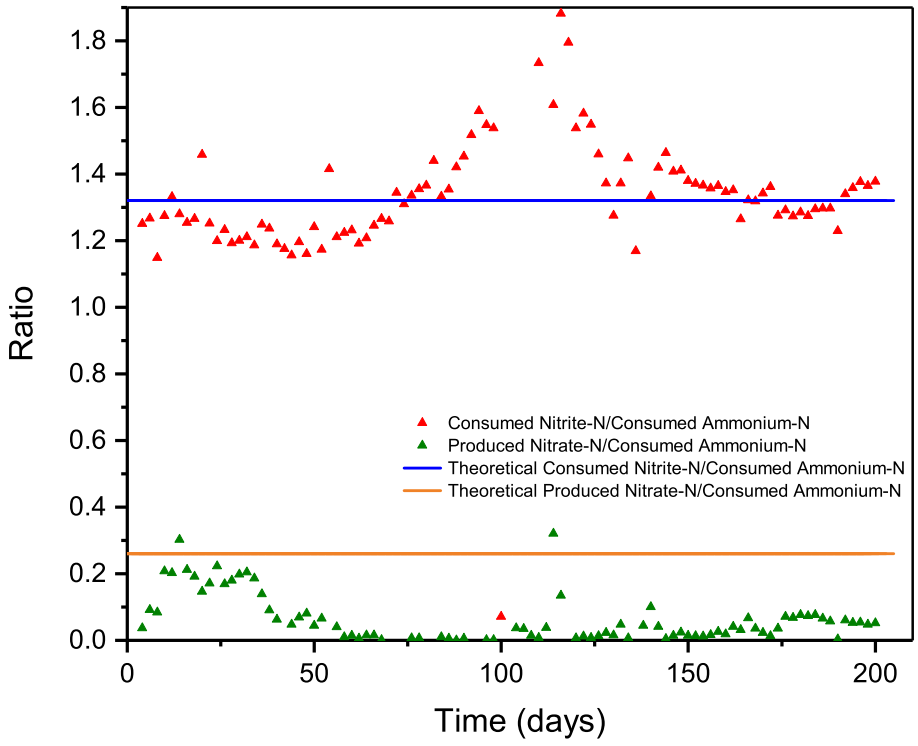


Figure 4.5: The stiochiometric ratios of ANAMMOX MBR fed with RS.

$NH_4^+ - N$ was around 0.01, lower than which of the system with RS feeding (Figure 4.7). The results stated that the inhibition was not caused by the substrate level, while it could be attributed to the high content of organic carbon in THP-S, which led to the growth of heterotrophic bacteria. The long-term study illustrated that long-term acclimation could not eliminate the inhibition of ANAMMOX by THP-S.

4.3.3 Microbial structures analysis

Six DNA samples were collected from the reactors treating SWW, RS, and THP-S. For each reactor, biomass samples were collected at two time points in the late phase of the experiments. A total of 2787863 effective sequences were obtained from 6 samples, which were clustered into 1392 OTUs at a distance of 0.03. The bacteria coverage described as the Good's value was between 99.80% and 99.97%, so the sequencing depth was sufficient to describe patterns (Table 4.1). Shannon, Ace, and Simpson diversity indexes were applied

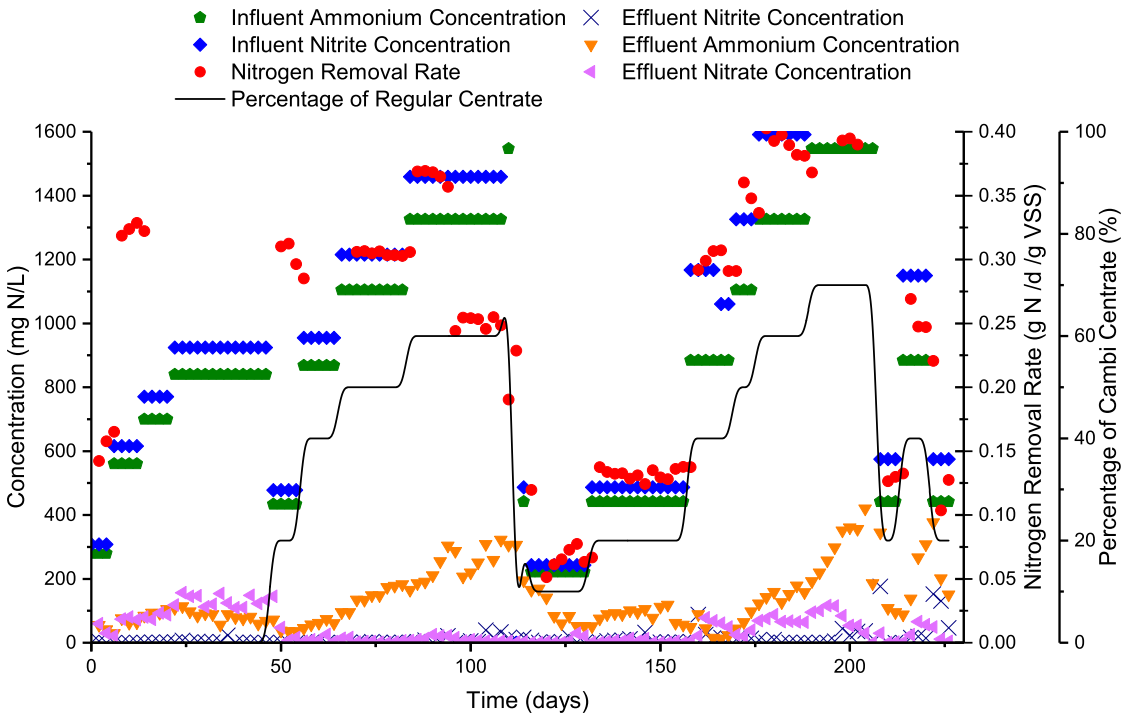


Figure 4.6: Performance of ANAMMOX MBR fed with THP-S.

to analyze the community richness and diversity (Table 4.1). These results demonstrated that the RS and THP-S samples had more community richness and diversity compared with SWW samples, because of the complex composition of sidestream. Figure 4.8 illustrates the phylum level distributions of bacterial sequences. The structures of microbial communities were significantly different across samples, and there was an obvious distinction between SWW and real wastewater communities. The phyla of *Proteobacteria* (47.4% - 51.3% of the identified 16S rRNA gene fragments) and *Planctomycetes* (31.5% - 36.8%) were dominant in SWW samples, while *Proteobacteria* (19.2% - 27.2%), *Bacteroidetes* (16.7% -30.1%) and *Ignavibacteriae* (17.6% - 21.9%) were dominant in both RS and THP-S samples. The average relative abundance of *Planctomycetes* in RS and THP-S samples were 7.95% and 3.20%, respectively. Previous studies reported that uncultured members of the phyla *Proteobacteria*, *Bacterioidetes*, *Chlorobi* and *Chloroflexi* are omnipresent in ANAMMOX bioreactors besides *Planctomycetes* [217, 218]. *Ignavibacteriae*, affiliated with *Chloroflexi*, are also frequently found in ANAMMOX reactors [216].

A total of 582 microbial genera were detected in six samples. The relative abundances of different genera and the phylogenetic tree were presented in Figure 4.9. The *Candidatus Brocadia* was the major AnAOB species in the system with the abundance of 35.9% (SWW_1),

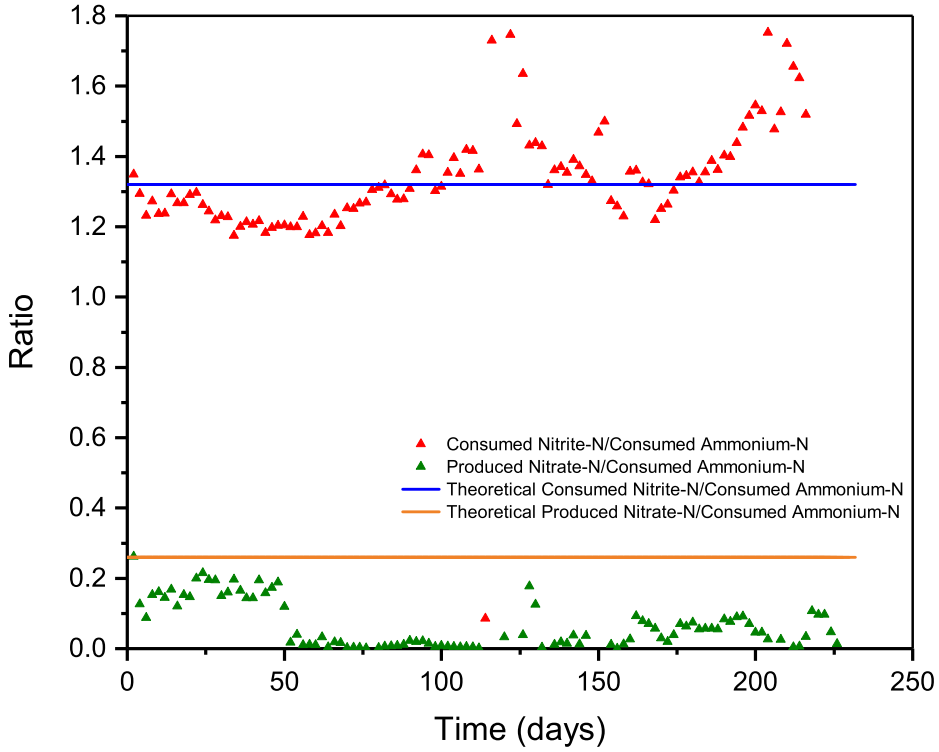


Figure 4.7: The stoichiometric ratios of ANAMMOX MBR fed with THP-S.

Sample	Sequence	Shannon	Simpson	Ace	Chao1	Coverage
SWW_1	440883	1.935351	0.283004	294.1963	286.2069	0.999689
SWW_2	554262	1.984516	0.281352	407.8227	418.3438	0.999593
RS_1	372980	3.884917	0.068093	1284.34	1301.162	0.998044
RS_2	439706	4.002663	0.056955	1211.569	1274.124	0.998398
THP-S_1	460097	3.451653	0.078091	863.9655	802.3684	0.998965
THP-S_2	519935	3.557315	0.068544	973.1314	872.7143	0.9987

Table 4.1: Number of sequence and estimated diversity indices.

ID	Completeness	Contamination	Genome size	Longest conting
102-*Proteobacteria*	98.37931034	5.205938697	3011495	102800
106-*Proteobacteria*	98.25949367	2.215189873	3692182	3413563
113-*Planctomycetes*	96.59090909	0	3376503	256355
115-*Planctomycetes*	98.9010989	1.648351648	3018561	268974
117-*Proteobacteria*	99.33127572	3.209876543	3459507	117234
119-*Deinococcus-Thermus*	90.04237288	1.200564972	2885193	188468
124-*Kryptonia*	43.10344828	0	1453824	177305
125-*Ignavibacteriae*	96.64804469	0.391061453	3552762	165826
127-*Bacteroidetes*	82.5136612	0.364298725	2054384	243136

Table 4.2: Summary of bin-genome reconstruction from metagenomes.

30.7% (SWW_2), 8.30% (RS_1), 4.35% (RS_2), 2.36% (THP-S_1) and 1.94% (THP-S_1), followed by SM1A02 (<1% in all samples). It was reported that *Candidatus Brocadia* was more competitive than other AnAOB in the presence of acetate [38, 219], and it was also found that the dominant *Candidatus Brocadia* did not contribute much to acetate oxidation [220]. The reactor also fostered a fairly high level of denitrifying bacteria, and the most predominant denitrifying bacteria were classified into the genus of *Denitratisoma*. The abundances of *Denitratisoma* in SWW_1, SWW_2, RS_1, RS_2, THP-S_1 and THP-S_2 were 39.2%, 43.1%, 0.591%, 0.569%, 3.02% and 2.73%. The observation was coincident with the study of Bae et al. (2010), which reported that the most predominant bacteria in the ANAMMOX UASB reactor were affiliated with *Denitratisoma oestradiolicum* (40%). Notably, the bacterial communities were diverse in the RS reactor with only 4.35% - 8.30% of *Candidatus Brocadia*, though high efficiency of $NH_4^+ - N$ and $NO_2^- - N$ removal was obtained. Furthermore, there was a sharp drop of denitrifier abundance in the community compared to SWW samples as well. It can be inferred that due to the lower growth rate of AnAOB (yield coefficient of 0.066 ± 0.01 g VSS/g $NH_4^+ - N$) [32], other heterotrophic bacteria, i.e., DNRA bacteria, multiplied with the application of sidestream influent.

4.3.4 Metagenomic analysis

A total of 392 884 712 reads from the samples metagenomes were filtered out after quality control and dynamic trimming, with an average length of 150 bp. Using de novo assembly, 451 Mbp of contigs with an average length of 4.4 Kbp were obtained. The coverages of the assembled contigs for the samples metagenomes were between 92.4% and 96%, which indicate a reliable accuracy of the de novo assembly. In total, 127 metagenome bins were retrieved, and 9 metagenome bins with relatively high coverage and long contig length were subjected to further analysis (Table 4.2). The bins were functionally annotated using the Kyoto Encyclopedia of Genes and Genomes (KEGG).

Among 9 metagenome bins, 115-*Planctomycetes* was discovered to have a complete

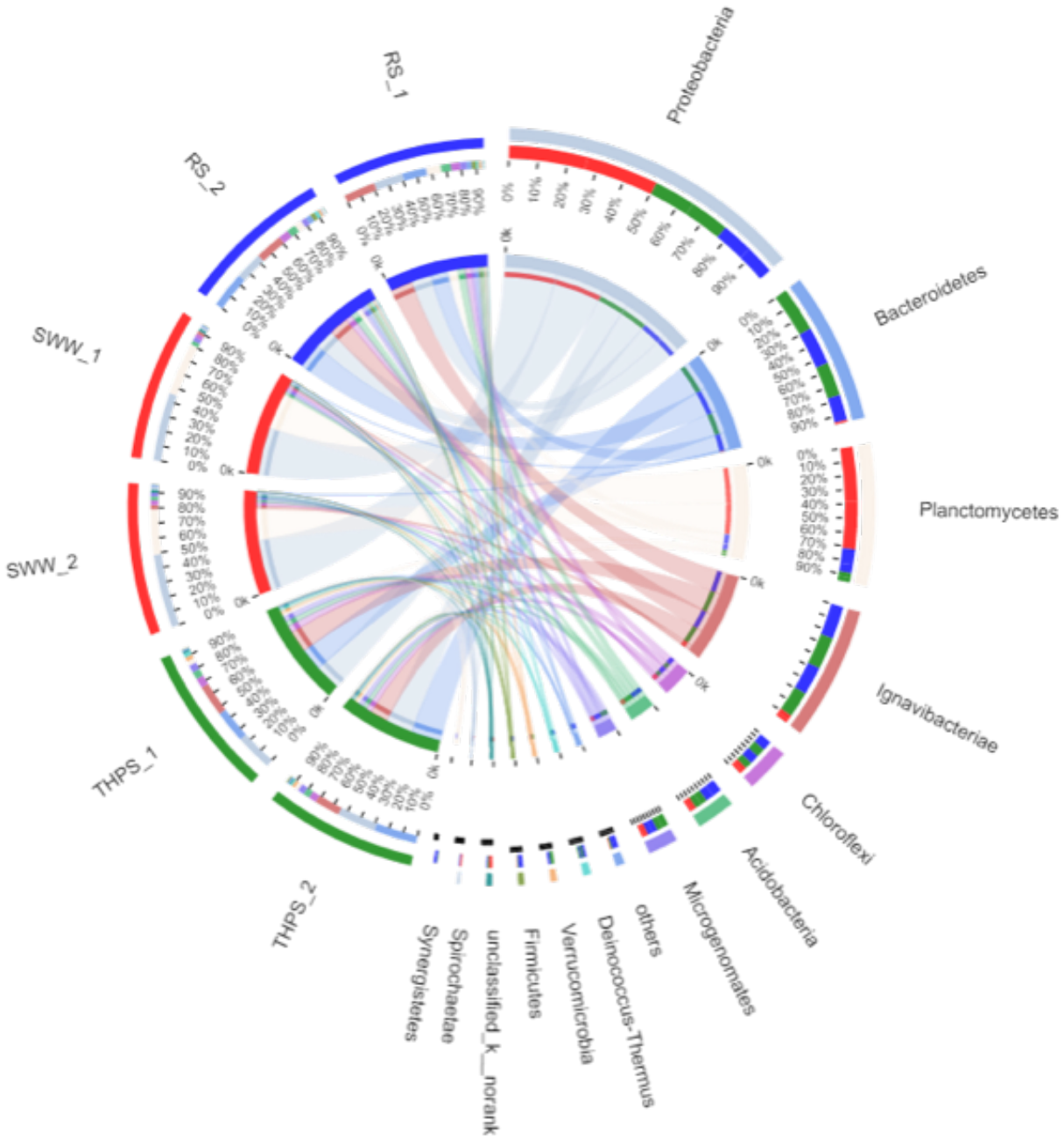


Figure 4.8: Relative abundances of detected phyla in the six samples. The data were visualized via Circos software [221].

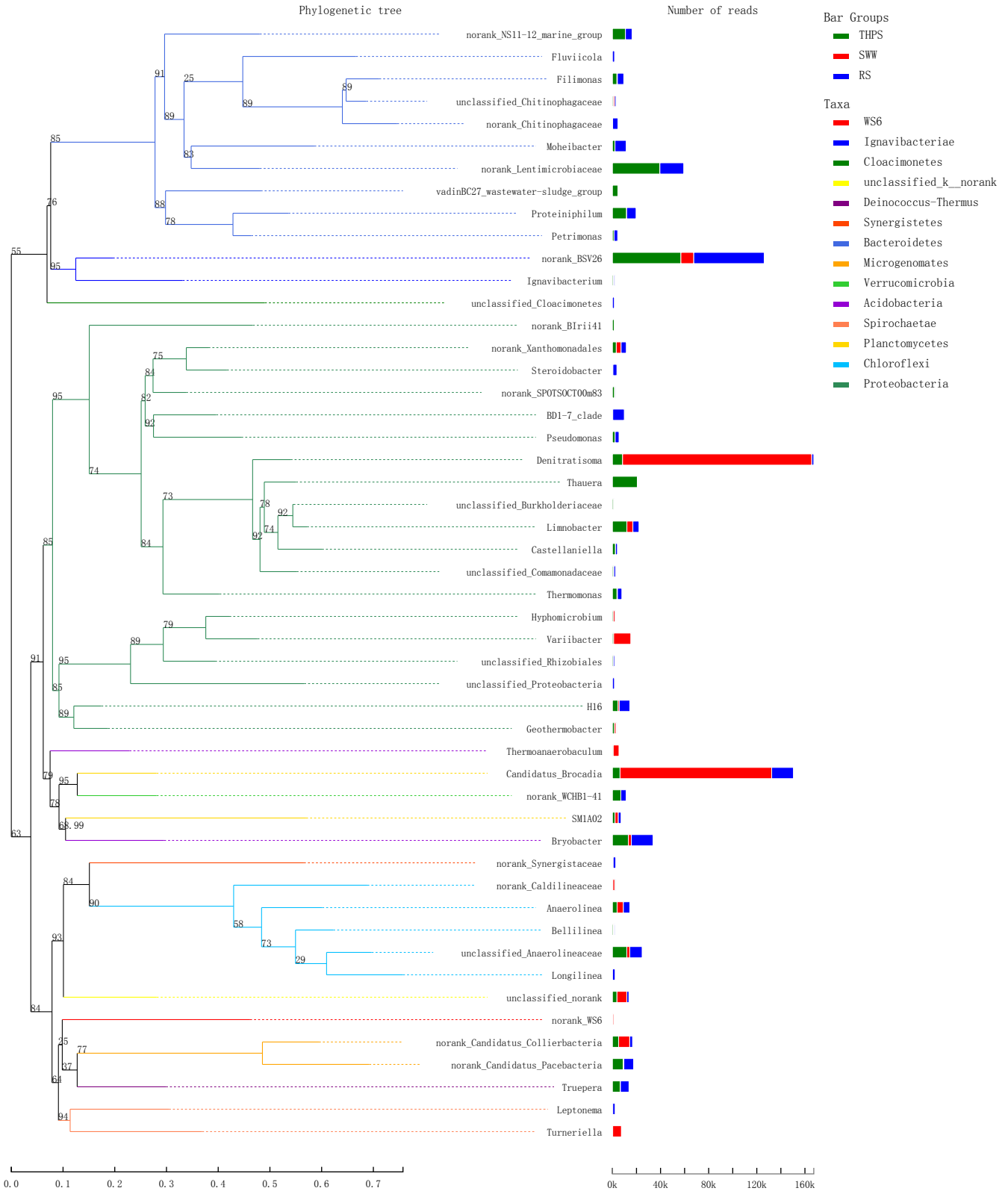


Figure 4.9: Sequences assignment results at the genus level.

ID	$\mathbf{SWW_1}$(%)	$\mathbf{SWW_2}$(%)	$\mathbf{THP\text{-}S_1}$(%)	$\mathbf{THP\text{-}S_2}$(%)	$\mathbf{RS_1}$(%)	$\mathbf{RS_2}$(%)
102-*Proteobacteria*	0.074	0.069	0.587	1.122	0.638	0.794
106-*Proteobacteria*	2.482	2.439	0.361	0.590	0.522	0.441
113-*Planctomycetes*	0.497	0.399	0.758	0.357	0.340	0.412
115-*Planctomycetes*	35.446	30.550	5.227	6.849	1.183	0.996
117-*Proteobacteria*	21.761	22.483	2.329	2.845	7.830	7.898
119-*Deinococcus-Thermus*	0.005	0.006	1.303	1.774	1.303	0.846
124-*Kryptonia*	1.490	1.789	14.832	12.360	10.931	9.091
125-*Ignavibacteriae*	18.512	18.778	16.907	17.823	15.633	15.659
127-*Bacteroidetes*	6.046	8.027	41.085	40.999	53.349	53.173

Table 4.3: Abundances of metagenome bins in the six samples.

ANAMMOX pathway, which contained the key ANAMMOX enzymes, including hydrazine synthase (HZS) and hydrazine dehydrogenase (HDH). It is notable that 115-*Planctomycetes* also contained a DNRA pathway, which indicated AnAOB can be rather versatile in their metabolisms (Figure 4.10) [165]. However, due to the limited metabolic pathway of organic carbon, DNRA could be an alternative pathway for AnAOB (Figure 4.11). In addition, there was a complete B12 synthetic pathway in 115-*Planctomycetes*, which was not found in other abundant metagenome bins. It indicated that AnAOB could be the source of B12 for other bacteria. The DNRA pathway was also discovered in many metagenome bins, including 106-*Proteobacteria*, 124-*Kryptonia* and 127-*Bacteroidetes*. 117-*Proteobacteria* and 119-*Deinococcus-Thermus* are related to denitrification. 125-*Ignavibacteriacea* is related to the degradation of starch, sugars, and peptides and thus involved in COD removal. 124-*Kryptonia* contains key metabolic enzymes for Embden-Meyerhof glycolysis and the pentose phosphate pathway. The abundances of metagenomes for the six samples were presented in Table 4.3. As shown, the percentage of 115-*Planctomycetes* in SWW_1, SWW_2, RS_1, RS_2, $THP\text{-}S_1$ and $THP\text{-}S_2$ were 35.446%, 30.550%, 5.227%, 6.849%, 1.183% and 0.996%, which was in line with the 16S results. The average abundances of metagenomes associated with DNRA in SWW, RS, and THP-S samples were 11.137%, 54.614% and 63.753%, respectively. The results implied that DNRA was one of the major pathways in the system. The DNRA bacteria more populated in the system with THP-S fed compared with RS.

Both DNRA and denitrification processes can be coupled with ANAMMOX for its NH_4^+ requirements. It was reported that DNRA should have certain competitive advantages over denitrifiers in nitrate-limiting and organic-rich settings [165, 169]. The co-existence of DNRA and ANAMMOX in the reactor illustrated the synergetic association for nitrogen removal. However, the overpopulation of DNRA bacteria could out-compete AnAOB by breaking ammonium to nitrite ratio for ANAMMOX feed, leading to the washing-out of AnAOB, which may elucidate the crash of the THP-S reactor(Figure 4.11).

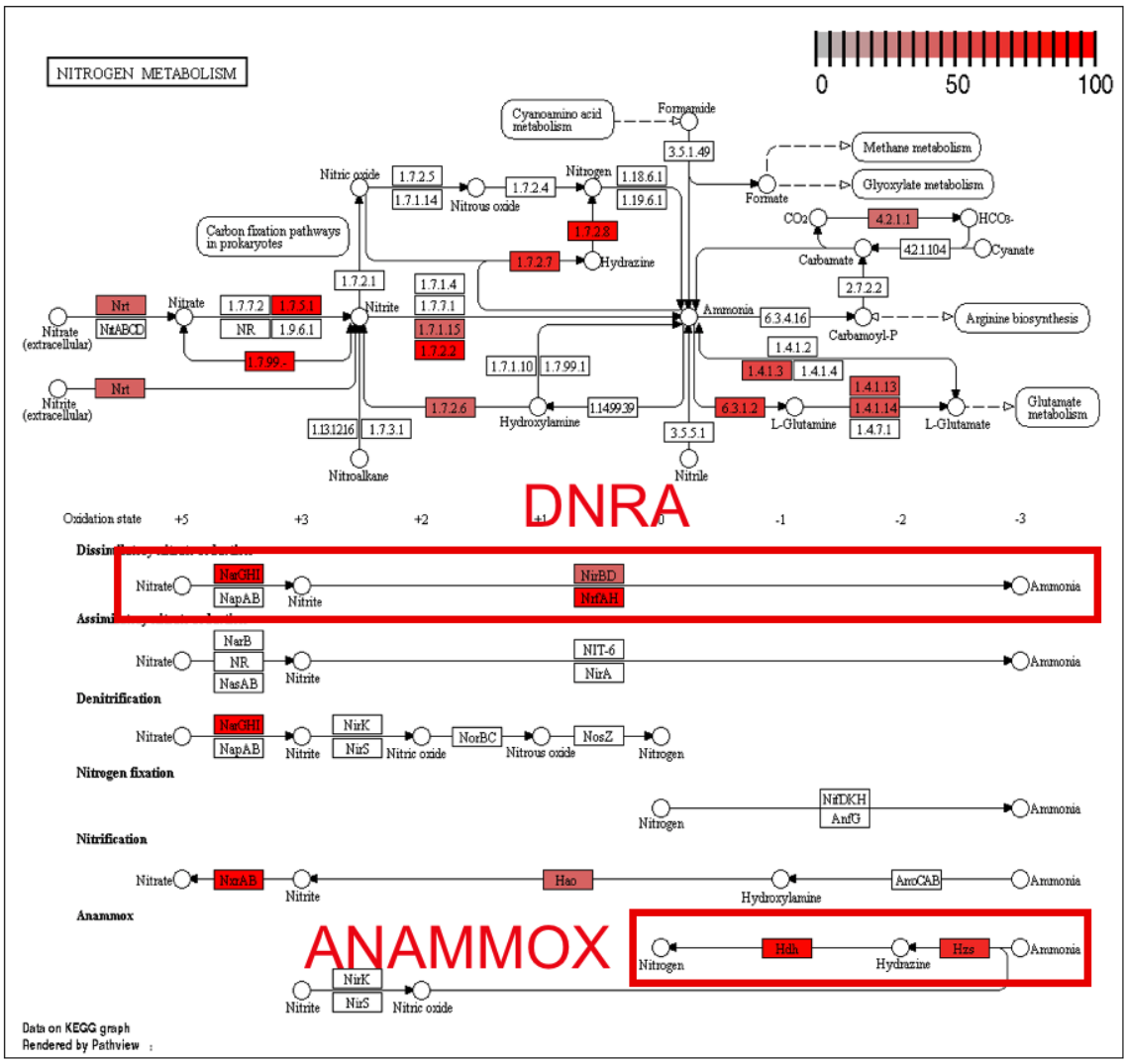


Figure 4.10: Nitrogen metabolism pathways of 115-*Planctomycetes* genomes.

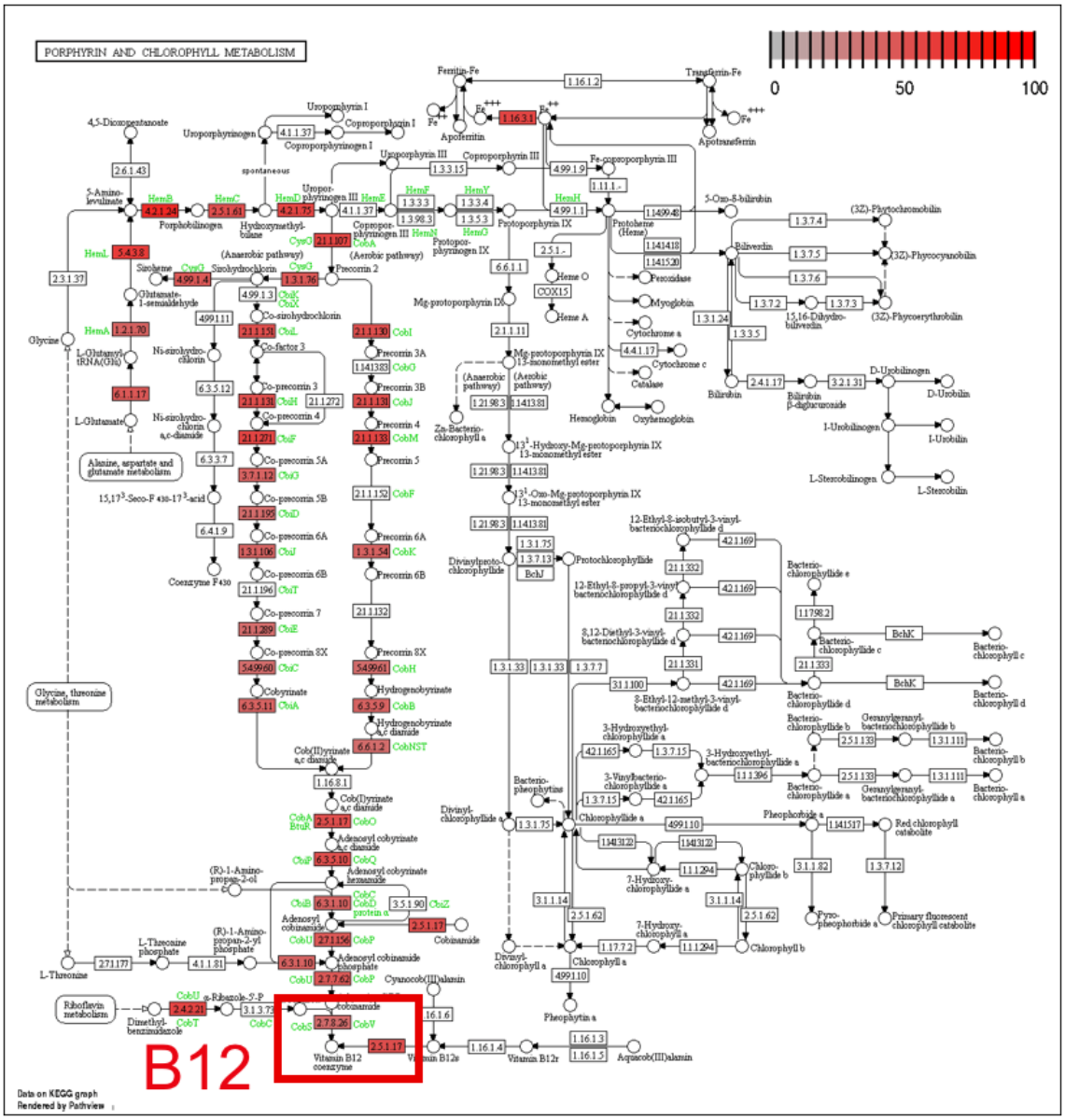


Figure 4.11: The complete B12 synthetic pathway found in 115-*Planctomycetes* genomes.

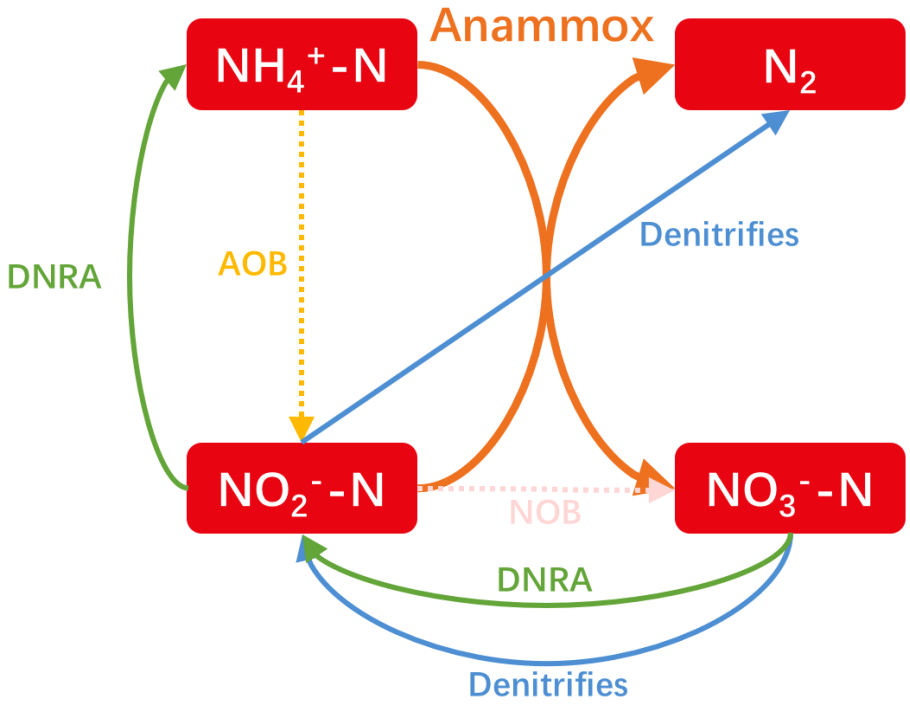


Figure 4.12: The relative nitrogen cycle involving ANAMMOX, DNRA and denitrification.

4.4 Conclusion

The thermal hydrolysis pre-treated sidestream(THP-S) had inhibitory effects on the activity of AnAOB, and long-term acclimation cannot eliminate the inhibition, with performance inhibition observed starting with 70% of THP-S. Meanwhile, ANAMMOX process worked well with regular sidestream under the help of dissimilatory nitrate reduction to ammonium. The reason for the inhibition could be high content of organic carbon in the THP-S, which caused the over-population of heterotrophic bacteria, leading to the washout of AnAOB. This study would assist the future design of ANAMMOX processes for THP-S treatment.

Chapter 5

The establishment of two-stage nitritation/ANAMMOX process treating thermal hydrolysis pre-treated sidestream

5.1 Introduction

Chapter 3 illustrated the inhibitory effects of thermal hydrolysis pre-treated sidestream (THP-S) on both the activity and the growth of ammonium-oxidizing bacteria (AOB). With the sludge retention time (SRT) of 8 days, most AOB was washed out from the system, as the doubling time of AOB in THP-S was longer than 8 days. To overcome the issue, longer SRT was applied for nitritation process, and the two-stage nitritation/ANAMMOX process was established for THP-S nitrogen removal. Compared with single-stage nitritation/ANAMMOX process, the two-stage configuration made it easier to control nitritation process [147]. The previous study reported that the presence of oxygen would inhibit the activity of ANAMMOX bacteria (AnAOB), leading to a decrease in nitrogen removal rate (NRR) of the system [222]. Moreover, it was believed that the high content of organic matters in THP-S caused the over-population of heterotrophic bacteria and resulted in AnAOB washout [223]. Having nitritation process as a pre-treatment for THP-S can effectively lower the organic matter concentrations, providing more suitable influent for the subsequent ANAMMOX process. As a result, the two-stage nitritation/ANAMMOX configuration would be a better choice to manipulate the operational parameters of the nitritation process, while not affecting and even promoting the efficiency of the ANAMMOX process treating THP-S.

This chapter focus on 1): the recovery of nitritation process using several operational strategies, including longer SRT, longer hydraulic retention time (HRT), higher dissolved oxygen (DO) control, etc; 2) the application of ANAMMOX process treating nitritation pre-treated THP-S; 3) the addition of chemical oxygen demand (COD) into ANAMMOX process

feed to disproof the effects of COD on the ANAMMOX process; 4) study the changes in microbial community structures of both nitritation and ANAMMOX processes with different operational strategies.

5.2 Details of Experiments

5.2.1 The operation of THP-S fed nitritation SBR

To stop the crash of THP-S fed nitritation SBR, the feeding of the reactor was stopped. As AOB was washed out from the system due to the THP-S feed, the THP-S fed nitritation SBR was re-seeded with the biomass collecting from regular sidestream (RS) fed nitritation SBR. The $NH_4^+ - N$ and $NO_2^- - N$ concentrations in the SBR were monitored. When almost half of $NH_4^+ - N$ was oxidized into $NO_2^- - N$, the THP-S feeding of the reactor was turned back on with the hydraulic retention time (HRT) of 2 days. The effluent concentrations of $NH_4^+ - N$, $NO_2^- - N$ and $NO_3^- - N$ had been monitored throughout the operation. This study was conducted in a 2.5-L sequencing batch reactor (SBR) (New Brunswick BioFlo 115, Eppendorf, Germany). Complete mixing was achieved using a mechanical stirrer, and air diffusers were placed at the bottom of the rector for aeration. The reactor was heat-jacketed, and the temperature was maintained at 37 °C using a thermometer. The pH was maintained at approximately 7.5 through the addition of sodium hydroxide (5N). The DO was controlled by mixing and aeration. The reactor was operated with 2-h cycles, consisting of 90 min of feeding under aeration, 20 min of settling, and 10 min of drawing. After the process performance was back to normal, THP-S was continuously fed into the reactor with an SRT of 20 days. The effluent of nitritation SBR was collected and stored in a plastic drum at 4 °C.

5.2.2 The operation of ANAMMOX reactors

Two identical 1-L submerged ANAMMOX MBRs were set-up. One set of the reactor was gradually fed with nitritation treated RS (NRS), and the other set of the reactor was gradually fed with nitritation treated THP-S (NTHP-S). Ammonium sulfate and/or sodium nitrite were added into the NRS and NTHP-S for making the $NH_4^+ - N$ to $NO_2^- - N$ ratio in the range of 1:1.1 to 1:1.2. Synthetic wastewater(SWW) with the same substrate levels of NRS and NTHP-S were prepared. The SWW to NRS and NTHP-S volume percentages were gradually increased from 0/100 to 100/0. The pH of the MBRs was controlled at 7.0 ± 0.1 by adding 1N hydrochloric acid and bubbling 95%Ar + 5% CO_2. The SRTs of the MBRs were controlled at 30 days.

5.3 Results

5.3.1 The recovery of THP-S fed nitritation SBR with extended SRT

According to our previous study, the crash of THP-S fed nitritation SBR was due to the reduced AOB activity together with the decreased AOB growth rate, leading to the washout of AOB from the system with the SRT of 8 days. Based on our high F: M growth rate kinetics tests, the SRT should be at least 15 days to avoid AOB washout. It was also believed that the high levels of particulate and colloidal organics in THP-S limited the diffusion of substrates and decreased AOB activity [204]. In order to improve the mass transfer of substrates and prevent AOB from being washed out, several operational strategies had been applied. Biomass collecting from RS fed nitritation SBR was re-seeded to the THP-S fed nitritation SBR. As half of the ammonium was oxidized into nitrite on the fifth day of re-seeding, the feeding of the nitritation process was turned back on with the HRT of 2 days. Compared with 0.5 days of HRT for nitritation SBR treating RS and SWW, a longer HRT can increase the contact time and lower the nitrogen loading rate, and therefore achieve better performance. Also, to avoid oxygen transfer limits, the set-point of dissolved oxygen (DO) level was increased by increasing agitation and gas flow rate. From day 5 to day 12, the DO set-point was gradually increased from 0.5 mg/L to 1.2 mg/L. With this action, the ammonium removal rate (ARR) increased from 41.1 % to 56.7 %, which is close to the ARR achieved by RS fed nitritation SBR (Figure 5.1). Moreover, the SRT of the process was controlled at 20 days to prevent AOB from being washed out. At these final conditions, a stable operation of nitritation process treating THP-S was achieved. Throughout the operation, high concentrations of ammonium and nitrite were accumulated in the system with the negligible amount of nitrate detected, indicating that AOB was the dominant species in the system. During the stable operation of 80 days, the average conversion efficiency of ammonium-N to nitrite-N and nitrate-N were 55.9% and <2%, respectively. This finding claims that nitritation process was successfully established for treating THP-S with manipulated operational conditions including extended SRT, increased HRT, and elevated DO set-point.

5.3.2 Sidestreams treated by nitritation process

After nitritation treatment, about half of ammonium was oxidized into nitrite, decreasing nitrogen loading to the subsequent ANAMMOX process. Also, the aeration in nitritation process lowered the organic content levels of sidestreams. The average concentrations of NRS and NTHP-S parameters are listed in Table 5.1. Compared with RS and THP-S (Table 2.3), the concentrations of total chemical oxygen demand (TCOD) and protein in NRS and NTHP-S decreased in half, while the polysaccharide levels in NRS and NTHP-S increased significantly. As the nitritation process was operated in the SBR, aggregated sludge was selected over suspended sludge due to better settling. Polysaccharide, as a component of

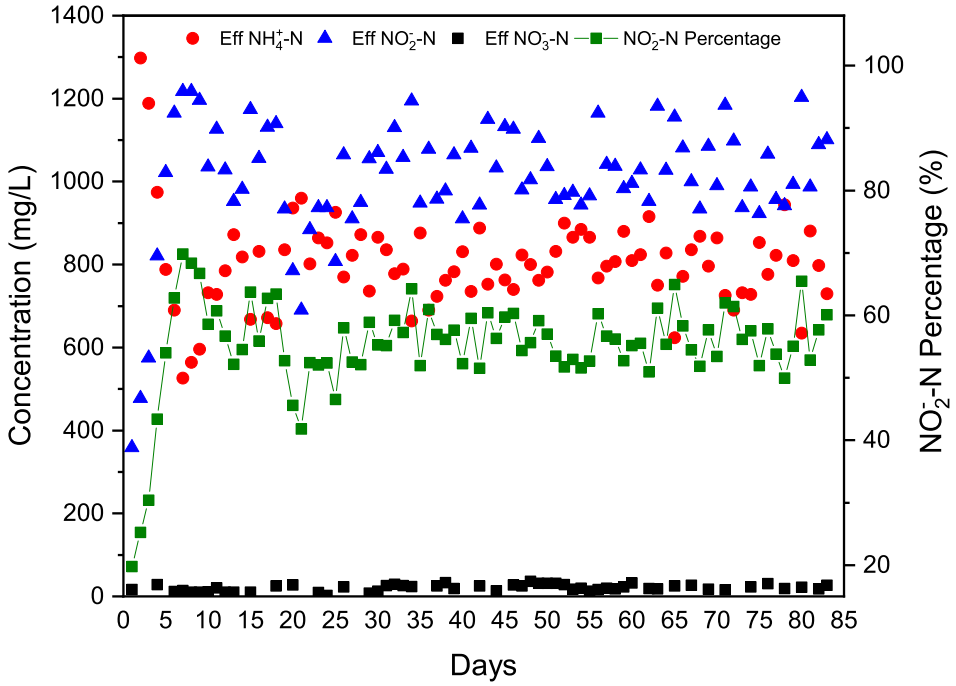


Figure 5.1: The performance of the nitritation SBR treating THP-S with extended SRT and increased aeration.

extracellular polymeric substances (EPS), could enhance biomass aggregation by working as the gelling agent in aerobic granulation [224, 225]. The increase of polysaccharide in NRS and NTHP-S indicates the generation of EPS and sludge aggregates during nitritation SBR operation. Besides, the ammonium oxidation consumed alkalinity (ALK), leading to large decreases of ALKs in both RS and THP-S after nitritation treatment. Three-dimensional EEM fluorescence spectroscopy was performed to identify the dissolved organic matters properties of NRS and NTHP-S (Figure 5.2 and Figure 5.3). Similar to RS and THP-S, three peaks for NRS were identified, while only one peak was identified for NTHP-S. However, compared with RS and THP-S (Figure 2.11 and Figure 2.12), the fluorescence intensities are much lower in NRS and NTHP-S. Peak B, which was reported as humic acid-like peak and observed at the EX/EM of 320-360/420-460 nm, has much weaker intensity in NRS than that in RS. At the same time, peak A, which was reported as refractory microorganism exudates and observed at the EX/EM of 320-360/420-460 nm, was lowered with nitritation treatment in both NRS and NTHP-S.

Parameters (mg/L)	**NRS**	**NTHP-S**
TCOD	352	1350
$NH_4^+ - N$	685	886
$NO_2^- - N$	670	1043
ALK (as $CaCO_3$)	610	850
Protein	134.1	179.48
Polysaccharide	693.2	1547.7

Table 5.1: The average concentrations of RS and THP-S parameters after nitritation treatment.

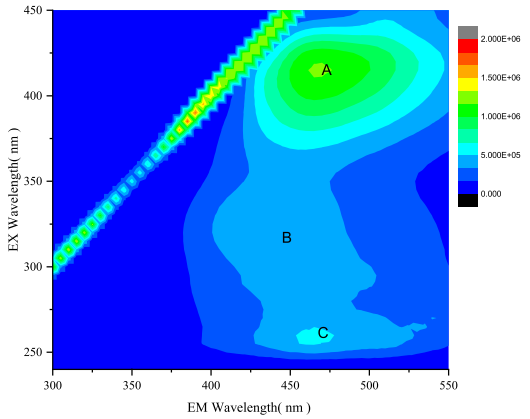


Figure 5.2: EEM fluorescence spectra of NRS.

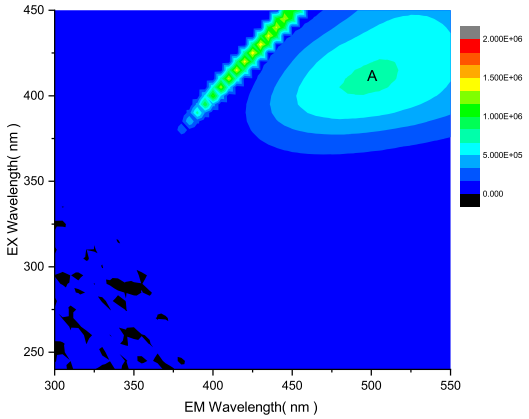


Figure 5.3: EEM fluorescence spectra of NTHP-S.

5.3.3 The performance of ANAMMOX process treating nitritation pre-treated sidestreams

ANAMMOX process was applied as the subsequent procedure treating NRS and NTHP-S. Figure 5.4 shows the performance of ANAMMOX process gradually fed with NRS. With the influent NRS percentage gradually increased from 20 % to 100 %, the effluent concentrations of $NH_4^+ - N$ and $NO_3^- - N$ decreased synchronously. This is possibly due to the presence of denitrifying bacteria in the system. Denitrifying bacteria could reduce $NO_3^- - N$ to $NO_2^- - N$, which can be coupled with $NH_4^+ - N$ to generate nitrogen gas in ANAMMOX process, resulting in the decrease of both $NH_4^+ - N$ and $NO_3^- - N$ in the effluent. At around day 80, the effluent $NH_4^+ - N$ concentration increased with the effluent $NO_3^- - N$ kept low, implying the possible presence of dissimilatory nitrate to ammonium (DNRA) process in the system. Also, the relatively high concentration of COD in NRS promoted the excessive proliferation of heterotrophic bacteria, increasing the mixed liquor volatile suspended solids (MLVSS)

concentration in the system from 6.01 g/L to 10.42 g/L. The large increase of MLVSS led to sludge decay and the release of $NH_4^+ - N$ to the system. Throughout the experiment, the effluent $NO_2^- - N$ concentration stayed low with the nitrogen removal rate (NRR) in the range of 0.2-0.3 $gN/d/gVSS$ (Figure 5.6), claiming good activity of ANAMMOX process. Also, the nitrogen removal efficiency of the process reached 95%. Figure 5.5 represents the stoichiometric ratios of ANAMMOX process treating RS. The removed $NO_2^- - N/$ removed $NH_4^+ - N$ ratio gradually decreased from near the theoretical value of 1.32 to about 1.2, and rose rapidly at the late stage of the experiment. On the other hand, the produced $NO_3^- - N/$ removed $NH_4^+ - N$ ratio gradually decreased from 0.18 and stabilized below 0.1. The changes of stoichiometric ratios match the changes in effluent nitrogen compounds concentrations, indicating the presence of heterotrophic nitrogen-associated processes in the system.

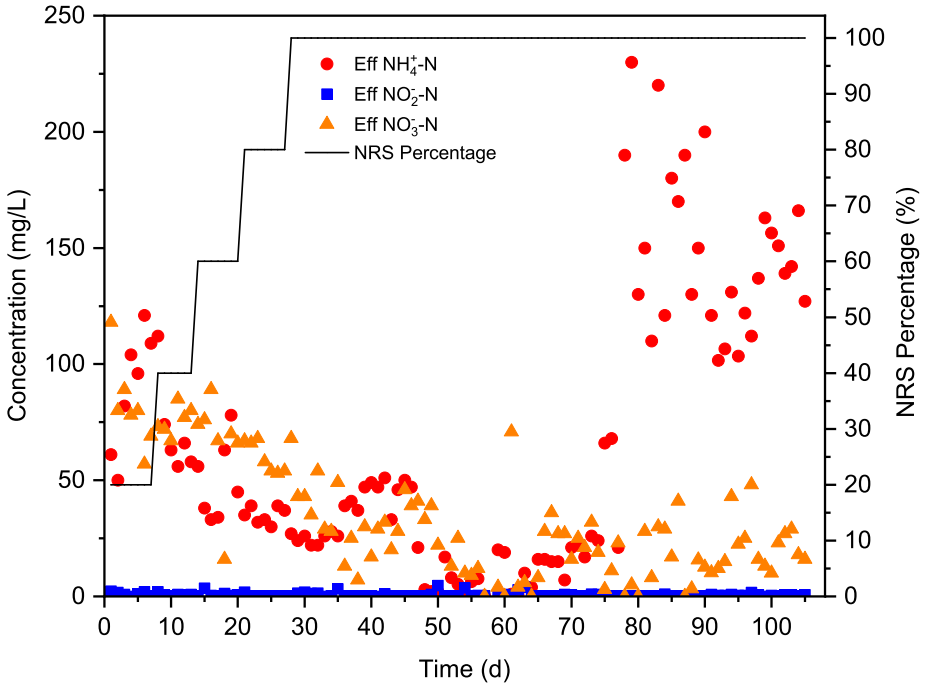


Figure 5.4: The performance of ANAMMOX process treating NRS.

Similar with ANAMMOX process treating NRS, stable performance was gained by using the ANAMMOX process treating NTHP-S (Figure 5.7). With the influent NTHP-S percentage gradually increased from 20 % to 100 %, the effluent $NH_4^+ - N$ and $NO_3^- - N$ concentrations stayed around 100 mg/L and 50 mg/L, while the effluent $NO_2^- - N$ con-

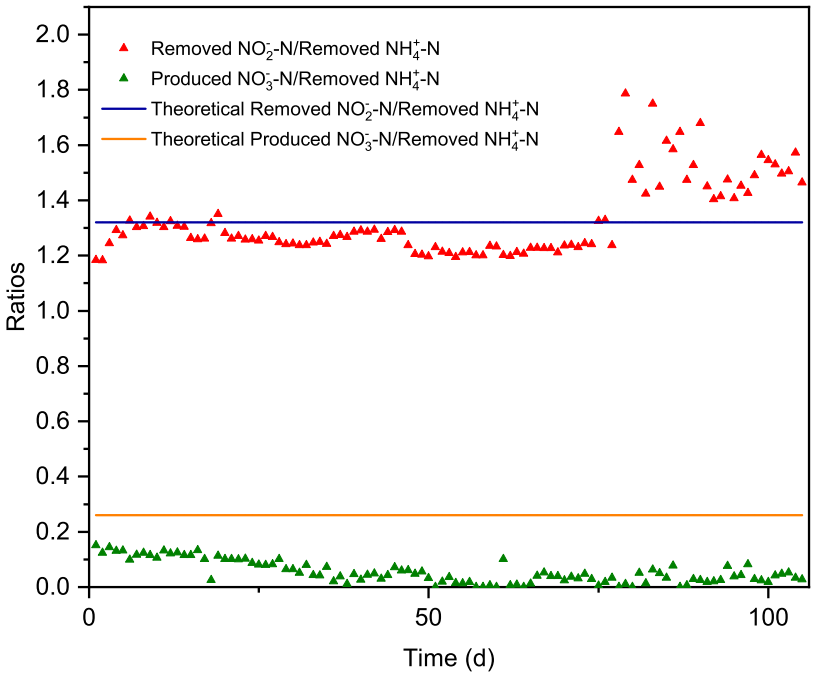


Figure 5.5: The stiochiometric ratios of ANAMMOX process treating NRS.

centration kept below 2 mg/L. The NRR of the system was above 0.3 $gN/d/gVSS$ with the nitrogen removal efficiency reached 95 %. Compared with treating THP-S by applying single-stage ANAMMOX process, the two-stage nitritation and ANAMMOX process effectively alleviate the inhibitory effects of THP-S on ANAMMOX process. Previous research proved that the high nitrogen concentration in wastewater would not cause ANAMMOX process performance failure [223]. It is believed that the inhibition was eliminated by the decreased COD levels in NTHP-S according to nitritation pre-treatment. To verify the inhibition of COD on the ANAMMOX process, 500 $mgCOD/L$ of CH_3COONa was added into the influent on day 83 of operation. After the addition of COD, the concentrations of effluent $NH_4^+ - N$ and $NO_2^- - N$ rapidly increased to above 400 mg/L and 100 mg/L, while the concentration of $NO_3^- - N$ decreased continuously. Moreover, the NRR sharply decreased after COD addition, and the removed $NO_2^- - N/$ removed $NH_4^+ - N$ ratio rapidly rose to 1.8 or more. All these phenomena indicate the appearance of a large portion of heterotrophic bacteria in the system, most probably DNRA or denitrifying bacteria, competing substrates with AnAOB and causing wash out of AnAOB.

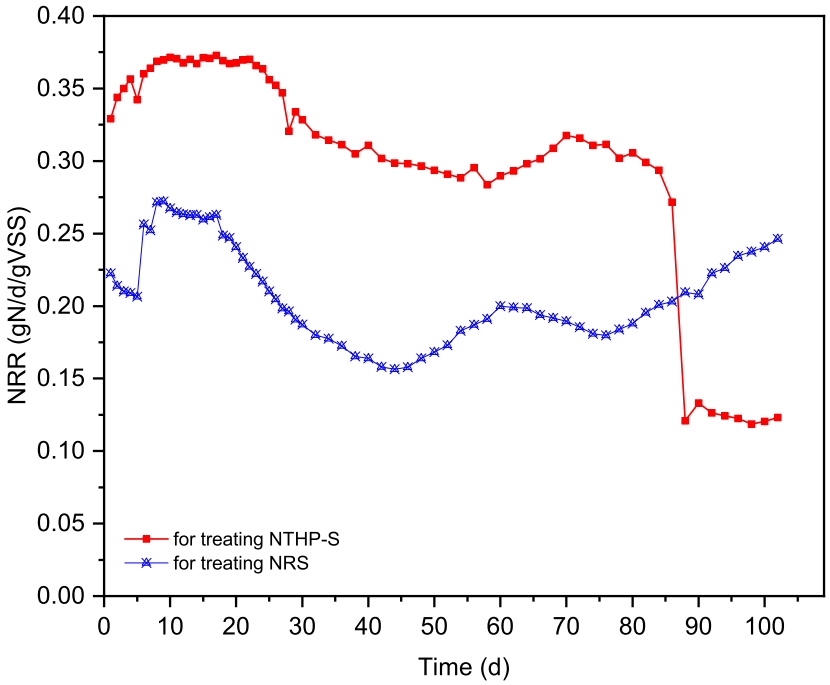


Figure 5.6: The nitrogen removal rate of ANAMMOX process treating NRS and NTHP-S.

5.3.4 Microbial structure analysis

5.3.4.1 Nitritation process

DNA samples were collected from nitritation process treating SWW (NSWW), RS at the early stage (NRS1), RS at the late stage (NRS2), THP-S at the early stage(NTHPS1), THP-S at the late stage(NTHPS2), and THP-S with extended SRT (NTHPSE). A total of 2612893 effective sequences were detected, which can be clustered into 799 OTUs at a distance of 0.03. According to RDP taxonomic category analysis, the detected bacteria were classified into 31 phyla, 69 classes, 125 orders, 205 families, 366 genera, and 506 species. Good's coverage values were measured to determine sequencing integrity. For all the samples, the Good's coverage values were approach 100%, indicating sufficient sequencing depth to describe patterns in this study (Table 5.2). Shannon, Simpson, Ace, Chao1 indexes were applied to analyze the microbial community richness and diversity (Table 5.2). The Simpson index value of NSWW was much higher than other samples, while the Shannon, Ace, and Chao1 values of NSWW were much lower, claiming that NSWW had less community richness and diversity. RS samples had more community richness and diversity than THP-S

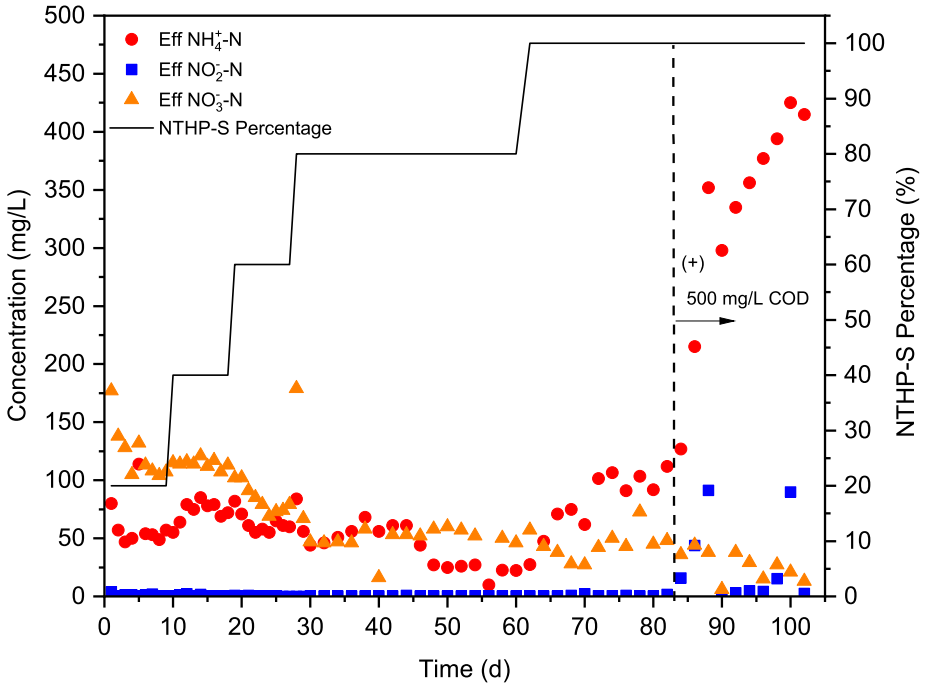


Figure 5.7: The performance of ANAMMOX process treating NTHP-S.

samples. However, with extended SRT and aeration, the bacterial community richness and diversity increased in the NTHPSE sample. Microbial community compositional differences among samples were revealed by principal coordinates analysis (PCoA) according to Bray-Curtis distance metrics. The principal coordinates (PCs), which explain the fractions of the variability observed in datasets, are plotted to create a visual representation of sample microbial compositional differences [226]. According to the plot, the microbial compositions of RS samples and THP-S samples were quite different, while NSWW was more similar to RS samples. Also, NTHPSE had a unique microbial composition, which was different from both RS and THP-S samples (Figure 5.9).

The phylum level distribution of bacterial sequences is shown in Figure 5.10. Compared with other samples, NSWW had a less diverse microbial composition in the phylum level. The major common dominant phyla in all the samples included *Proteobacteria* (68.5-29%), *Bacteoidetes*(39.2-24.5%), *Deinococcus-Thermus*(15.9-1.3%), *Firmicutes* (7.7-0.033%) and *Chloroflexi* (3.1-0.64%). All those phyla were widely distributed and dominated in nitrifying bioreactor and wastewater treatment plants [227, 228]. AOBs usually restricted to a few groups within β- and γ- *Proteobacteria*. Besides, some *alpha*- and γ- *Proteobacte-*

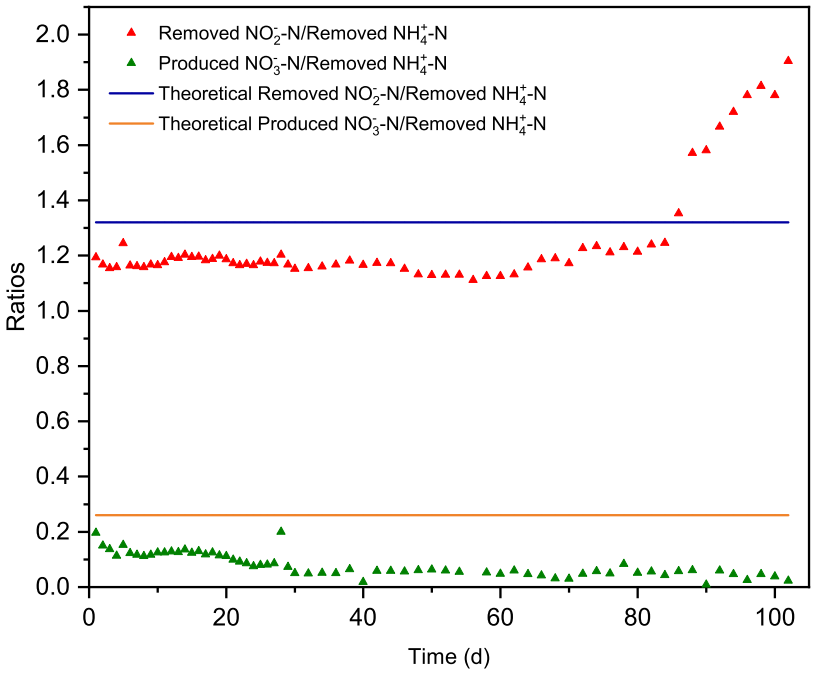


Figure 5.8: The stiochiometric ratios of ANAMMOX process treating NTHP-S.

ria populations can utilize low molecular-weight organic matter from utilization-associated products (UAP) [229]. Members of *Bacteoidetes* were known to be able to degrade high molecular-weight compounds of both dissolved and particulate organic matters. Containing genes encoding hydrolytic enzymes, *Bacteoidetes* possessed capabilities of polymeric carbon degradation. Also, as members of particle-associated microbial communities, *Bacteoidetes* had potential for surface adhesion by creating metal cation bridge to trigger organic aggregation, and therefore promoted carbon sequestration [230]. NTHPSE had the highest abundance of *Deinococcus-Thermus* (15.9%), which was known for having high resistant to environmental hazards [231]. The previous study found that saline water could motivate the blossom of *Deinococcus-Thermus*, as it was the predominant phylum in the seawater-processing wastewater treatment plant [232]. Some species of *Firmicutes* can degrade soluble microbial product (SMP) , while *Chloroflexi* was able to utilize refractory organics from nitrifying bacteria decay [233]. With complete inorganic components of feeds, lowest abundances of *Firmicutes* and *Chloroflexi* were seen in NSWW. Also, denitrifying bacteria was detected among *Firmicutes* and *Chloroflexi* [223, 234, 235]. Other than the common phyla, specific phyla were detected in different samples. *Verrucomicrobia* was only found in NSWW(13.3%),

Sample	Sequence	Shannon	Simpson	Ace	Chao1	Coverage
NSWW	503936	1.8179	0.2709	322.0860	357.6667	0.999879
NRS1	447132	4.1419	0.0776	1803.8464	1824.6899	0.999388
NRS2	456164	3.5634	0.1095	1639.8381	1639.7692	0.999371
NTHPS1	310390	3.1653	0.0933	615.7379	672.0811	0.999634
NTHPS2	413878	3.1482	0.1011	651.7808	651.1754	0.999737
NTHPSE	481393	3.8474	0.0531	1259.7426	1275.5140	0.999575
ASWW	156908	2.4827	0.1627	432.6307	435.65	0.999832
ARS1	341255	4.0309	0.0522	1612.6777	1656.7863	0.99946
ARS2	263082	3.9747	0.0506	1368.0501	1424.0095	0.999366
ATHPS1	207126	3.4307	0.1125	1234.4904	1280.6774	0.999502
ATHPS2	221724	3.4031	0.1095	1223.2823	1261.8191	0.999585
ATHPS3	203935	3.3338	0.1084	1197.9145	1203.875	0.999549

Table 5.2: Number of sequence and estimated diversity indices of nitritation process and the subsequence ANAMMOX process.

NRS1(2.4%) and NRS2(1.8%). Previous studies reported the appearance of *Verrucomicrobia* in the municipal anaerobic digester and their ability of methane oxidation [228, 236]. *Spirochaetae* and *Cloacimonetes* only showed up in NRS1 (4.6% and 4.7%), NRS2(2.1% and 2%) and NTHPSE(2% and 1.4%). It was reported that species of *Spirochaetae* were associated with cellulose degradation and glucose fermentation, producing hydrogen, carbon dioxide, acetate and lactate as end products [237]. Similarly, species of *Cloacimonetes* observed in anaerobic digestion can contribute to propionate degradation [227].Other minor phyla, including *Thermotogae* in NRS1 (1.7%) and NRS2 (0.68%), *Gemmatimonadetes* in NTHPS1 (0.99%) and NTHPS2 (1.1%), and *Tenericutes* in NTHPSE (1.7%) were also detected.

Figure 5.11 represents the abundances of different genera and the phylogenetic tree of bacterial sequences. Clear distinctions of microbial community structures were found across samples. *Nitrosomonas* was the major AOB species in the system with abundance of 43.3% (NSWW), 25.6% (NRS1), 28.8%(NRS2), 5.3% (NTHPS1), 1.3% (NTHPS2) and 4.8% (NTHPSE). The significant decrease of *Nitrosomonas* abundance in THP-S samples correlates with the finding that THP-S could inhibit AOB growth. The *Nitrosomonas* abundance in NTHPSE was promoted by SRT extension, indicating that longer SRT could prevent AOB from being washed out from THP-S fed nitritation system. Prevalent nitrite-oxidizing bacteria (NOB) such as *Nitrospira*, *Nitrobacter* and *Candidatus Nitrotoga* were not detected [238]. Genus *Moheibacter*, which was found omnipresent in nitritation process [229, 233, 238], was also detected in all the samples. It was reported that *Moheibacter*, the heterotrophic aerobic bacteria, was closely related to SMP consumption [229, 239]. *Truepera* took a large portion in NTHPSE (15.9 %). Being detected in the biological nitrogen removal process treating

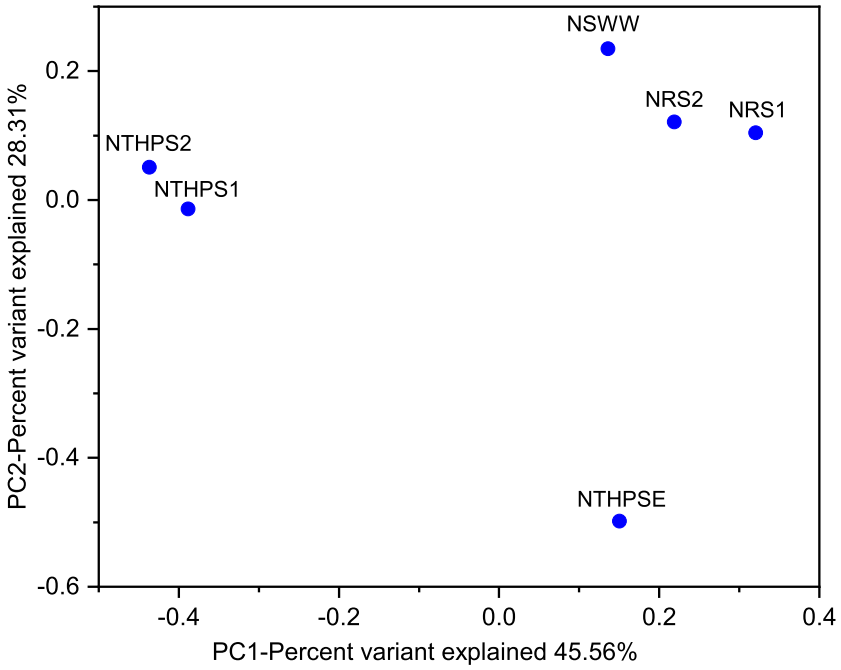


Figure 5.9: The application of principal coordinates analysis to determine microbial compositional differences among nitritation process samples.

mature landfill leachate, it was believed that *Truepera* could tolerate hazards in the wastewater while utilizing a large variety of organic matters [240]. The relatively high abundance of *Truepera* in NTHPSE implied that *Truepera* could stabilize the nitritation process by treating THP-S. *Castellaniella* and *Rhodobacteraceae* took Large portions in NTHPS1 (9.5% and 21.9%) and NTHPS2 (19.8% and 7.3%). However, the abundance of both *Castellaniella* and *Rhodobacteraceae* decreased largely in NTHPSE (1.5% and 0.3%). *Castellaniella* was identified as a group of facultatively anaerobic denitrifying bacteria [241]. *Rhodobacteraceae* possessed highly diverse metabolism including anoxic nitrate-mediated sulfide oxidation and anaerobic denitrification [242, 243]. The decreases of *Castellainella* and *Rhodobacteraceae* in NTHPSE were possibly due to the increased aeration in the nitritation process. On the contrary, *Chitinophagaceae* was mostly observed in NRS1 (3%), NRS2 (6.1%), NSWW (5.4%) and NTHPSE (9.5%). It was reported that *Chitinophagaceae* populations contained glycosyl hydrolases, which can catalyze the hydrolysis of glycosidic bonds in complex sugars, and metabolized starch [244]. Minor genera including *Xiphinematobacter*, *Comamonas*, *Phaeodactylibacter*, *Xanthomonadaceae*, *Piscirickettsiaceae*, *Pontibaca* and *Lysobacter* were also

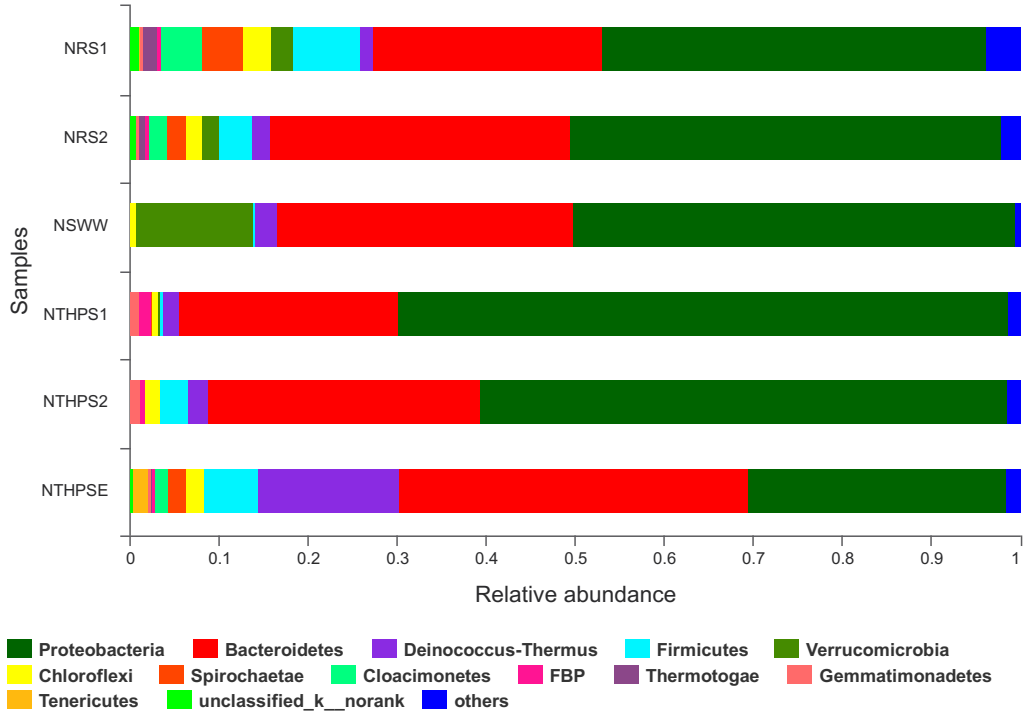


Figure 5.10: Relative abudances of detected phyla in the nitritation samples

detected. *Xiphinematobacter* was a group of endosymbiotic species detected in activated sludge [245]. 13.2% of *Xiphinematobacter* was observed in NSWW. *Xanthomonadaceae*, a group of bacteria involved in nitrification process under low-DO conditions ($<0.3\,mg/L$), was not detected in RS samples [246].The aerobic chemoheterotrophic genus *Phaeodactylibacter* was specifically observed in RS samples, occupying 6% in NRS1 and 6.4% in NRS2. Differently, *Piscirickettsiaceae* and *Pontibaca* were specifically observed in THP-S samples. *Piscirickettsiaceae* populations possessed abilities of sulfur oxidation under aerobic condition took 9.1% in NTHPS1 and 1.5% in NTHPS2, while the facultatively anaerobic genus *Pontibaca* took 1.3% in NTHPS1 and 7.4% in NTHPS2 [247, 248]. *Lysobacter* was only observed in NTHPSE (5.2%). The previous study reported that *Lysobacter* can degrade a variety of phenolic pollutants [249].

5.3.4.2 ANAMMOX process

DNA samples were collected from ANAMMOX process treating SWW (ASWW), RS at the early stage (ARS1), RS at the late stage (ARS2), RS with additional COD (ARS3), THP-S at the early stage(ATHPS1) and THP-S at the late stage(ATHPS2). A total of 1394030 effective sequences were detected from the six samples. The sequences can be clustered

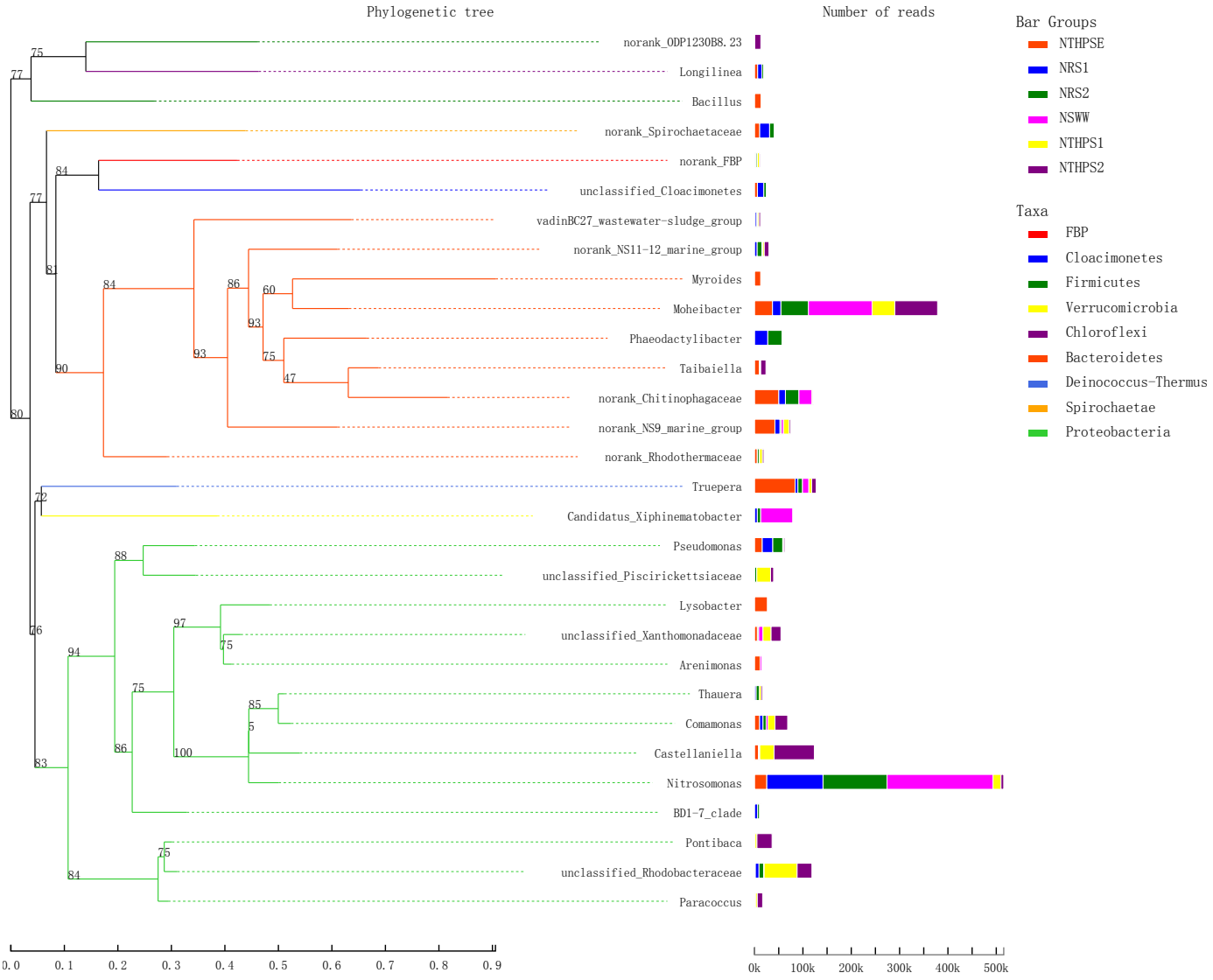


Figure 5.11: Phylogenetic tree and the relevant sequences assignment results at the genus level of nitritation process.

into 759 OTUs at a distance of 0.03. The bacteria coverages, which can be described as Good's coverage values, all approach 100%, indicating sufficient sequencing depth to describe patterns in this study (Table 5.2). The detected bacteria were classified into 36 phyla, 85 classes, 140 orders, 212 families, 342 genera, and 484 species. Alpha indexes were applied to analyze the microbial community richness and diversity (Table 5.2). Similar with the samples from the nitritation process, the Simpson index value of ASWW was much higher than other samples, while the Shannon, Ace and Chao1 values of ASWW were much lower,

claiming that ASWW had less community richness and diversity. Also, the Simpson index values of RS were the lowest, while the values of other indexes were the highest, indicating RS samples had more community richness and diversity than THP-S samples. There were no obvious distinctions between THP-S samples and THP-S samples with additional COD as feed. PCoA showed the microbial community compositional differences among samples. Clear differences were shown among SWW sample, RS samples, and THP-S samples, while THP-S samples and THP-S samples with additional COD were quite similar (Figure 5.12).

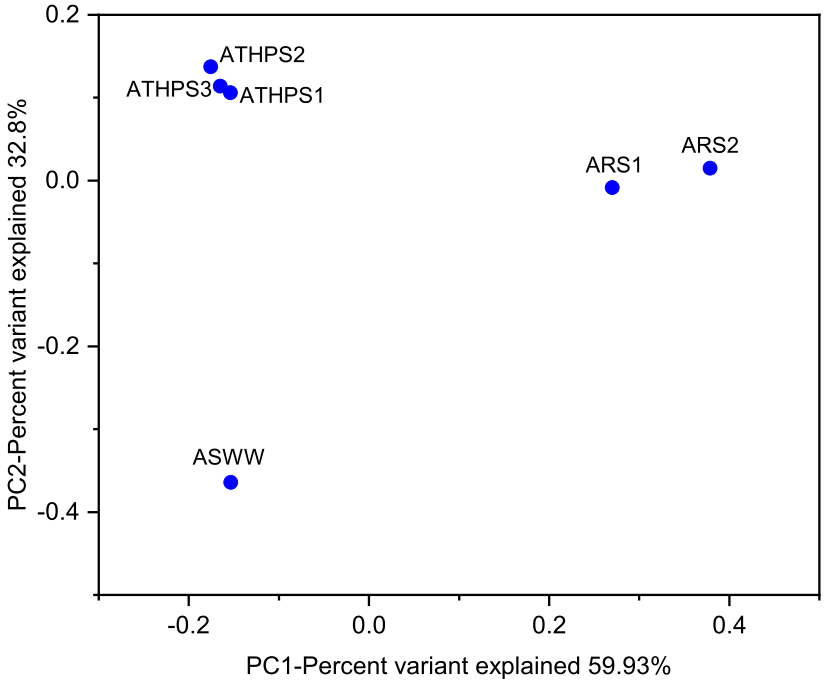


Figure 5.12: The application of principal coordinates analysis to determine microbial compositional differences among ANAMMOX process samples.

Taxonomic assignment indicating diversity differences among all the samples at phylum level was shown in Figure 5.13. The predominant phyla of all the samples were the same. Within the major phyla, *Chlorobi* (33.9- 20.6%) was predominant in all the samples, followed by *Planctomycetes*(24- 1.1%), *Chloroflexi* (17.7- 11.1%), *Proteobacteria* (12.1- 6.3%) and *Ignavibacteriae* (12.7- 3.1%). *Bacteroidetes* and *Firmicutes* were barely detected in ASWW, which was more abundant with *Armatimonadetes*. Compared with THP-S samples, some phyla in ARS1 and ARS2, such as *Cloacimonetes*, *Spirochaetae* and *Bacteroidetes*, had higher abundance, whereas others, such as *Chlorobi*, *Chloroflexi*, *Proteobacteria* and *Ignavibacte-*

riae were lower in abundance. Among all these phyla, *Chlorobi*, *Chloroflexi*, *Proteobacteria*, *Ignavibacteriae Bacteroidetes* and *Firmicutes* were often detected with *Planctomycetes* in ANAMMOX reactors [234, 250–253]. The phylum *Acidobacteria*, which was frequently detected in ANAMMOX process, was not observed [254]. Denitrification ability was widespread in bacterial domains, including phyla *Proteobacteria*, *Chlorobi*, *Chloroflexi*, *Bacteroidetes* and *Firmicutes* [234]. The high abundances of the phyla were possibly inherited from the previous nitritation process. In addition, higher abundances of *Spirochaetae*, together with *Cloacimonetes* and *Bacteroidetes* in RS samples illustrated that NRS contained lower levels of easily biodegradable organic matters and polysaccharides. The average relative abundances of *Planctomycetes* in RS and THP-S samples were 1.27% and 1.28%, respectively. The different abundance levels of *Planctomycetes* between the two groups can be negligible, which was different from the single-stage ANAMMOX process illustrated in Chapter 4. The fewer differences might be due to the lower COD concentrations in both NRS and NTHP-S. Also, the bacterial community structure of ATHPS3 did not show many differences from ATHPS1 and ATHPS2, indicating that the addition of COD in THP-S feed did not affect the bacterial community structure and the reactor operation failure was possibly due to the changes in gene levels. To find out the reason of reactor failure, more research needs to be done in functional gene levels, such as metagenomic analysis.

5.4 Conclusion

The THP-S fed nitritation SBR was successfully recovered with re-seeding and influent shut-down. The stable operation of nitritation process treating THP-S was achieved by extended SRT from 8 days to 20 days, increased HRT from 0.5 days to 2 days, and elevated DO set-point from 0.5 mg/L to 1.2 mg/L. After the treatment of nitritation process, both NRS and NTHP-S contained much lower concentrations of proteins and CODs, especially refractory CODs. Stable ANAMMOX process performance was also achieved, treating both nitritation pre-treated RS and THP-S. It is believed that the inhibition of THP-S on ANAMMOX process was mediated by the decreased COD levels in NTHP-S. To prove this hypothesis, additional COD was added into NTHP-S and fed into the ANAMMOX process. The rapid decrease of NRR was observed, indicating that the heterotrophic bacteria in the system competed for substrates with AnAOB and led to AnAOB washout. 16s rRNA sequencing showed that all the samples from the nitritation process contained *Proteobacteria* , *Bacteoidetes*, *Deinococcus-Thermus*, *Firmicutes* and *Chloroflexi*. Among these phyla, *Deinococcus-Thermus* had the highest abundance in NTHPSE. NRS samples contained relatively higher abundances of anaerobic digestion associated phyla, including *Bacteoidetes*, *Verrucomicrobia*, *Spirochaetae* and *Cloacimonetes*. Genus level analysis showed that *Nitrosomonas* was the major AOB species in the system, and large decreases of *Nitrosomonas* abundances in NTHPS samples were observed. The *Nitrosomonas* abundance increased in NTHPSE with the decrease of denitrification associated bacteria, indicating that the extended SRT and aeration can promote the process stability. Also, the relatively high abun-

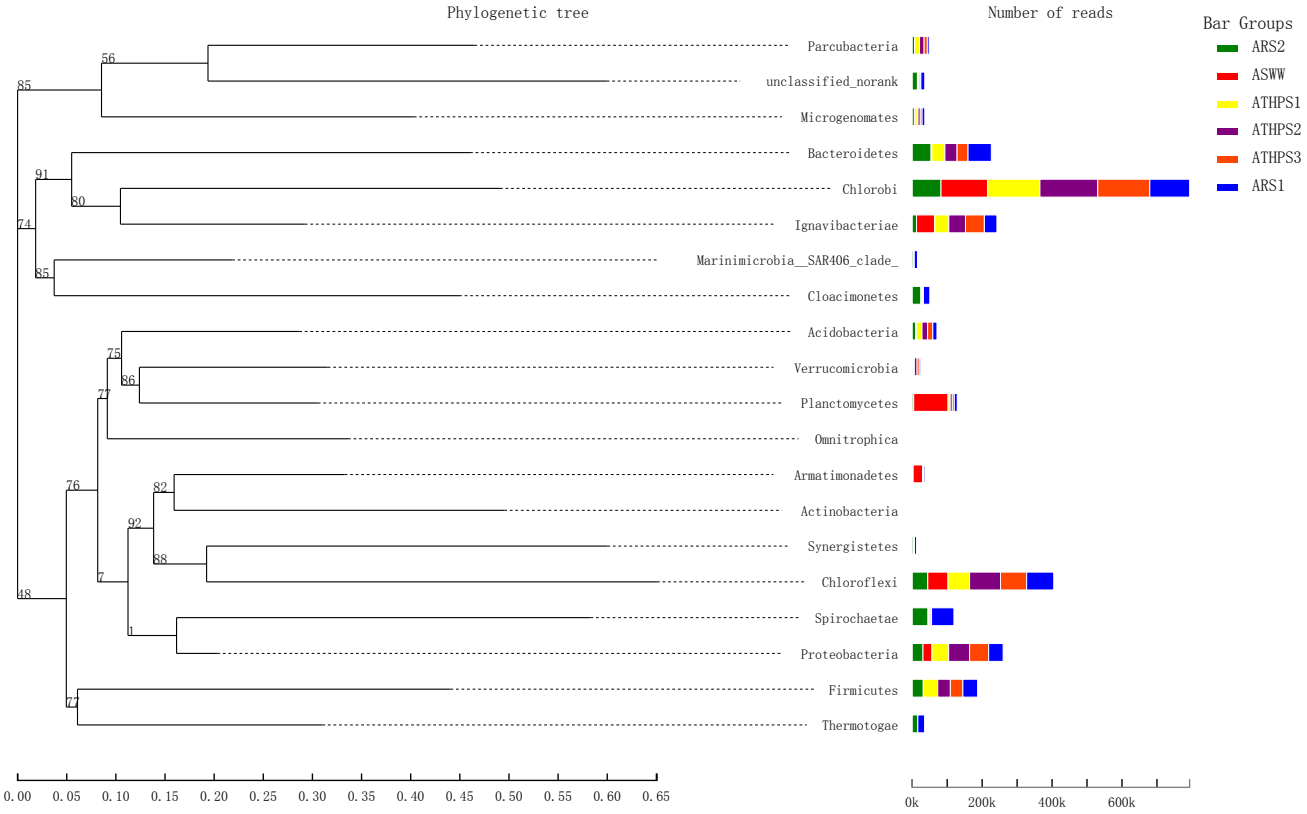


Figure 5.13: Phylogenetic tree and the relevant sequences assignment results at the phylum level of ANAMMOX process.

dance of *Truepera* and *Lysobacter* in NTHPSE implied that these bacteria can do benefit to the nitritation process treating THP-S. The major phyla detected in nitritation samples were also observed in the ANAMMOX process. It is possible that these phyla were partially inherited from the previous nitritation process. Moreover, the ANAMMOX samples had similar traits with the nitritation samples. For example, ARS samples also contained *Bacteoidetes*, *Spirochaetae* and *Cloacimonetes*. The similarity with NRS samples indicates that NRS contained more refractory CODs than NTHP-S. The abundances of *Planctomycetes* were quite similar in both ARS samples and ATHP-S samples. Even with additional COD added to the THP-S influent, the abundance of *Planctomycetes* did not have many differences. Further research such as metagenomic analysis needs to be performed to study the reason of ANAMMOX process failure with COD addition in the gene levels.

Chapter 6

The effects of different reactor configurations on nitritation/ANAMMOX process to treat sidestream

6.1 Introduction

With the development of automatic controls in recent years, the establishments of single-stage systems became the mainstream. The single-stage nitritation/ANAMMOX process can save operational cost while reducing the footprints of the wastewater treatment plant. Also, with continuous consumption of nitrite, the one-stage systems avoid the potential toxic feed for the second step. One-stage reactors including sequencing batch reactor (SBR), biofilm reactor, up-flow reactor, have been established for developing nitritation/ANAMMOX process [32, 157, 159, 255]. SBR, which offers advantages including efficient biomass retention, homogeneous mixture, and reliability for long-term operation, is the most commonly applied implementation for the one-stage nitritation/ANAMMOX process [32, 87]. Biofilm reactor such as moving-bed biofilm reactor (MBBR) also works as an effective tool for developing nitritation/ANAMMOX process. The porous biomass carriers in MBBR can provide large specific areas for biomass attachment, which enhances biomass aggregation and diminishes biomass washout. With the advantage of effectively retaining biomass, MBBR has been applied to shorten the start-up time of nitritation/ANAMMOX process. By applying MBBR, nitritation/ANAMMOX process was started up within 4 months with the ammonium removal rate reached 1.2 $kg/m^3/d$ [159]. The performance of MBBR can be further improved by integrated fixed-biofilm activated sludge (IFAS) configuration. By incorporating a settler in the MBBR system, the IFAS configuration can achieve 2 to 2.5 times higher NRR than MBBR itself. The system performance can benefit from the suspended sludge retained from the effluents, which can be enriched under lower DO and substrate levels due to less mass

transfer limitations [160].

In this study, two one-stage nitritation/ANAMMOX pilots have been built up. One of them is running as an SBR, and the other is operating in an IFAS system. According to long-term feeding the pilots with RS and THP-S, the performances of the pilots are evaluated. Also, by applying 16s rRNA sequencing, this study investigates the effects of different reactor configurations on the structures of the bacterial community. The findings from this study can provide evidence for establishing robust nitritation/ANAMMOX process treating THP-S. What's more, the study on microbial evolution can enable us to have a better understanding of THP-S inhibition mechanism on nitritation/ANAMMOX process.

6.2 Details of Experiments

6.2.1 The setup of SBR pilot

With the diameter of 1-foot and height of 4-foot, the SBR pilot was set up for establishing the one-stage nitritation/ANAMMOX process. Having a volume of 89 L and an active volume of 72 L, the SBR pilot was operated with $8h$ per cycle. Each cycle consisted of filling of $6.75h$, $1h$ settling phase ended by $0.25h$ of decanting. The process was automatically controlled by a Programmable Logic Controller (PLC) according to the setpoints and equipped with sensors that monitored the real-time data of pH, dissolved oxygen(DO), water level and feed rate. pH and DO were monitored by pH/ORP model 3900VP sensor and Rosemont Analytical RDO sensor, respectively. To provide aeration into the system, air was introduced to the pilot via a coarse bubble diffuser at the bottom of the pilot, while the air flow rates were controlled by a Sierra Smart-Trak 50 Series mass flow controller. The water level in the pilot was monitored by a Pulsar Model dBi3 ultrasonic level sensor. Also, a peristaltic pump was used for feeding. In the SBR pilot, mixing was achieved mainly through aeration, as agitation and recirculation tended to shear biomass granules. The temperature of the pilot depended on the temperature of the sidestream fed into the system. Without any extra heating equipment, the temperature of the pilot was 32.6±1.4°C [256].

The pH-based control strategy was applied for the SBR operation. pH was controlled within a tight interval of 0.1 (with lower and higher setpoints of ±0.05) by aeration and sidestream feeding. Oxygen inputs promoted nitritation, which produced H^+ and drove pH to the lower setpoint. Once the pH dropped to the lower setpoint, aeration was stopped, and sidestream feeding was provided. Together with ANAMMOX and denitrification processes, the sidestream feeding recovered alkalinity (ALK) in the system and brought up pH. The alkaline sidestream feeding was introduced to the system until pH reached the upper setpoint. DO levels were kept below 0.2 mg/L to avoid ANAMMOX inhibition. The solid retention time (SRT) of the SBR pilot was ranging from 1.25 days to 130 days, depending on the pilot performance and the concentrations of volatile suspended solids (VSS) in the effluent.

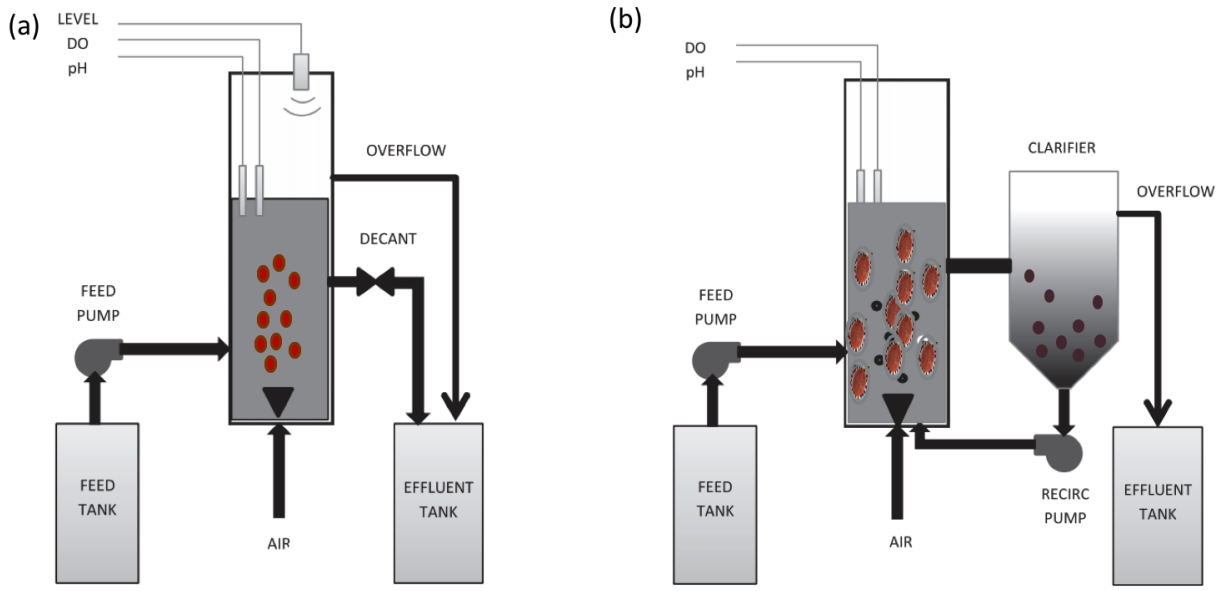


Figure 6.1: The diagram of **a** SBR pilot. **b** IFAS pilot.

6.2.2 The setup of IFAS pilot

The MBBR pilot was set up in the IFAS configuration, which consisted of an MBBR pilot with identical dimensions as the SBR pilot and a 55 L clarifier (Figure 6.2). The clarifier collected effluents from the MBBR and settled solids. AnoxKaldnes K5 carriers with a filling ratio of about 50% were applied in the IFAS. A centrifugal pump was installed to periodically return the settled solids from the clarifier to the reactor. Different from the SBR pilot which had periodically decanting, the IFAS pilot drained effluent through an overflow port at the top of the clarifier. Aeration was provided continuously. Mixing was gained by aeration and sludge recirculation. Same with the SBR, the PLC control was used to manipulate air flow rate, sidestream feeding, and sludge recirculation according to the pH-based control strategy. Also, pH, DO, water level, and sidestream feeding were monitored in real-time. The SRT of the IFAS pilot was ranging from 0.88 days to 50 days, depending on the pilot performance and the concentration of VSS in the effluent.

6.3 Results

6.3.1 Nitritation/ANAMMOX pilots treating RS

Both SBR and IFAS pilots were operated since 2014. After the operation of about 500 days, reliable nitrogen removal performance was achieved for both the pilot systems. Figure 6.3a

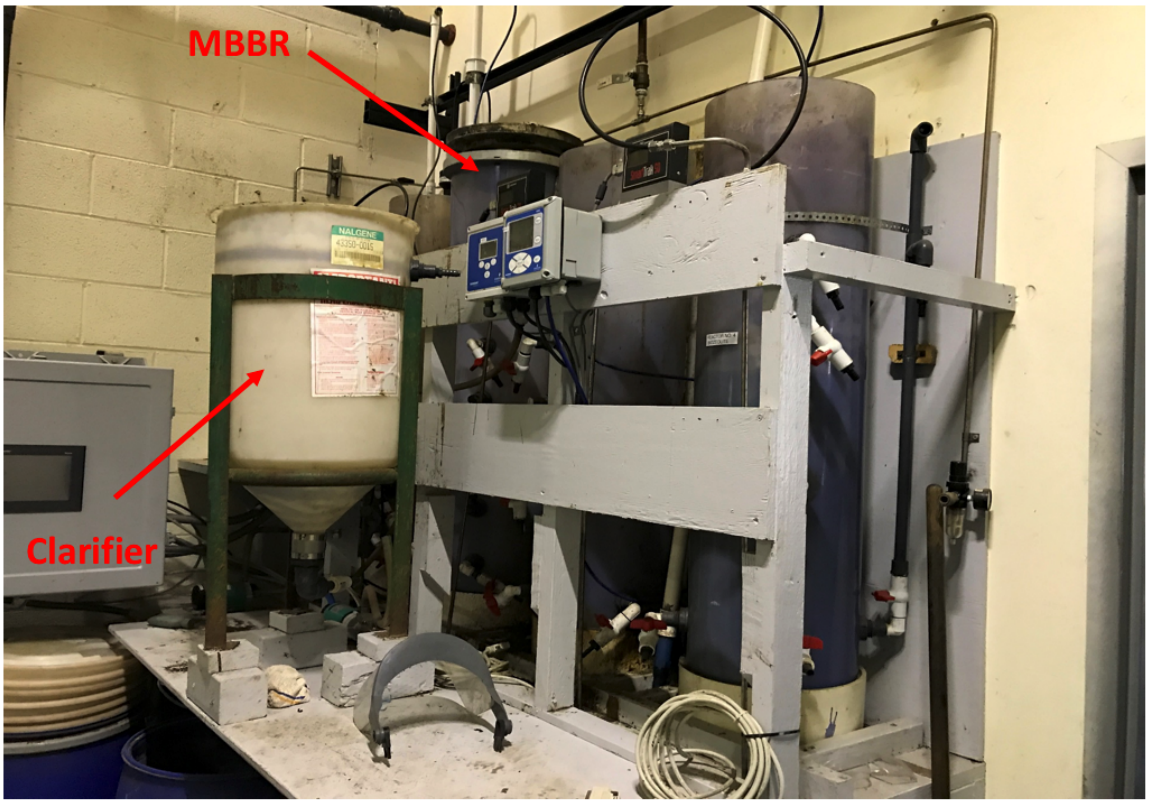


Figure 6.2: The picture of IFAS pilot.

and 6.3b represents the performance of SBR and IFAS treating RS, respectively. With RS directly feed into the systems, the hydraulic retention times (HRTs) of both the systems decreased gradually to increase the nitrogen loading rates (NLRs) of the systems. The HRT of the SBR pilot was decreased from about 24 days to about 1.4 days, getting a maximum NLR of 1.11 $gN/L/d$. A much higher NLR of 3.57 $gN/L/d$ was gained by the IFAS pilot with the HRT decreased to about 0.5 days. The higher NLR of the IFAS pilot also led to higher nitrogen removal rate (NRR). The maximum NRR of the IFAS pilot was 3.03 $gN/L/d$, which was more than 4.5 times higher than the maximum NRR of 0.67 $gN/L/d$ for the SBR pilot. One possibility of the higher NRR of the IFAS pilot was the higher VSS in the system. Figure 1c represents the evolution of VSS and the specific nitrogen removal rate (sNRR) of the two systems. During about 500-day's cultivation, the VSS of the IFAS pilot was fluctuating from 1.26 g/L to 6.77 g/L. Having a lower VSS in general, the VSS of the SBR pilot was fluctuating from 1.09 g/L to 5.69 g/L. Despite the higher VSS in the IFAS pilot, a much higher maximum sNRR of 0.88 $gN/d/gVSS$ was achieved compared with the SBR maximum sNRR of 0.28 $gN/d/gVSS$. This finding indicated that the IFAS configuration had higher efficiency in RS nitrogen removal than the SBR configuration.

From Figure 6.3a and 6.3b, nitrite accumulations were barely detected in both systems. Similar levels of effluent ammonium and effluent nitrate were also found in both systems. The average total nitrogen removal efficiencies (TNREs) of 76.2 % and 73.3 % were achieved in the SBR pilot and the IFAS pilot, respectively. The limited supply of inorganic carbon in the RS was the cause of the limited TN removal efficiencies in both systems. With an average ALK/N molar ratio of 0.94, only about 47 % of ammonium was oxidized into nitrite, leading to the nitrite-N/ammonium-N ratio of only about 0.88. As a result, an excess of ammonium was left untreated in the system, causing lower TNREs. It was believed that the TNRE would be over 90 % with excess ALK available in the influent [26, 160, 256, 257]. Besides the ability of nitrogen removal, the IFAS pilot had higher sCOD RE than the SBR pilot throughout the experiment (Fig 1d). Moreover, both systems have average $NO_3, produced/NH_4, removed$ percentages below 8 %, which was lower than the stoichiometric value of 11%, claiming that heterotrophic denitrification process happened in the systems by consuming nitrate and sCOD.

6.3.2 Nitritation/ANAMMOX pilots treating THP-S

Same with the findings of Zhang et al. in 2016 [182], THP-S had higher levels of ammonium, COD, COD/N ratio but a lower alkalinity/N molar ratio than RS. Figure 6.4 presents the performance of both the SBR pilot and the IFAS pilot feeding with different percentages of THP-S. The operation was performed in two phases, with each phase characterized by different percentages of RS and THP-S in the influent. In phase I, stable operation for both systems were achieved within the course of 29 days by having up to 25 % of THP-S as feed. With the higher COD concentration in the influent, lower average $NO_3, produced/NH_4, removed$ percentages of 2.21 % and 5.17 % were achieved by the SBR pilot and the IFAS pilot, respectively. Compared with the SBR pilot, the IFAS pilot had an average 26.4 % lower effluent ammonium concentration and 117.3 % higher effluent nitrate concentration. Same with treating RS, nitrite was barely detected in both systems. During phase I, the maximum NRRs of 0.65 $gN/L/d$ and 1.76 $gN/L/d$ were achieved by the SBR pilot and the IFAS pilot, with the average TN removal efficiencies of 79.4% and 81.7%. The average sCOD REs of the SBR pilot and the IFAS pilot also reached 52.2 % and 64.8 %, respectively.

More THP-S was introduced to both systems in phase II. During the operation of 36 days, the stable performance was gained by the IFAS pilot, with the average TN removal efficiency of 79.2 % and the maximum NRR of 1.38 $gN/L/d$. Compared with phase I, the average $NO_3, produced/NH_4, removed$ percentage increased to 7.55 %, which was mainly due to the increase of effluent nitrate concentration from 66.56 ± 29.11 mgN/L to 123.46 ± 44.49 mgN/L. Different from the IFAS pilot, the SBR pilot seemed to be much less stable with adding THP-S. Having more THP-S introduced to the SBR pilot, the effluent nitrogen concentrations increased significantly. At day 56, the effluent nitrite concentration surged to 660 mgN/L. Also, the effluent ammonium increased to 827 mgN/L with the effluent nitrate concentration reached to 168 mgN/L, which was much higher than the effluent nitrate

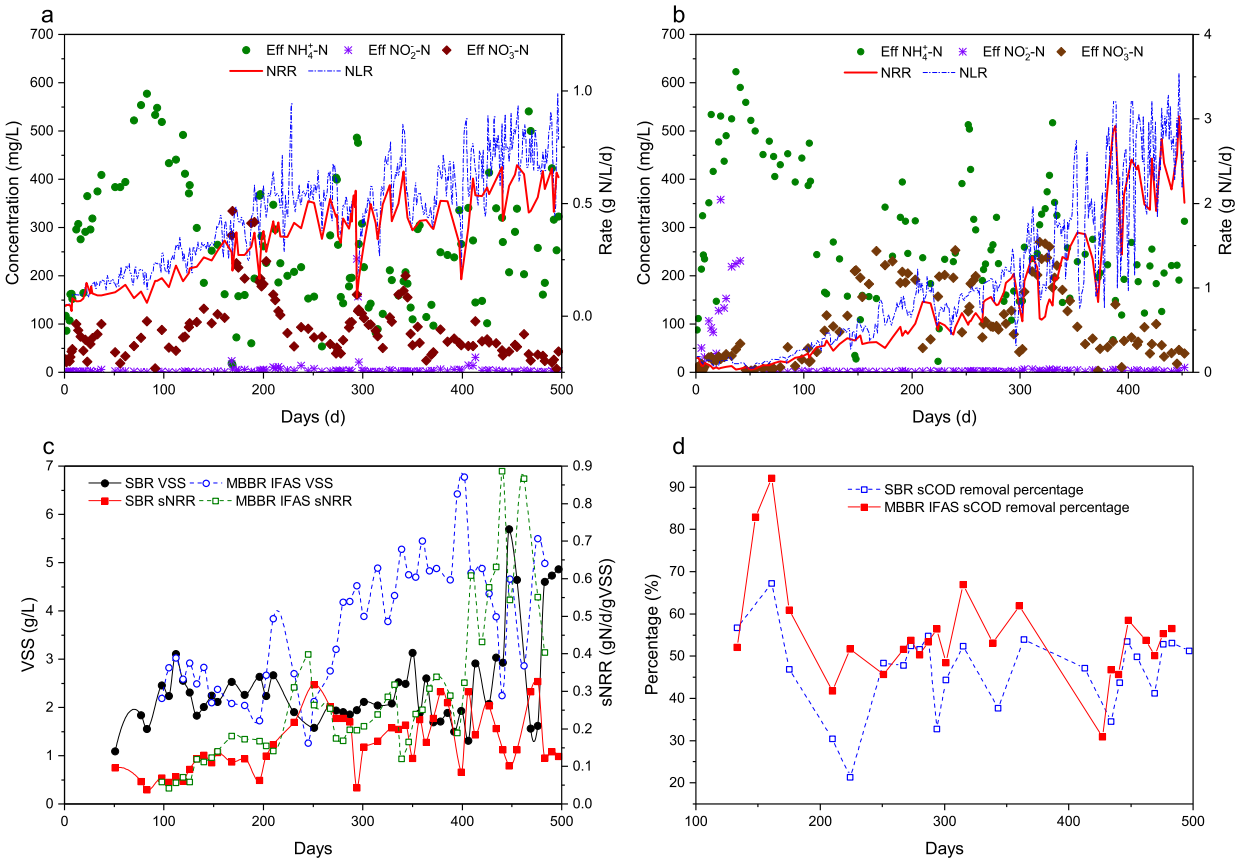


Figure 6.3: **a** The performance of the SBR pilot treating RS. **b** The performance of the IFAS pilot treating RS. **c** The evolution of VSS and sNRR of the two systems. **d** The sCOD RE of the two systems.

concentration of 27.3 ± 9.01 mgN/L during day 31 to day 50. The increase of effluent nitrogen concentrations led to the decrease of NRR and sCOD removal efficiency. Table 6.1 summarizes operational performance throughout the experimental period.

6.3.3 Diversity analysis of microbial structures

Nine DNA samples collected from the SBR pilot and the IFAS pilot were analyzed by 16S rRNA sequencing. The DNA samples and the relevant sampling time are listed in Table 6.2. After performing a series of analytical methods with the sequencing result, 158603 (IFAS-M-1), 168309 (IFAS-M-2), 158133 (IFAS-M-3), 171409 (IFAS-S-1), 162466 (IFAS-S-2), 172973 (IFAS-S-3), 146470 (SBR-1), 142099 (SBR-2), and 139124 (SBR-3) effective

	SBR			IFAS		
	RS	THP-S phase I	THP-S phase II	RS	THP-S phase I	THP-S phase II
NLR ($gN/L/d$)	0.45 ± 0.22	0.72 ± 0.12	0.72 ± 0.14	0.99 ± 0.88	1.13 ± 0.6	1.12 ± 0.48
NRR ($gN/L/d$)	0.34 ± 0.18	0.56 ± 0.083	0.66-0.069	0.83 ± 0.79	1.08 ± 0.4	0.94 ± 0.29
TNRE (%)	76.21 ± 9.89	79.4 ± 8.32	86.28-9.69	73.27 ± 12.14	81.77 ± 5.32	79.21 ± 8.05
Ammonium RE (%)	82.63 ± 8.98	81.13 ± 8.15	87.47-54.96	80.76 ± 10.52	85.67 ± 4.15	87.69 ± 4.43
sCOD RE (%)	46.89 ± 9.93	52.19 ± 7.58	58.76-25.95	55.32 ± 12.3	64.79 ± 9.94	65.19 ± 18.59
$NO_3, produced/NH_4, removed$ Percentage (%)	7.66 ± 5.72	2.21 ± 0.73	1.42-16.65	7.96 ± 6.3	5.17 ± 1.67	7.56 ± 2.81

Table 6.1: The performance of the SBR pilot and the IFAS pilot treating RS and THP-S.

sequences were obtained from each sample. A total of 644 OUTs were achieved at a distance of 0.03. Sequencing integrity was measured using Good's coverage, which approached 100 % in this study, indicating sufficient sequencing depth was detected to describe patterns in the study. After assigning OTUs to the taxonomic category by RDP, the detected bacteria were classified into 31-35 phyla, 50-60 classes, 64-77 orders, 100-116 families, and 107-129 genera.

Alpha diversity indexes including Ace, Chao1, Shannon and Simpson indexes were used to analyze the microbial community richness and diversity (Table 6.2). These results demostrated that DNA samples collected during THP-S Phase II had more community richness and diversity than other DNA samples, which was possibly due to the more complex composition and higher COD/N ratio of influent water by introducing more THP-S. The differences in compositions of communities among samples were calculated according to Bray-Curtis distance metrics. NJ tree was generated to show the change in diversities of species between environments. As shown in Figure 6.5, the cluster analysis reveals the significant changes in the SBR pilot microbial community after feeding with THP-S containing influent. On the other hand, the microbial community structures in the IFAS pilot had less differences. Also, obvious differences of bacterial community structures were shown among the samples of the SBR pilot, the IFAS biofilm and the IFAS suspension.

6.3.4 Microbial community composition analysis by 16s rRNA sequencing

Taxonomic assignments also indicated diversity differences among all the samples at phylum and genus levels. Fig 6.6 illustrates the relative abundances of each major phylum in all the samples. Feeding with RS, differences of microbial community structures were observed between biofilm samples and suspended samples. Predominant phyla of IFAS-M-1 included *Bacterodietes* (22.91 %), *Chloroflexi* (21.52 %), *Ignavibacteriae* (20.5 %), emphProteobacteria (17.03 %) and *Acidobacteria* (13.96 %), while *Bacteroidetes* (32.11 % and 37.45 %), *Proteobacteria* (30.21 % and 29.97 %), *Ignavibacteriae* (14.98 % and 7.84 %), *Chloroflexi* (8.02 % and 11.71 %)were dominant in IFAS-S-1 and SBR-1, respectively. Nitrifying bacteria and denitrifying bacteria were affiliated with *Proteobacteria*. Besides, denitrifying bacteria was also found among *Bacteroidetes*, *Actinomycetes*, *Chloroflexi* and *Firmicutes* [223, 234, 235]. Previous studies reported that *Proteobacteria*, *Chloroflexi*, *Ignavibacteriae*, *Acidobacteria* and *Bacteroidetes* were often detected with *Planctomycetes* in ANAMMOX reactors [234, 250–252, 254]. Small amounts of *Planctomycetes* were detected in IFAS-M-1 (0.74 %), IFAS-S-1 (0.23 %) and SBR-1 (1.29 %), which were similar with 1.09 % of *Planctomycetes* reported in an ANAMMOX upflow anaerobic sludge blanket (UASB) reactor treating high-strength wastewater [258]. *Nitrospira* was also detected with low abundances in IFAS-M-1 (0.25 %), IFAS-S-1 (0.72 %) and SBR-1 (0.74 %).

With THP-S introducing to the systems, distinctions of relative abundances at phylum levels were also observed. From IFAS-M-1 to IFAS-M-3 and IFAS-S-1 to IFAS-S-3, the relative abundances of *Bacteroidetes* were reduced, while that of *Chloroflexi* and *Nitrospira*

Samples	Sampling time	Sampling location	Ace	Chao1	Shannon	Simpson	Good's coverage
SBR-1	Late phase of RS feed	SBR	441.248	447.676	4.962	0.934	1
SBR-2	Late phase of THP-S phase I	SBR	404.944	404.676	5.018	0.923	1
SBR-3	Late phase of THP-S phase II	SBR	455.854	461	5.86	0.955	1
IFAS-M-1	Late phase of RS feed	IFAS biofilm	473.593	469.45	4.951	0.925	1
IFAS-M-2	Late phase of THP-S phase I	IFAS biofilm	485.574	488.037	4.918	0.9	1
IFAS-M-3	Late phase of THP-S phase II	IFAS biofilm	514.939	519.577	5.05	0.902	1
IFAS-S-1	Late phase of RS feed	IFAS suspension	480.549	479.5	5.041	0.917	1
IFAS-S-2	Late phase of THP-S phase I	IFAS suspension	505.058	514.357	4.834	0.903	1
IFAS-S-3	Late phase of THP-S phase II	IFAS suspension	513.084	513.207	6.078	0.965	1

Table 6.2: Sampling information and comparison of alpha diversity indexes amonge all the DNA samples.

were increased. The relative abundances of *Proteobacteria*, *Ignavibacteriae*, *Acidobacteria* and *Planctomycetes* were quite constant among IFAS biofilm samples. However, the relative abundances of *Proteobacteria* and *Planctomycetes* were increased to 36.28 % and 0.85 % from IFAS-S-1 to IFAS-S-3. From SBR-1 to SBR-3, *Proteobacteria* was largely enriched to 41.74 % and became the major phylum. Conversely, *Bacterodietes*, *Chloroflexi*, *Ignavibacteriae*, *Planctomycetes* and *Nitrospira* were reduced.

Fig 6.7 represents the relative abundances of different genera among all the DNA samples. 59.19-79.47 % of reads were unclassified, which might be caused by the complex composition of wastewater. Further study needs to be performed to identify the unclassified reads. *Candidatus Brocadia* was the major ANAMMOX bacteria genus in both the systems. The bacterial community is discussed in two parts: (1) nitrogen cycle bacteria (NB) which is consisted of AnAOB, AOB, nitrite-oxidizing bacteria (NOB) and denitrifying bacteria; (2) other heterotrophic bacteria (HB). In the IFAS pilot, *Candidatus Brocadia* (502-1070 reads, 0.41-0.66 %) mostly presented in the immobilized biofilm rather than the suspended sludge. The finding was coincident with previous studies, which reported that *Candidatus Brocadia* tended to grow in biofilms [234, 259, 260]. The feeding of THP-S slightly decreased *Candidatus Brocadia* abundances in the biofilm. Despite the small amount of *Candidatus Brocadia*, high efficiencies of TN, NH_4^+-N and COD removal rates were achieved by the IFAS pilot treating with both RS and THP-S. In the SBR pilot, *Candidatus Brocadia* was reduced from 1.23 % (1479 reads) to 0.01 % (9 reads) by increasing THP-S percentage in the feed. *SM1A02* was believed to be another genus that can carry out ANAMMOX [261, 262]. Mainly present in the suspended sludge of the IFAS pilot, the relative abundance of *SM1A02* even increased with the increase of THP-S in the feed. Different from *Candidatus Brocadia*, AOB was mainly found in the suspended sludge of the IFAS pilot. Being the major AOB genus, *Nitrosomonas* abundances were relatively constant in both immobilized biofilm samples and suspended samples of the IFAS pilot feeding THP-S. From SBR-1 to SBR-2, *Nitrosomonas* was enriched from 1.93 % (2360 reads) to 4.69 % (5728 reads), while *Nitrosomonas* was decreased to 2.84 % (3466 reads) in SBR-3 with more THP-S in the feed. Denitrifying bacteria classified into genus *H16*, *Denitratisoma*, *Hyphomicrobium*, *Thermomonas*, *Flavobacterium*, *Thauera*, *Pseudomonas* and *Paracoccus* were also detected in both the systems. Notably, NOB genus *Nitrospira* was shown in IFAS-M-1(153 reads, 0.13 %), IFAS-M-2 (428 reads, 0.35 %), IFAS-M-3 (379 reads, 0.31 %), IFAS-S-1 (872 reads, 0.71 %), IFAS-S-2 (625 reads, 0.51 %), IFAS-S-3 (1343 reads, 1.1 %) and SBR-1 (873 reads, 0.72 %).

Besides NB, various HB genera were also observed. For example, *Ignavibacterium* was the most predominant genus in all the DNA samples. Higher relative abundance of *Phaeodactylibacter* genus, which was capable of organic matters removal [263], was found in IFAS-S-1 and SBR samples. *Bryobacteria* (3276-4887 reads, 2.68-4 %), which was affiliated with phlyum *Acidobacteria*, mostly presented in the IFAS biofilm samples. In addition, *Filimonas* (449-1302 reads, 0.37-1.07 %) and *Limnobacter* (738-1248 reads, 0.6-1.02 %) were dominant genera found in the IFAS suspension samples. The increase of THP-S percentage in the feed didn't largely affect the structures of bacterial communities among the IFAS suspension samples. On the contrary, changes of structures of bacterial communities were detected

among IFAS suspension samples and SBR samples feeding with THP-S. Genera with relatively higher abundances including *Mycobacterium* (3508 reads, 2.87%)and *Fastidiosipila* (1133 reads, 0.93 %) were observed in IFAS-S-1, whereas, *Truepera* (1399 reads, 1.15 %), *Sandaracinus* (1745 reads, 1.43 %), *Gelria* (1080 reads, 0.88 %), *Smithella* (1073 reads, 0.88 %) were enriched in IFAS-S-3. In SBR-1, *Turneriella* (2207 reads, 1.81 %) and *Sandaracinus* (1406 reads, 1.15 %) had higher relative abundances. With THP-S introducing into the feed, the dominant heterophic bacteria genera in SBR-3 included *Fastidiosipila* (1279 reads, 1.05 %), *Proteiniphilum* (1642 reads, 1.35 %), *Methanosarcina* (935 reads, 0.77 %), *Gelria* (1837 reads, 1.51 %), *Smithella* (1163 reads, 0.95 %), *Comamonas* (1147 reads, 0.95 %), and *vandinBC27*(628 reads, 0.51 %).

6.4 Discussion

Stable performance was achieved by both the IFAS pilot and the SBR pilot treating RS. With a much higher NRR, the IFAS configuration seems to be a better option. The application of immobilization techniques can effectively improve reactor performance by retaining biomass. The biomass carriers can not only provide the large-specific area for biomass attachment but can also work as the nuclei for enhancing biofilm development. Also, with periodically recycling settled solids in the IFAS configuration, the SRT was extended, and AOB was more likely to grow as flocculated biomass in suspension (Fig 6.8). Having less substrate diffusion limitations in flocs than the thick biofilm, higher efficiency can be achieved by having AOB in suspension. The larger population of AOB in suspension further promoted the production of nitrite. Moreover, AOB inhabited in suspended soils resulting AnAOB on biofilm with a fine outer layer of oxygen scavengers (AOB or other heterotrophic bacteria). The finer out layer on biofilm also improved substrate diffusions for AnAOB, enhancing the activity of AnAOB [160]. As a result, the IFAS configuration can boost TNRE according to biomass retention and better substrate diffusion.

Being the primary genera carrying out ANAMMOX, *Candidatus Brocadia* was mainly observed on the biofilm carriers. It was reported that *Candidatus Brocadia* with a lower polysaccharide/protein ratio preferred to grow in biofilm, as proteins and hydrophobic amino acids were important factors responsible for the formation of AnAOB aggregates [259, 264]. Genera *SM1A02* was also able to carry out ANAMMOX. Previous studies reported the presences of *SM1A02* in an SBR treating municipal wastewater, a one-stage nitritation/ANAMMOX system treating synthetic wastewater, and a hybrid fixed/fluidized beds nitritation/ANAMMOX reactor treating synthetic wastewater [261, 262, 265]. More evidence is required to prove the functions of *SM1A02*. Denitrifying bacteria were also detected in the systems, which explained the lower achieved $NO_3, produced/NH_4, removed$ compared with the stoichiometric ratio. What's more, the ALK produced by denitrification process can compensate the ALK consumed by nitritation and maintain pH balance in the systems. Although the co-existence of NOB was detected in both systems, the small amounts of NOB did not affect the reactor performance. This finding was coincident with the study of Pereira et al. (2014),

which reported that small amounts of NOB could inhibit nitrite accumulate, consume excess DO and benefit ANAMMOX process [234, 266, 267].

With THP-S introducing into the systems during phase I, better performance was achieved in both systems than feeding RS (Table 6.1). In spite of the lower denitrifying bacteria in IFAS biofilm samples and SBR samples, the sCOD RE increased. The observation might be due to the increase of HB, causing by higher COD/N ratio in the influent. AnAOB was increased in the IFAS pilot. Mostly existence in the suspended sludge of the IFAS pilot, *SM1A02* was even enriched with THP-S feed. The phenomenon revealed in this study implied that *SM1A02* might have higher tolerances toward THP-S. Moreover, the increase of *SM1A02* with THP-S feed was probably due to the increase of nitrogen loading. Future studies need to be performed to verify this hypothesis (Fig 6.8). Both AOB and NOB in the IFAS pilot were slightly increased with THP-S feeding, resulting in higher TNRE and ammonium RE. On the other hand, AnAOB and NOB were decreased significantly in the SBR pilot by feeding THP-S, while AOB was increased. However, the nitrite accumulation was barely observed in this phase, claiming the bacterial community in SBR could maintain the nitrogen removal performance. During phase II, the COD/N ratio further increased in the influent via 50 % of THP-S introducing into both the systems. Besides the increase of *SM1A02* in the IFAS suspended sludge, NOB was also increased. It was reported that the proliferation of HB by the increase of COD/N ratio could affect the activity of autotrophic bacteria but not NOB, which would assimilate simple organic compounds under substrate-limited conditions [260, 268]. Conversely, AnAOB and NOB could barely be detected in SBR-3, resulting in the SBR pilot performance failure. The different dynamics of AnAOB in the IFAS pilot and the SBR pilot indicated that the immobilized AnAOB had better tolerances to THP-S than the suspended AnAOB.

Supported by organic matters from influent water, the soluble microbial products (SMP) and extracellular polymeric substances (EPS) released by autotrophs, HB also played important roles in sustaining stable structures of the bacterial community for treating THP-S. For example, *Ignavibacterium*, which was detected in all the samples, is a facultatively anaerobic bacteria being frequently found in ANAMMOX reactor and can utilize nitrite as electron acceptor [269]. Moreover, different HBs were detected between suspended samples and biofilm samples. Higher abundance of phylum *Chloroflexi* was found in biofilm samples. It was reported that the filamentous *Chloroflexi* generated frameworks for initiating granulation and provided stabilizing backbones for microbial aggregates. Also, previous studies revealed that *Chloroflexi* would degrade complex compounds such as polysaccharides and proteins [265, 270, 271]. According to Gu et al. (2018), much higher levels of polysaccharides and proteins were detected in THP-S, explaining the increase of *Chloroflexi* in the IFAS pilot feeding THP-S [223]. Genera *limnobacter* and *Bryobacter* were also detected in biofilm samples. Being able to degrade bio-refractory organics, these aerobic bacteria could protect AnAOB from the inhibition of oxygen and organic matters. Wang et al. (2018) reported the co-occurrence through positive correlative among AnAOB, *limnobacter* and *Bryobacter* in an IFAS reactor treating mainstream, and illustrated that the HB could protect AnAOB from hostile environments and provide great benefits to AnAOB in organic matter environment

[240, 260, 272, 273]. THP-S addition significantly increased the abundances of *Truepera* and *Sandaracinus* in the IFAS suspended samples. *Truepera* is affiliated with the extremophile phylum *Dienococcus-Thermus*. It was believed that *Truepera* could tolerate the hazards in industrial wastewater and acclimate to mature landfill leachate, benefiting the stabilization of simultaneous nitritation, ANAMMOX and denitrification (SNAD) process treating mature landfill leachate [240]. *Sandaracinus*, a starch-degrading myxobacterium, was also observed in a two-stage nitritation/ANAMMOX process treating mature landfill leachate [274]. In the SBR pilot, the increase of THP-S resulted in the abundance reductions of *Sandaracinus* and *Turneriella*, which is an aerobic chemo-organotroph similar with *Limnobacter* and *Bryobacter* [275]. Differently, various fermentation bacteria were raised in the SBR with increasing of THP-S, such as *Fastidiosipila*, *vandinBC27* and *Methanosarcina*. Besides, proteolytic anaerobic bacteria *Proteinphilum*, which was applied for polycyclic aromatic hydrocarbons removal in sewage sludge, was increased with the increase of THP-S [269, 276]. The large increase of fermentation bacteria implied that the symbiotic HB had been taken over by fermentation bacteria, which might be related to the unstabilized structures of the bacterial community in the SBR pilot. It is possible that the turn over of HB structures in the SBR caused the diminished AnAOB abundance, which was due to loss of granulation backbone and protection from mutually symbiotic HB. In summary, the IFAS configuration can benefit the stabilization of bacterial community structures by raising mutually symbiotic HB, while the structures of the bacterial community in the SBR was unstabilized with increasing THP-S.

6.5 Conclusions

Treating RS, a much higher maximum sNRR of 0.88 $gN/d/gVSS$ was gained by the IFAS pilot compared to the sNRR of 0.28 $gN/d/gVSS$ by the SBR pilot. Also, the IFAS pilot had more resistant to THP-S than the SBR pilot. Feeding with THP-S, the IFAS pilot achieved NRR of 1.38 $gN/L/d$ while the effluent nitrogen concentrations of the SBR pilot increased significantly, leading to the SBR pilot crash. 16s rRNA sequencing revealed the distribution of AOB and AnAOB in the IFAS pilot, where AOB was mostly observed in the suspended samples, and AnAOB was mostly detected in the biofilm samples. The distribution decreased the diffusion limits of substrates, improving the NRR of IFAS. Moreover, despite the change of feed from RS to THP-S, much more stable bacterial community structures of the IFAS samples were shown with high abundances of mutually symbiotic HB. On the other hand, the abundances of fermentation bacteria were increased in SBR samples with the increasing of THP-S feed. At the same time, the abundance of AnAOB was significantly reduced. This study concludes that IFAS configuration would be a better choice for nitritation/ANAMMOX process treating THP-S. With biomass carriers providing the surface for biomass accumulating, the IFAS configuration can retain biomass and improve the build-up of the robust bacterial ecosystem, enabling nitritation/ANAMMOX process to work under a hostile environment.

%	Phase I	Phase II
RS	100-75	50
THPS	0-25	50

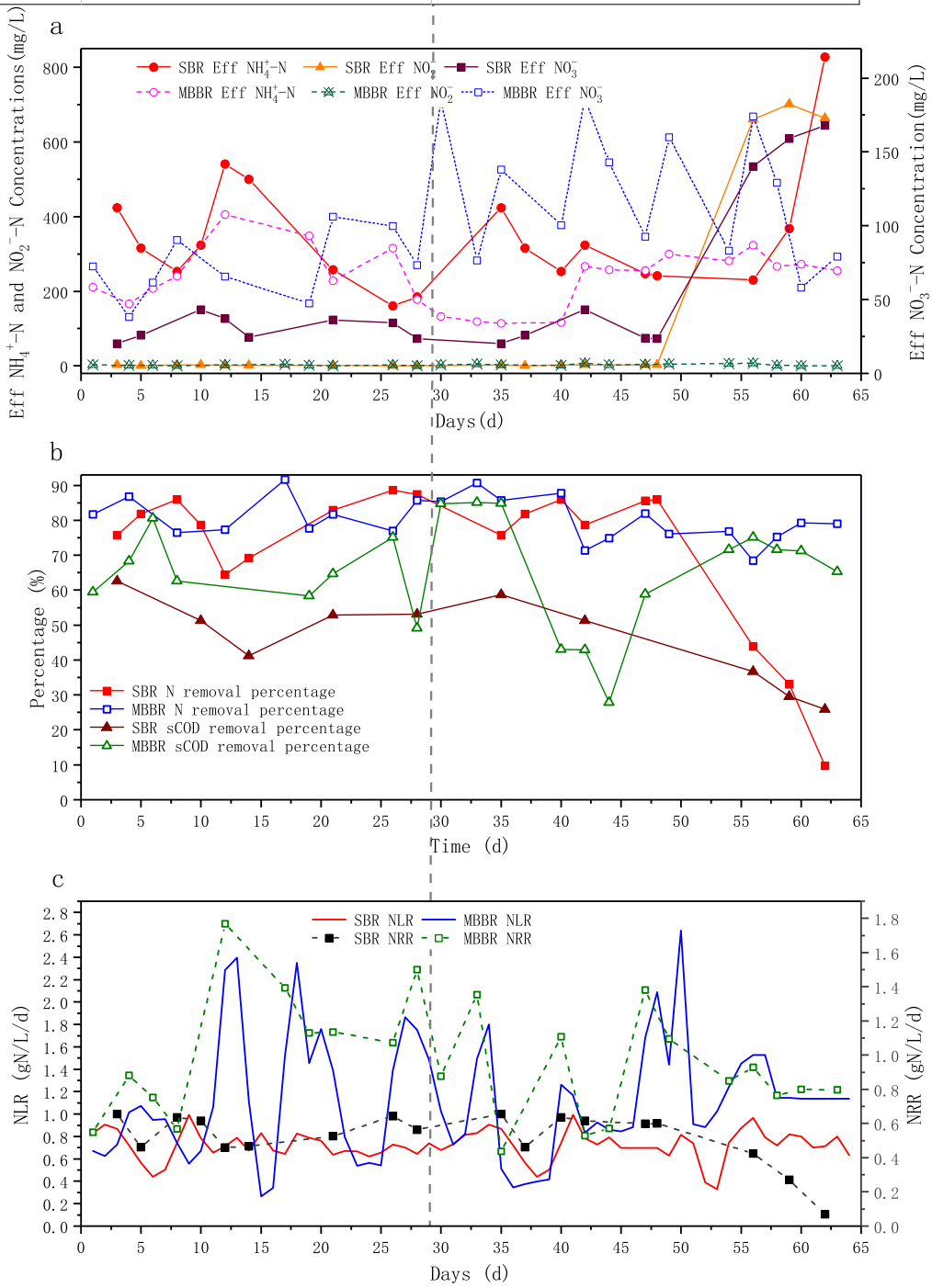


Figure 6.4: The performance of the SBR pilot and the IFAS pilot treating THP-S.

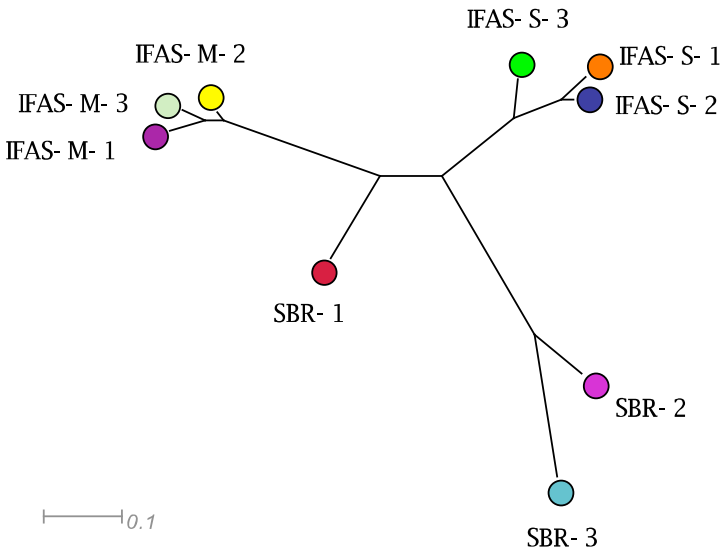


Figure 6.5: Phylogenetic tree of 16s rRNA gene sequences. The tree illustrates the relationships of the 9 samples collected in this study using Bay-Curtis distances with NJ analysis. The scale bar represents 10 % sequence divergence.

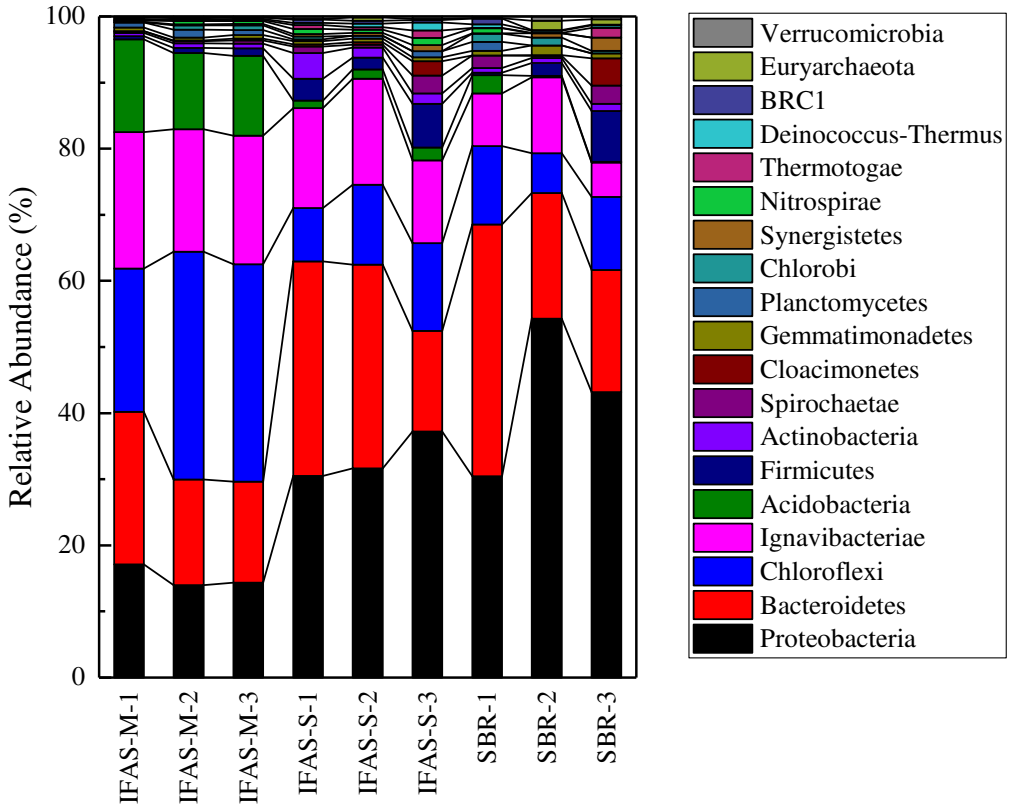


Figure 6.6: Relative abundances of each major phylum. The figure only shows the phlum with relative abundaces $> 0.5\%$

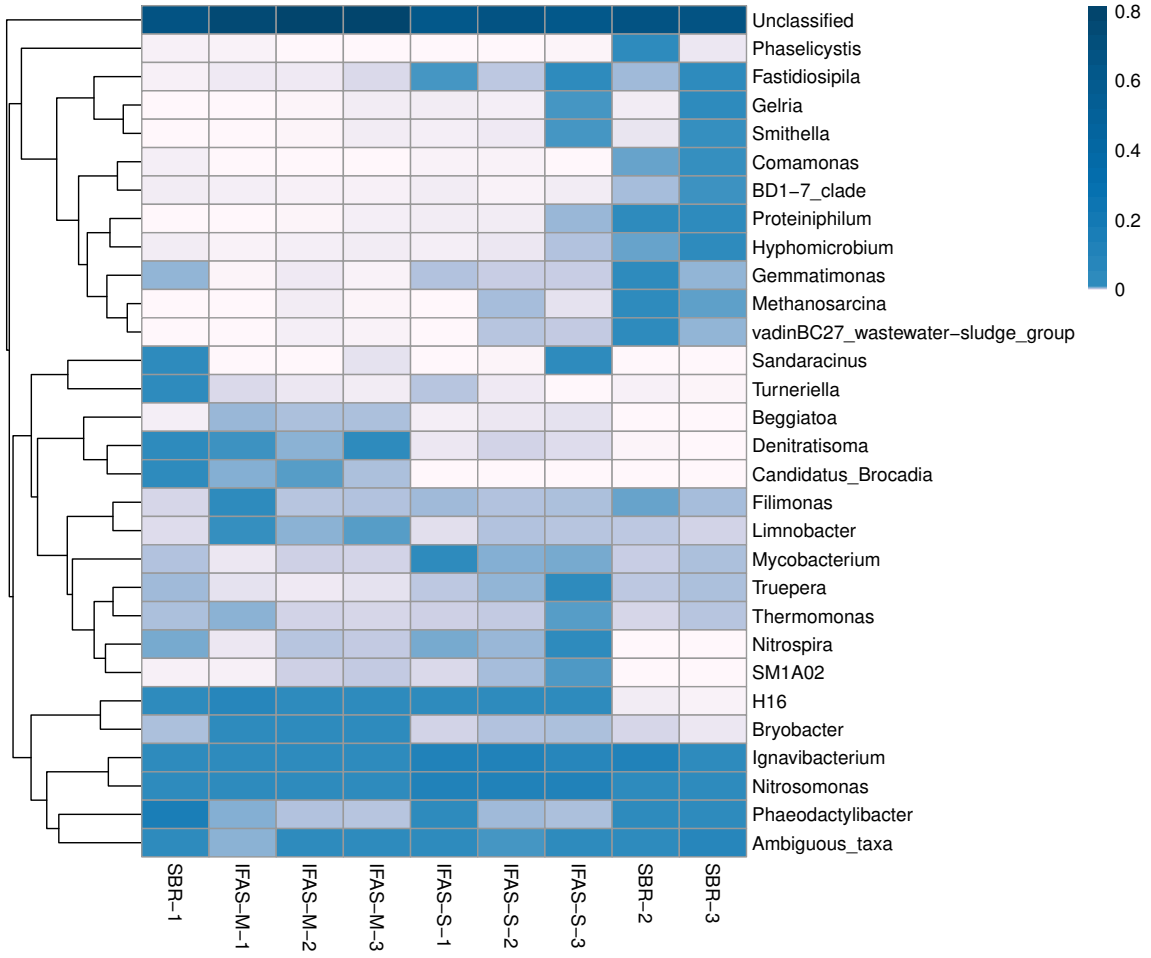


Figure 6.7: Relative abundances of bacterial community composition detected in different samples at genus levels showing in a heatmap. Titles for rows are genus names, and title for columns are sample information. The left side of the graph is the genus clustering tree, and the top is the sample clustering tree.

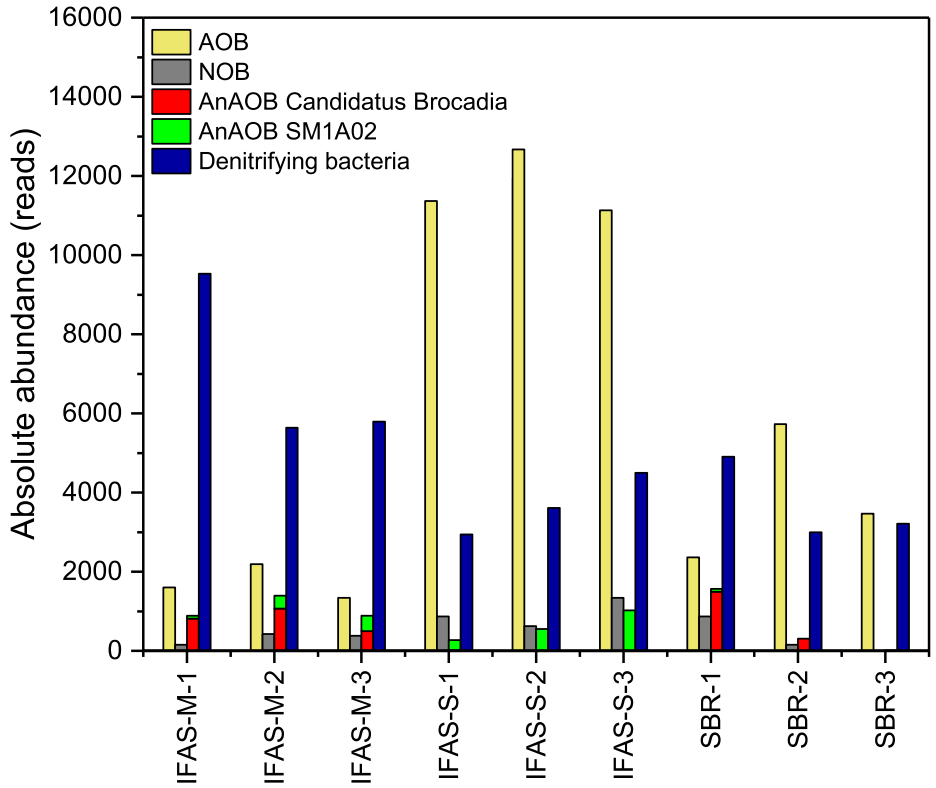


Figure 6.8: Absolute abudances of nitrogen cycle related bacterial communities detected in different samples.

Chapter 7

Conclusions

7.1 Summary of Major Findings

The overall objective of this dissertation is to determine the inhibition mechanism of thermal hydrolysis pre-treated sidestream (THP-S) on nitritation/ANAMMOX process. Specifically, the dissertation has quantified the inhibition kinetics of THP-S on nitritation process and ANAMMOX process, respectively, and has analyzed the inhibitory effects on the levels of microbial community structures and relevant functional genes, while providing practical references for establishing robust nitritation/ANAMMOX process treating THP-S by applying optimized operational strategies and techniques.

Chapter 3 presented the inhibitory effects of THP-S on an independent nitritation process. Being major functional species in the nitritation process, ammonium-oxidizing bacteria (AOB), were exposed to THP-S in both short-term and long-term. The short-term tests revealed the inhibitory effects of THP-S on AOB activity. Also, the inhibition kinetics can be described with the Luong inhibition model, which presented a relationship between the decrease in the AOB activity with the increase of THP-S percentage in the influent. With long-term exposure to THP-S, the nitrite accumulation percentage and the ammonium conversion rate decreased significantly in the nitritation process, indicating that long-term acclimation cannot mediate the inhibition of AOB activity by THP-S. The study on the changes of AOB concentrations during long-term exposure indicated a strong correlation between the decrease in the activity and the decrease in AOB concentrations, implying that the nitritation performance failure might be the result of AOB concentration decrease. High F: M growth kinetic study confirmed that THP-S reduced the effective maximum specific growth rate of AOB from 0.77 to 0.068 d^{-1}, which resulted in the washout of AOB from the nitritation process. This finding verified that THP-S inhibited both activity and growth of AOB while providing useful operational references for establishing robust nitritation process treating THP-S.

Chapter 4 studied the inhibitory effects of THP-S on an independent ANAMMOX process. THP-S contained a higher concentration of chemical oxygen demand (COD) compared

with regular sidestream (RS). Short-term ANAMMOX bacteria activity tests were performed using different dilutions of THP-S and RS, as well as different concentrations of CODs. Similar trends were observed between the two groups of short-term tests, implying that the high COD concentration in THP-S inhibited ANAMMOX activity. The quantitative relationship between the inhibition response and the concentration of COD can be described by the non-competitive inhibition kinetic model. The long-term study successfully established one-stage ANAMMOX process treating 100% RS, while 70% of THP-S inhibited ANAMMOX process performance. 16s rRNA sequencing detected 4.35-8.3% of *Candidatus Brocadia* in RS fed ANAMMOX process, but only 1.94-2.36% of *Candidatus Brocadia* in THP-S fed ANAMMOX process. The metagenomic analysis found out that rather than denitrifier, dissimilatory nitrate to ammonium (DNRA) bacteria took a large portion in the systems, and THP-S fed ANAMMOX system had more DNRA than RS fed ANAMMOX system. It was concluded that the DNRA bacteria could out-compete ANAMMOX bacteria by breaking ammonium to nitrite ratio for ANAMMOX feed, leading to ANAMMOX bacteria washout.

Chapter 5 focused on the recovery of nitritation process by applying optimized operational strategies and implemented THP-S nitrogen removal using two-stage nitritation/ANAMMOX process. Extended sludge retention time (SRT), longer hydraulic retention time (HRT) and elevated dissolved oxygen(DO) set-point were applied to overcome the inhibition of THP-S on both the activity and the growth of AOB. After the operation of 80 days, an average ammonium to nitrite conversion efficiency of 55.9% was achieved. Microbial structure analysis showed that the AOB species including *Nitrosomonas*, increased from 1.3% to 4.8% with the optimized operational strategies. The nitritation pre-treatment can effectively decrease the COD and protein contents in both RS and THP-S, providing more suitable feed to the subsequent ANAMMOX process. Stable performance was achieved in the ANAMMOX process treating both nitritation pre-treated RS and nitritation pre-treated THP-S. To verify the effects of COD on the ANAMMOX process, an extra 500 mg/L of COD was added to the nitritation pre-treated THP-S feed, and a decrease of ANAMMOX process performance was observed. Microbial structure analysis did not show much difference between the samples with extra COD inputs and without extra COD input.

Chapter 6 presented results of two one-stage nitritation/ANAMMOX systems, which were integrated fixed-biofilm activated sludge system (IFAS) and sequencing batch reactor (SBR), to treat both RS and THP-S and to compare the feasibilities and efficiencies of the two systems. With RS as feed, IFAS gained a much higher nitrogen removal rate (NRR) of 3.03 $gN/L/d$ than SBR, of which the NRR was 0.67 $gN/L/d$. Also, IFAS was a better choice for treating THP-S. With THP-S as feed, IFAS gained an NRR of 1.38 %, while performance failure was observed in SBR. Microbial structure analysis revealed a much more stable bacterial structure in IFAS with most ANAMMOX bacteria found in the biofilm samples and most AOB found in the suspended samples. The distribution can effectively reduce the diffusion limits of substrates, improving the NRR of IFAS. Also, a high abundance of mutually symbiotic heterotrophic bacteria was observed in IFAS, while a high abundance of fermentation bacteria was observed in SBR treating THP-S. It was concluded that IFAS being a better option for treating THP-S can retain biomass and improve the build-up of

the robust bacterial ecosystem, enabling nitritation/ANAMMOX process to work under a hostile environment.

7.2 Recommendations for Future Research

The results from chapter 3 indicated that THP-S could not only inhibit AOB activity but can also suppress the growth rate of AOB. Even though in Chapter 5, the nitritation process was recovered through a series of operational strategies adjustments, the longer HRT will significantly decrease the NRR for the entire nitrogen removal process. Previous study reported that the inhibition of AOB by THP-S was closely associated with particulate and colloidal organics, which can limit the diffusion of substrates and cause a decrease of AOB activity [204]. As a result, the operation of nitritation process can benefit from the pre-treatment of THP-S to reduce the contents of particulate and colloidal CODs and the optimization of the dewatering process to eliminate the inhibitors.

The two-stage nitritation/ANAMMOX process studied in Chapter 5 illustrated that the pre-treatment of THP-S by the nitritation process can reduce the COD levels in THP-S and provide more suitable influent for the ANAMMOX process. However, the two-stage configuration is not favorable for practical industrial application. Based on the results from Chapter 4, ANAMMOX bacteria was washout out from the system due to the high COD concentration, which can stimulate the enrichment of heterotrophic bacteria in the ANAMMOX process. Therefore, the application of immobilization techniques became a good option for implementing the single-stage nitritation/ANAMMOX process treating THP-S. The IFAS configuration studied in Chapter 6 revealed that the immobilization can effectively prevent ANAMMOX bacteria from being washed out. Other immobilization technique, such as gel entrapment, might also be a good option for establishing nitritation/ANAMMOX process.

Compared with conventional nitrification and denitrification process, the nitritation/ANAMMOX process is much more economical and environmentally favorable. The widespread application of nitritation/ANAMMOX process is mainly limited due to the long start-up time and slow growth rate of ANAMMOX bacteria. Fast enrichment of ANAMMOX bacteria would always be an interesting topic because of this reason. Moreover, wastewater nitrogen removal can benefit a lot form the commercial ANAMMOX bacteria seeds.

Bibliography

[1] James N Galloway, II Hiram Levy, and Prasad S Kasibhatla. "Year 2020: Consequences of population growth and development on deposition of oxidized nitrogen". In: *Ambio* (1994), pp. 120–123.

[2] Vaclav Smil. "Global population and the nitrogen cycle". In: *Scientific American* 277.1 (1997), pp. 76–81.

[3] Vaclav Smil. "Nitrogen and food production: proteins for human diets". In: *AMBIO: A Journal of the Human Environment* 31.2 (2002), pp. 126–131.

[4] Rosa María Martínez-Espinosa et al. *Enzymology and ecology of the nitrogen cycle*. 2011.

[5] James N Galloway et al. "The nitrogen cascade". In: *AIBS Bulletin* 53.4 (2003), pp. 341–356.

[6] James N Galloway et al. "Nitrogen cycles: past, present, and future". In: *Biogeochemistry* 70.2 (2004), pp. 153–226.

[7] Jan Willem Erisman et al. "How a century of ammonia synthesis changed the world". In: *Nature Geoscience* 1.10 (2008), p. 636.

[8] Jing Huang et al. "Nitrogen and phosphorus losses and eutrophication potential associated with fertilizer application to cropland in China". In: *Journal of Cleaner Production* 159 (2017), pp. 171–179.

[9] K Lassey and M Harvey. "Nitrous oxide: the serious side of laughing gas". In: *Water Atmos* 15.2 (2007), pp. 10–11.

[10] James E Cloern and Alan D Jassby. "Drivers of change in estuarine-coastal ecosystems: Discoveries from four decades of study in San Francisco Bay". In: *Reviews of Geophysics* 50.4 (2012).

[11] Phoebe Grow et al. "Development of a Conceptual Nutrient Trading Program for San Francisco Bay". In: *Proceedings of the Water Environment Federation* 2017.15 (2017), pp. 753–771.

[12] Perry L McCarty, Jaeho Bae, and Jeonghwan Kim. *Domestic wastewater treatment as a net energy producer–can this be achieved?* 2011.

[13] Young-Ho Ahn. "Sustainable nitrogen elimination biotechnologies: a review". In: *Process Biochemistry* 41.8 (2006), pp. 1709–1721.

[14] A Teske et al. "Evolutionary relationships among ammonia-and nitrite-oxidizing bacteria." In: *Journal of bacteriology* 176.21 (1994), pp. 6623–6630.

[15] Jia You et al. "Ammonia-oxidizing archaea involved in nitrogen removal". In: *Water Research* 43.7 (2009), pp. 1801–1809.

[16] Pilar Junier et al. "Phylogenetic and functional marker genes to study ammonia-oxidizing microorganisms (AOM) in the environment". In: *Applied Microbiology and Biotechnology* 85.3 (2010), pp. 425–440.

[17] Yutaka Okano et al. "Application of real-time PCR to study effects of ammonium on population size of ammonia-oxidizing bacteria in soil". In: *Applied and environmental microbiology* 70.2 (2004), pp. 1008–1016.

[18] Timothy A Hovanec et al. "Nitrospira-like bacteria associated with nitrite oxidation in freshwater aquaria". In: *Applied and environmental microbiology* 64.1 (1998), pp. 258–264.

[19] P Tavares et al. "Metalloenzymes of the denitrification pathway". In: *Journal of inorganic biochemistry* 100.12 (2006), pp. 2087–2100.

[20] Julián Carrera, Teresa Vicent, and Javier Lafuente. "Effect of influent COD/N ratio on biological nitrogen removal (BNR) from high-strength ammonium industrial wastewater". In: *Process Biochemistry* 39.12 (2004), pp. 2035–2041.

[21] Leonidia Maria Castro Daniel et al. "Removal of ammonium via simultaneous nitrification–denitrification nitrite-shortcut in a single packed-bed batch reactor". In: *Bioresource Technology* 100.3 (2009), pp. 1100–1107.

[22] Shuai Yang and Fenglin Yang. "Nitrogen removal via short-cut simultaneous nitrification and denitrification in an intermittently aerated moving bed membrane bioreactor". In: *Journal of hazardous materials* 195 (2011), pp. 318–323.

[23] Xiong Zheng et al. "Increasing municipal wastewater BNR by using the preferred carbon source derived from kitchen wastewater to enhance phosphorus uptake and short-cut nitrification-denitrification". In: *Chemical Engineering Journal* 344 (2018), pp. 556–564.

[24] Vel M Vadivelu, Jurg Keller, and Zhiguo Yuan. "Effect of free ammonia and free nitrous acid concentration on the anabolic and catabolic processes of an enriched Nitrosomonas culture". In: *Biotechnology and bioengineering* 95.5 (2006), pp. 830–839.

[25] Yuan Xue et al. "The influence of controlling factors on the start-up and operation for partial nitrification in membrane bioreactor". In: *Bioresource Technology* 100.3 (2009), pp. 1055–1060.

[26] Christian Fux et al. "Biological treatment of ammonium-rich wastewater by partial nitritation and subsequent anaerobic ammonium oxidation (anammox) in a pilot plant". In: *Journal of biotechnology* 99.3 (2002), pp. 295–306.

[27] A Mulder et al. "Anaerobic ammonium oxidation discovered in a denitrifying fluidized bed reactor". In: *FEMS microbiology ecology* 16.3 (1995), pp. 177–183.

[28] Boran Kartal et al. "Anammoxgrowth physiology, cell biology, and metabolism". In: *Advances in microbial physiology*. Vol. 60. Elsevier, 2012, pp. 211–262.

[29] Mamoru Oshiki et al. "Physiological characteristics of the anaerobic ammonium-oxidizing bacterium Candidatus Brocadia sinica". In: *Microbiology* 157.6 (2011), pp. 1706–1713.

[30] E1 Broda. "Two kinds of lithotrophs missing in nature". In: *Zeitschrift für allgemeine Mikrobiologie* 17.6 (1977), pp. 491–493.

[31] Astrid A Van de Graaf et al. "Anaerobic oxidation of ammonium is a biologically mediated process." In: *Applied and environmental microbiology* 61.4 (1995), pp. 1246–1251.

[32] Mare Strous et al. "The sequencing batch reactor as a powerful tool for the study of slowly growing anaerobic ammonium-oxidizing microorganisms". In: *Applied microbiology and biotechnology* 50.5 (1998), pp. 589–596.

[33] Mike SM Jetten et al. "Biochemistry and molecular biology of anammox bacteria". In: *Critical reviews in biochemistry and molecular biology* 44.2-3 (2009), pp. 65–84.

[34] John A Fuerst. *Planctomycetes: Cell Structure, Origins and Biology*. Springer, 2013.

[35] Mumtazah Ibrahim et al. "Enrichment of anaerobic ammonium oxidation (anammox) bacteria for short start-up of the anammox process: a review". In: *Desalination and Water Treatment* 57.30 (2016), pp. 13958–13978.

[36] Laura van Niftrik and Mike SM Jetten. "Anaerobic ammonium-oxidizing bacteria: unique microorganisms with exceptional properties". In: *Microbiology and molecular biology reviews* 76.3 (2012), pp. 585–596.

[37] Jianwei Li et al. "A Critical Review of One-stage Anammox Processes for Treating Industrial Wastewater: Optimization Strategies Based on Key Functional Microorganisms". In: *Bioresource technology* (2018).

[38] Boran Kartal et al. "Anammox bacteria disguised as denitrifiers: nitrate reduction to dinitrogen gas via nitrite and ammonium". In: *Environmental microbiology* 9.3 (2007), pp. 635–642.

[39] Boran Kartal et al. "Candidatus Anammoxoglobus propionicus a new propionate oxidizing species of anaerobic ammonium oxidizing bacteria". In: *Systematic and applied microbiology* 30.1 (2007), pp. 39–49.

[40] Boran Kartal et al. "Candidatu s Brocadia fulgida: an autofluorescent anaerobic ammonium oxidizing bacterium". In: *FEMS microbiology ecology* 63.1 (2008), pp. 46–55.

[41] Marc Strous et al. "Deciphering the evolution and metabolism of an anammox bacterium from a community genome". In: *Nature* 440.7085 (2006), p. 790.

[42] Sitong Liu et al. "Application of anaerobic ammonium-oxidizing consortium to achieve completely autotrophic ammonium and sulfate removal". In: *Bioresource technology* 99.15 (2008), pp. 6817–6825.

[43] Bo Thamdrup and Tage Dalsgaard. "Production of N2 through anaerobic ammonium oxidation coupled to nitrate reduction in marine sediments". In: *Applied and environmental microbiology* 68.3 (2002), pp. 1312–1318.

[44] C Ryan Penton, Allan H Devol, and James M Tiedje. "Molecular evidence for the broad distribution of anaerobic ammonium-oxidizing bacteria in freshwater and marine sediments". In: *Applied and environmental microbiology* 72.10 (2006), pp. 6829–6832.

[45] Hui Li et al. "Molecular detection of anaerobic ammonium-oxidizing (anammox) bacteria in high-temperature petroleum reservoirs". In: *Microbial ecology* 60.4 (2010), pp. 771–783.

[46] Marcel MM Kuypers et al. "Anaerobic ammonium oxidation by anammox bacteria in the Black Sea". In: *Nature* 422.6932 (2003), p. 608.

[47] Rikke Louise Meyer, Nils Risgaard-Petersen, and Diane Elizabeth Allen. "Correlation between anammox activity and microscale distribution of nitrite in a subtropical mangrove sediment". In: *Applied and environmental microbiology* 71.10 (2005), pp. 6142–6149.

[48] Andrea Jaeschke et al. "16S rRNA gene and lipid biomarker evidence for anaerobic ammonium-oxidizing bacteria (anammox) in California and Nevada hot springs". In: *FEMS microbiology ecology* 67.3 (2009), pp. 343–350.

[49] Mariusz Tomaszewski, Grzegorz Cema, and Aleksandra Ziembińska-Buczyńska. "Influence of temperature and pH on the anammox process: a review and meta-analysis". In: *Chemosphere* 182 (2017), pp. 203–214.

[50] J Gijs Kuenen. "Anammox bacteria: from discovery to application". In: *Nature Reviews Microbiology* 6.4 (2008), p. 320.

[51] Marc Strous et al. "Missing lithotroph identified as new planctomycete". In: *Nature* 400.6743 (1999), p. 446.

[52] Bao-lan Hu et al. "Identification and quantification of anammox bacteria in eight nitrogen removal reactors". In: *Water research* 44.17 (2010), pp. 5014–5020.

[53] Boran Kartal et al. "Candidatu s Brocadia fulgida: an autofluorescent anaerobic ammonium oxidizing bacterium". In: *FEMS microbiology ecology* 63.1 (2008), pp. 46–55.

[54] JC Araujo et al. "Anammox bacteria enrichment and characterization from municipal activated sludge". In: *Water Science and Technology* 64.7 (2011), pp. 1428–1434.

[55] Yuko Narita et al. "Enrichment and physiological characterization of an anaerobic ammonium-oxidizing bacterium Candidatus Brocadia sapporoensis". In: *Systematic and applied microbiology* 40.7 (2017), pp. 448–457.

[56] Hongkeun Park et al. "Discovery and metagenomic analysis of an anammox bacterial enrichment related to Candidatus Brocadia caroliniensis in a full-scale glycerol-fed nitritation-denitritation separate centrate treatment process". In: *Water research* 111 (2017), pp. 265–273.

[57] Hiroyuki Okamoto et al. "Development of a fixed-bed anammox reactor with high treatment potential". In: *Biodegradation* 24.1 (2013), pp. 99–110.

[58] Markus Schmid et al. "Molecular evidence for genus level diversity of bacteria capable of catalyzing anaerobic ammonium oxidation". In: *Systematic and applied microbiology* 23.1 (2000), pp. 93–106.

[59] Zhe-Xue Quan et al. "Diversity of ammonium-oxidizing bacteria in a granular sludge anaerobic ammonium-oxidizing (anammox) reactor". In: *Environmental Microbiology* 10.11 (2008), pp. 3130–3139.

[60] Muhammad Ali et al. "Physiological characterization of anaerobic ammonium oxidizing bacterium C andidatus J ettenia caeni". In: *Environmental microbiology* 17.6 (2015), pp. 2172–2189.

[61] SV Khramenkov et al. "A novel bacterium carrying out anaerobic ammonium oxidation in a reactor for biological treatment of the filtrate of wastewater fermented sludge". In: *Microbiology* 82.5 (2013), pp. 628–636.

[62] Boran Kartal et al. "Candidatus Anammoxoglobus propionicus a new propionate oxidizing species of anaerobic ammonium oxidizing bacteria". In: *Systematic and applied microbiology* 30.1 (2007), pp. 39–49.

[63] Yi-Guo Hong et al. "Residence of habitat-specific anammox bacteria in the deep-sea subsurface sediments of the South China Sea: analyses of marker gene abundance with physical chemical parameters". In: *Microbial ecology* 62.1 (2011), pp. 36–47.

[64] Clara A Fuchsman et al. "Free-living and aggregate-associated Planctomycetes in the Black Sea". In: *FEMS microbiology ecology* 80.2 (2012), pp. 402–416.

[65] Markus Schmid et al. "Candidatus Scalindua brodae, sp. nov., Candidatus Scalindua wagneri, sp. nov., two new species of anaerobic ammonium oxidizing bacteria". In: *Systematic and applied microbiology* 26.4 (2003), pp. 529–538.

[66] Dagmar Woebken et al. "A microdiversity study of anammox bacteria reveals a novel Candidatus Scalindua phylotype in marine oxygen minimum zones". In: *Environmental Microbiology* 10.11 (2008), pp. 3106–3119.

[67] Jack van de Vossenberg et al. "The metagenome of the marine anammox bacterium Candidatus Scalindua profundaillustrates the versatility of this globally important nitrogen cycle bacterium". In: *Environmental microbiology* 15.5 (2013), pp. 1275–1289.

[68] Joost Brandsma et al. "A multi-proxy study of anaerobic ammonium oxidation in marine sediments of the Gullmar Fjord, Sweden". In: *Environmental microbiology reports* 3.3 (2011), pp. 360–366.

[69] Huosheng Li et al. "Fast start-up of ANAMMOX reactor: operational strategy and some characteristics as indicators of reactor performance". In: *Desalination* 286 (2012), pp. 436–441.

[70] Chong-Jian Tang et al. "Characterization and quantification of anammox start-up in UASB reactors seeded with conventional activated sludge". In: *International Biodeterioration & Biodegradation* 82 (2013), pp. 141–148.

[71] Yasunori Kawagoshi et al. "Temperature effect on nitrogen removal performance and bacterial community in culture of marine anammox bacteria derived from sea-based waste disposal site". In: *Journal of bioscience and bioengineering* 113.4 (2012), pp. 515–520.

[72] Søren Rysgaard et al. "Denitrification and anammox activity in Arctic marine sediments". In: *Limnology and Oceanography* 49.5 (2004), pp. 1493–1502.

[73] Ren-Cun Jin et al. "The inhibition of the Anammox process: a review". In: *Chemical Engineering Journal* 197 (2012), pp. 67–79.

[74] Kazuichi Isaka, Tatsuo Sumino, and Satoshi Tsuneda. "High nitrogen removal performance at moderately low temperature utilizing anaerobic ammonium oxidation reactions". In: *Journal of bioscience and bioengineering* 103.5 (2007), pp. 486–490.

[75] J Dosta et al. "Short-and long-term effects of temperature on the Anammox process". In: *Journal of hazardous materials* 154.1-3 (2008), pp. 688–693.

[76] Michele Laureni et al. "Activity and growth of anammox biomass on aerobically pre-treated municipal wastewater". In: *Water research* 80 (2015), pp. 325–336.

[77] Qiong Guo et al. "Anaerobic ammonium oxidation (anammox) under realistic seasonal temperature variations: Characteristics of biogranules and process performance". In: *Bioresource technology* 192 (2015), pp. 765–773.

[78] AC Anthonisen et al. "Inhibition of nitrification by ammonia and nitrous acid". In: *Journal (Water Pollution Control Federation)* (1976), pp. 835–852.

[79] Marc Strous et al. "Effects of aerobic and microaerobic conditions on anaerobic ammonium-oxidizing (anammox) sludge." In: *Applied and environmental microbiology* 63.6 (1997), pp. 2446–2448.

[80] Wouter RL Van der Star et al. "Startup of reactors for anoxic ammonium oxidation: experiences from the first full-scale anammox reactor in Rotterdam". In: *Water research* 41.18 (2007), pp. 4149–4163.

[81] Ikuo Tsushima et al. "Development of high-rate anaerobic ammonium-oxidizing (anammox) biofilm reactors". In: *Water research* 41.8 (2007), pp. 1623–1634.

[82] Yujie Qin et al. "Impact of substrate concentration on anammox-UBF reactors start-up". In: *Bioresource technology* 239 (2017), pp. 422–429.

[83] Shou-Qing Ni et al. "Effect of organic matter on the performance of granular anammox process". In: *Bioresource technology* 110 (2012), pp. 701–705.

[84] Zhen Bi et al. "Fast start-up of Anammox process with appropriate ferrous iron concentration". In: *Bioresource technology* 170 (2014), pp. 506–512.

[85] Sarah EJ Bowman and Kara L Bren. "The chemistry and biochemistry of heme c: functional bases for covalent attachment". In: *Natural product reports* 25.6 (2008), pp. 1118–1130.

[86] Sen Qiao et al. "Long term effects of divalent ferrous ion on the activity of anammox biomass". In: *Bioresource technology* 142 (2013), pp. 490–497.

[87] Tao Wang et al. "Enrichment of Anammox bacteria in seed sludges from different wastewater treating processes and start-up of Anammox process". In: *Desalination* 271.1-3 (2011), pp. 193–198.

[88] Astrid A Van de Graaf et al. "Autotrophic growth of anaerobic ammonium-oxidizing micro-organisms in a fluidized bed reactor". In: *Microbiology* 142.8 (1996), pp. 2187–2196.

[89] Chong-Jian Tang et al. "Enrichment features of anammox consortia from methanogenic granules loaded with high organic and methanol contents". In: *Chemosphere* 79.6 (2010), pp. 613–619.

[90] C Trigo et al. "Start-up of the Anammox process in a membrane bioreactor". In: *Journal of Biotechnology* 126.4 (2006), pp. 475–487.

[91] Shou-Qing Ni et al. "Fast start-up, performance and microbial community in a pilot-scale anammox reactor seeded with exotic mature granules". In: *Bioresource Technology* 102.3 (2011), pp. 2448–2454.

[92] Jianbo Guo et al. "Rapid start-up of the anammox process: Effects of five different sludge extracellular polymeric substances on the activity of anammox bacteria". In: *Bioresource technology* 220 (2016), pp. 641–646.

[93] Tao Wang et al. "Start-up and long-term operation of the Anammox process in a fixed bed reactor (FBR) filled with novel non-woven ring carriers". In: *Chemosphere* 91.5 (2013), pp. 669–675.

[94] Tao Wang et al. "Start-up performance of Anammox process in a fixed bed reactor (FBR) filled with honeycomb-like polypropylene carriers". In: *Water Science and Technology* 73.8 (2016), pp. 1848–1854.

[95] Chong-jun Chen et al. "Improving anammox start-up with bamboo charcoal". In: *Chemosphere* 89.10 (2012), pp. 1224–1229.

[96] Takao Fujii et al. "Characterization of the microbial community in an anaerobic ammonium-oxidizing biofilm cultured on a nonwoven biomass carrier." In: *Journal of bioscience and bioengineering* 94.5 (2002), pp. 412–418.

[97] Li Zhang et al. "Treatment capability of an up-flow anammox column reactor using polyethylene sponge strips as biomass carrier". In: *Journal of bioscience and bioengineering* 110.1 (2010), pp. 72–78.

[98] I Fernández et al. "Biofilm and granular systems to improve Anammox biomass retention". In: *Biochemical Engineering Journal* 42.3 (2008), pp. 308–313.

[99] Li Zhang et al. "High-rate nitrogen removal from anaerobic digester liquor using an up-flow anammox reactor with polyethylene sponge as a biomass carrier". In: *Journal of bioscience and bioengineering* 111.3 (2011), pp. 306–311.

[100] Hui-Ping Chuang et al. "Anoxic ammonium oxidation by application of a down-flow hanging sponge (DHS) reactor". In: *J. Environ. Eng. Manage* 18 (2008), pp. 409–417.

[101] Yanning Gao et al. "Mechanical shear contributes to granule formation resulting in quick start-up and stability of a hybrid anammox reactor". In: *Biodegradation* 23.3 (2012), pp. 363–372.

[102] Marc Strous et al. "Ammonium removal from concentrated waste streams with the anaerobic ammonium oxidation (anammox) process in different reactor configurations". In: *Water Research* 31.8 (1997), pp. 1955–1962.

[103] Yi-Feng Lu et al. "Improvement of start-up and nitrogen removal of the anammox process in reactors inoculated with conventional activated sludge using biofilm carrier materials". In: *Environmental technology* 39.1 (2018), pp. 59–67.

[104] Muhammad Ali et al. "Rapid and successful start-up of anammox process by immobilizing the minimal quantity of biomass in PVA-SA gel beads". In: *Water research* 79 (2015), pp. 147–157.

[105] Kyungjin Cho et al. "Comparison of inoculum sources for long-term process performance and fate of ANAMMOX bacteria niche in poly (vinyl alcohol)/sodium alginate gel beads". In: *Chemosphere* 185 (2017), pp. 394–402.

[106] Yuya Kimura et al. "Effects of nitrite inhibition on anaerobic ammonium oxidation". In: *Applied microbiology and biotechnology* 86.1 (2010), pp. 359–365.

[107] Umapathy Manonmani and Kurian Joseph. "Research advances and challenges in anammox immobilization for autotrophic nitrogen removal". In: *Journal of Chemical Technology & Biotechnology* (2018).

[108] Hyokwan Bae et al. "Enrichment of ANAMMOX bacteria from conventional activated sludge entrapped in poly (vinyl alcohol)/sodium alginate gel". In: *Chemical Engineering Journal* 281 (2015), pp. 531–540.

[109] Albert Magrí, Matias B Vanotti, and Ariel A Szögi. "Anammox sludge immobilized in polyvinyl alcohol (PVA) cryogel carriers". In: *Bioresource technology* 114 (2012), pp. 231–240.

[110] Gang-Li Zhu, Jia Yan, and Yong-You Hu. "Anaerobic ammonium oxidation in polyvinyl alcohol and sodium alginate immobilized biomass system: a potential tool to maintain anammox biomass in application". In: *Water Science and Technology* 69.4 (2014), pp. 718–726.

[111] Kazuichi Isaka et al. "Ammonium removal performance of anaerobic ammonium-oxidizing bacteria immobilized in polyethylene glycol gel carrier". In: *Applied microbiology and biotechnology* 76.6 (2007), pp. 1457–1465.

[112] Kazuichi Isaka et al. "Novel autotrophic nitrogen removal system using gel entrapment technology". In: *Bioresource technology* 102.17 (2011), pp. 7720–7726.

[113] Muhammad Ali, Mamoru Oshiki, and Satoshi Okabe. "Simple, rapid and effective preservation and reactivation of anaerobic ammonium oxidizing bacterium Candidatus Brocadia sinica". In: *Water research* 57 (2014), pp. 215–222.

[114] Lai Minh Quan et al. "Reject water treatment by improvement of whole cell anammox entrapment using polyvinyl alcohol/alginate gel". In: *Biodegradation* 22.6 (2011), pp. 1155–1167.

[115] CHARLES Bédard and ROGER Knowles. "Physiology, biochemistry, and specific inhibitors of CH4, NH4+, and CO oxidation by methanotrophs and nitrifiers." In: *Microbiological reviews* 53.1 (1989), pp. 68–84.

[116] Lisa Y Juliette, Michael R Hyman, and Daniel J Arp. "Inhibition of ammonia oxidation in Nitrosomonas europaea by sulfur compounds: thioethers are oxidized to sulfoxides by ammonia monooxygenase". In: *Applied and environmental microbiology* 59.11 (1993), pp. 3718–3727.

[117] GW McCarty. "Modes of action of nitrification inhibitors". In: *Biology and Fertility of Soils* 29.1 (1999), pp. 1–9.

[118] A Delgado et al. "The effect of volatile fatty acids on the nitrification of a saline effluent". In: *Environmental technology* 25.4 (2004), pp. 413–422.

[119] Zhiqiang Hu et al. "Effect of nickel and cadmium speciation on nitrification inhibition". In: *Environmental science & technology* 36.14 (2002), pp. 3074–3078.

[120] Sheng-Jie You, Yung-Pin Tsai, and Ru-Yi Huang. "Effect of heavy metals on nitrification performance in different activated sludge processes". In: *Journal of hazardous materials* 165.1-3 (2009), pp. 987–994.

[121] SR Juliastuti et al. "The inhibitory effects of heavy metals and organic compounds on the net maximum specific growth rate of the autotrophic biomass in activated sludge". In: *Journal of hazardous materials* 100.1-3 (2003), pp. 271–283.

[122] Krist Gernaey et al. "Fast and sensitive acute toxicity detection with an enrichment nitrifying culture". In: *Water environment research* 69.6 (1997), pp. 1163–1169.

[123] Paolo Madoni, Donatella Davoli, and Lorena Guglielmi. "Response of SOUR and AUR to heavy metal contamination in activated sludge". In: *Water Research* 33.10 (1999), pp. 2459–2464.

[124] Silvie Hartmann, Hana Skrobankova, and Jarmila Drozdova. "Inhibition of activated sludge respiration by heavy metals". In: *Proceedings of the 2013 International Conference on Environment, Energy, Ecosystem and Development*. 2013, pp. 28–30.

[125] Vel M Vadivelu et al. "The inhibitory effects of free nitrous acid on the energy generation and growth processes of an enriched Nitrobacter culture". In: *Environmental Science & Technology* 40.14 (2006), pp. 4442–4448.

[126] Vel M Vadivelu, Jurg Keller, and Zhiguo Yuan. "Effect of free ammonia on the respiration and growth processes of an enriched Nitrobacter culture". In: *Water Research* 41.4 (2007), pp. 826–834.

[127] Stijn Wyffels et al. "Nitrogen removal from sludge reject water by a two-stage oxygen-limited autotrophic nitrification denitrification process". In: *Water science and technology* 49.5-6 (2004), pp. 57–64.

[128] JY Jung et al. "Factors affecting the activity of anammox bacteria during start up in the continuous culture reactor". In: *Water Science and Technology* 55.1-2 (2007), pp. 459–468.

[129] Chong-jian Tang et al. "Effect of substrate concentration on stability of anammox biofilm reactors". In: *Journal of Central South University of Technology* 17.1 (2010), pp. 79–84.

[130] I Fernández et al. "Short-and long-term effects of ammonium and nitrite on the Anammox process". In: *Journal of Environmental Management* 95 (2012), S170–S174.

[131] Kazuichi Isaka et al. "Anaerobic ammonium oxidation (anammox) irreversibly inhibited by methanol". In: *Applied microbiology and biotechnology* 81.2 (2008), p. 379.

[132] Didem Güven et al. "Propionate oxidation by and methanol inhibition of anaerobic ammonium-oxidizing bacteria". In: *Applied and environmental microbiology* 71.2 (2005), pp. 1066–1071.

[133] S Toh and N Ashbolt. "Adaptation of anaerobic ammonium-oxidising consortium to synthetic coke-ovens wastewater". In: *Applied Microbiology and Biotechnology* 59.2-3 (2002), pp. 344–352.

[134] A Dapena-Mora et al. "Evaluation of activity and inhibition effects on Anammox process by batch tests based on the nitrogen gas production". In: *Enzyme and microbial technology* 40.4 (2007), pp. 859–865.

[135] José M Carvajal-Arroyo et al. "Inhibition of anaerobic ammonium oxidizing (anammox) enrichment cultures by substrates, metabolites and common wastewater constituents". In: *Chemosphere* 91.1 (2013), pp. 22–27.

[136] Ren-Cun Jin et al. "The effect of sulfide inhibition on the ANAMMOX process". In: *Water research* 47.3 (2013), pp. 1459–1469.

[137] Ruth Pietri, Elddie Román-Morales, and Juan López-Garriga. "Hydrogen sulfide and hemeproteins: knowledge and mysteries". In: *Antioxidants & redox signaling* 15.2 (2011), pp. 393–404.

[138] Boran Kartal et al. "Adaptation of a freshwater anammox population to high salinity wastewater". In: *Journal of biotechnology* 126.4 (2006), pp. 546–553.

[139] T Lotti et al. "Inhibition effect of swine wastewater heavy metals and antibiotics on anammox activity". In: *Water Science and Technology* 66.7 (2012), pp. 1519–1526.

[140] Guangbin Li et al. "Inhibition of anaerobic ammonium oxidation by heavy metals". In: *Journal of Chemical Technology & Biotechnology* 90.5 (2015), pp. 830–837.

[141] Yuya Kimura and Kazuichi Isaka. "Evaluation of inhibitory effects of heavy metals on anaerobic ammonium oxidation (anammox) by continuous feeding tests". In: *Applied microbiology and biotechnology* 98.16 (2014), pp. 6965–6972.

[142] Zheng-Zhe Zhang et al. "Long-term effects of heavy metals and antibiotics on granule-based anammox process: granule property and performance evolution". In: *Applied microbiology and biotechnology* 100.5 (2016), pp. 2417–2427.

[143] I Fernandez et al. "Operation of an Anammox SBR in the presence of two broad-spectrum antibiotics". In: *Process Biochemistry* 44.4 (2009), pp. 494–498.

[144] Ramon Ganigué et al. "Long-term operation of a partial nitritation pilot plant treating leachate with extremely high ammonium concentration prior to an anammox process". In: *Bioresource technology* 100.23 (2009), pp. 5624–5632.

[145] Taichi Yamamoto et al. "Long-term stability of partial nitritation of swine wastewater digester liquor and its subsequent treatment by Anammox". In: *Bioresource Technology* 99.14 (2008), pp. 6419–6425.

[146] Stefano Milia et al. "Biological treatment of nitrogen-rich refinery wastewater by partial nitritation (SHARON) process". In: *Environmental technology* 33.13 (2012), pp. 1477–1483.

[147] Susanne Lackner et al. "Full-scale partial nitritation/anammox experiences–an application survey". In: *Water research* 55 (2014), pp. 292–303.

[148] UGJM Van Dongen, Mike SM Jetten, and MCM Van Loosdrecht. "The SHARON®-Anammox® process for treatment of ammonium rich wastewater". In: *Water science and technology* 44.1 (2001), pp. 153–160.

[149] B Wett. "Solved upscaling problems for implementing deammonification of rejection water". In: *Water science and technology* 53.12 (2006), pp. 121–128.

[150] B Wett et al. "Syntrophy of aerobic and anaerobic ammonia oxidisers". In: *Water science and technology* 61.8 (2010), pp. 1915–1922.

[151] Adriano Joss et al. "Full-scale nitrogen removal from digester liquid with partial nitritation and anammox in one SBR". In: *Environmental Science & Technology* 43.14 (2009), pp. 5301–5306.

[152] B Wett et al. "Key parameters for control of DEMON deammonification process". In: *Water Practice* 1.5 (2007), pp. 1–11.

[153] WR Abma et al. "Upgrading of sewage treatment plant by sustainable and cost-effective separate treatment of industrial wastewater". In: *Water science and technology* 61.7 (2010), pp. 1715–1722.

[154] KA Third et al. "The CANON system (completely autotrophic nitrogen-removal over nitrite) under ammonium limitation: interaction and competition between three groups of bacteria". In: *Systematic and applied microbiology* 24.4 (2001), pp. 588–596.

[155] A Olav Sliekers et al. "Completely autotrophic nitrogen removal over nitrite in one single reactor". In: *Water research* 36.10 (2002), pp. 2475–2482.

[156] Young-Ho Ahn and Hoon-Chang Choi. "Autotrophic nitrogen removal from sludge digester liquids in upflow sludge bed reactor with external aeration". In: *Process Biochemistry* 41.9 (2006), pp. 1945–1950.

[157] Siegfried E Vlaeminck et al. "Nitrogen removal from digested black water by one-stage partial nitritation and anammox". In: *Environmental Science & Technology* 43.13 (2009), pp. 5035–5041.

[158] Kim Windey, Inge De Bo, and Willy Verstraete. "Oxygen-limited autotrophic nitrification–denitrification (OLAND) in a rotating biological contactor treating high-salinity wastewater". In: *Water research* 39.18 (2005), pp. 4512–4520.

[159] Magnus Christensson et al. "Experience from start-ups of the first ANITA Mox plants". In: *Water Science and Technology* 67.12 (2013), pp. 2677–2684.

[160] Hong Zhao et al. "One-stage deammonification process-MBBR versus IFAS configurations-Development updates and application considerations". In: *Proceedings of the Water Environment Federation* 2014.2 (2014), pp. 1–16.

[161] Takaaki Tokutomi et al. "Application of the nitritation and anammox process into inorganic nitrogenous wastewater from semiconductor factory". In: *Journal of Environmental Engineering* 137.2 (2011), pp. 146–154.

[162] Xin Wen et al. "Efficient simultaneous partial nitrification, anammox and denitrification (SNAD) system equipped with a real-time dissolved oxygen (DO) intelligent control system and microbial community shifts of different substrate concentrations". In: *Water research* 119 (2017), pp. 201–211.

[163] FangZhai Zhang et al. "A novel simultaneous partial nitrification Anammox and denitrification (SNAD) with intermittent aeration for cost-effective nitrogen removal from mature landfill leachate". In: *Chemical Engineering Journal* 313 (2017), pp. 619–628.

[164] Zhaoming Zheng et al. "Nitrogen removal via simultaneous partial nitrification, anammox and denitrification (SNAD) process under high DO condition". In: *Biodegradation* 27.4-6 (2016), pp. 195–208.

[165] Phyllis Lam and Marcel MM Kuypers. "Microbial nitrogen cycling processes in oxygen minimum zones". In: *Annual review of marine science* 3 (2011), pp. 317–345.

[166] Anne E Giblin et al. "The importance of dissimilatory nitrate reduction to ammonium (DNRA) in the nitrogen cycle of coastal ecosystems". In: *Oceanography* 26.3 (2013), pp. 124–131.

[167] Zackary L Jones et al. "Sulfide-induced dissimilatory nitrate reduction to ammonium supports anaerobic ammonium oxidation (anammox) in an open-water unit process wetland". In: *Applied and Environmental Microbiology* 83.15 (2017), e00782–17.

[168] Fleur AE Roland et al. "Denitrification, anaerobic ammonium oxidation, and dissimilatory nitrate reduction to ammonium in an East African Great Lake (Lake Kivu)". In: *Limnology and Oceanography* 63.2 (2018), pp. 687–701.

[169] Liang F Dong et al. "Dissimilatory reduction of nitrate to ammonium, not denitrification or anammox, dominates benthic nitrate reduction in tropical estuaries". In: *Limnology and Oceanography* 56.1 (2011), pp. 279–291.

[170] Celia M Castro-Barros et al. "Evaluating the potential for dissimilatory nitrate reduction by anammox bacteria for municipal wastewater treatment". In: *Bioresource technology* 233 (2017), pp. 363–372.

[171] Naomichi Nishio and Yutaka Nakashimada. "Recent development of anaerobic digestion processes for energy recovery from wastes". In: *Journal of Bioscience and Bioengineering* 103.2 (2007), pp. 105–112.

[172] Lise Appels et al. "Anaerobic digestion in global bio-energy production: potential and research challenges". In: *Renewable and Sustainable Energy Reviews* 15.9 (2011), pp. 4295–4301.

[173] Lise Appels et al. "Influence of low temperature thermal pre-treatment on sludge solubilisation, heavy metal release and anaerobic digestion". In: *Bioresource technology* 101.15 (2010), pp. 5743–5748.

[174] Jason Dwyer et al. "Decreasing activated sludge thermal hydrolysis temperature reduces product colour, without decreasing degradability". In: *Water research* 42.18 (2008), pp. 4699–4709.

[175] Valérie Penaud, Jean-Philippe Delgenès, and René Moletta. "Characterization of soluble molecules from thermochemically pretreated sludge". In: *Journal of Environmental Engineering* 126.5 (2000), pp. 397–402.

[176] Ursula Kepp et al. "Enhanced stabilisation of sewage sludge through thermal hydrolysis-three years of experience with full scale plant". In: *Water science and technology* 42.9 (2000), pp. 89–96.

[177] E Neyens and J Baeyens. "A review of thermal sludge pre-treatment processes to improve dewaterability". In: *Journal of hazardous materials* 98.1-3 (2003), pp. 51–67.

[178] Bryce Figdore et al. "Deammonification of dewatering sidestream from thermal hydrolysis-mesophilic anaerobic digestion process". In: *Proceedings of the Water Environment Federation* 2011.1 (2011), pp. 1037–1052.

[179] Domenec Jolis. "High-solids anaerobic digestion of municipal sludge pretreated by thermal hydrolysis". In: *Water Environment Research* 80.7 (2008), pp. 654–662.

[180] Camilla Maria Braguglia et al. "The impact of sludge pre-treatments on mesophilic and thermophilic anaerobic digestion efficiency: Role of the organic load". In: *Chemical Engineering Journal* 270 (2015), pp. 362–371.

[181] Shireen M Kotay et al. "Anaerobic ammonia oxidation (ANAMMOX) for side-stream treatment of anaerobic digester filtrate process performance and microbiology". In: *Biotechnology and Bioengineering* 110.4 (2013), pp. 1180–1192.

[182] Qi Zhang et al. "Deammonification for digester supernatant pretreated with thermal hydrolysis: overcoming inhibition through process optimization". In: *Applied microbiology and biotechnology* 100.12 (2016), pp. 5595–5606.

[183] Matthew Higgins et al. "Dewatering characteristics of cambi thermal hydrolysis biosolids: centrifuges vs. BFPs". In: *Proceedings of the Water Environment Federation* 2011.17 (2011), pp. 678–684.

[184] Zhiwei Wang, Zhichao Wu, and Shujuan Tang. "Extracellular polymeric substances (EPS) properties and their effects on membrane fouling in a submerged membrane bioreactor". In: *Water research* 43.9 (2009), pp. 2504–2512.

[185] Wen Chen et al. "Fluorescence excitation- emission matrix regional integration to quantify spectra for dissolved organic matter". In: *Environmental science & technology* 37.24 (2003), pp. 5701–5710.

[186] Kadiya Calderón et al. "Comparative analysis of the bacterial diversity in a lab-scale moving bed biofilm reactor (MBBR) applied to treat urban wastewater under different operational conditions". In: *Bioresource technology* 121 (2012), pp. 119–126.

[187] HJAF McTavish, JA Fuchs, and AB Hooper. "Sequence of the gene coding for ammonia monooxygenase in Nitrosomonas europaea." In: *Journal of bacteriology* 175.8 (1993), pp. 2436–2444.

[188] Jeanette M Norton et al. "Diversity of ammonia monooxygenase operon in autotrophic ammonia-oxidizing bacteria". In: *Archives of microbiology* 177.2 (2002), pp. 139–149.

[189] J Gregory Caporaso et al. "Global patterns of 16S rRNA diversity at a depth of millions of sequences per sample". In: *Proceedings of the national academy of sciences* 108.Supplement 1 (2011), pp. 4516–4522.

[190] Alma E Parada, David M Needham, and Jed A Fuhrman. "Every base matters: assessing small subunit rRNA primers for marine microbiomes with mock communities, time series and global field samples". In: *Environmental microbiology* 18.5 (2016), pp. 1403–1414.

[191] Mads Albertsen et al. "Genome sequences of rare, uncultured bacteria obtained by differential coverage binning of multiple metagenomes". In: *Nature biotechnology* 31.6 (2013), p. 533.

[192] Donovan H Parks et al. "CheckM: assessing the quality of microbial genomes recovered from isolates, single cells, and metagenomes". In: *Genome research* (2015), gr–186072.

[193] Doug Hyatt et al. "Gene and translation initiation site prediction in metagenomic sequences". In: *Bioinformatics* 28.17 (2012), pp. 2223–2230.

[194] Weijun Luo and Cory Brouwer. "Pathview: an R/Bioconductor package for pathway-based data integration and visualization". In: *Bioinformatics* 29.14 (2013), pp. 1830–1831.

[195] Robert D Finn et al. "The Pfam protein families database: towards a more sustainable future". In: *Nucleic acids research* 44.D1 (2015), pp. D279–D285.

[196] P Antoniou et al. "Effect of temperature and pH on the effective maximum specific growth rate of nitrifying bacteria". In: *Water research* 24.1 (1990), pp. 97–101.

[197] Henryk Melcer. *Methods for wastewater characterization in activated sludge modelling*. IWA publishing, 2004.

[198] Seongjun Park and Wookeun Bae. "Modeling kinetics of ammonium oxidation and nitrite oxidation under simultaneous inhibition by free ammonia and free nitrous acid". In: *Process Biochemistry* 44.6 (2009), pp. 631–640.

[199] Murray Moo-Young, William A Anderson, and Ananda M Chakrabarty. *Environmental biotechnology: principles and applications*. Springer Science & Business Media, 2013.

[200] Albert Magrí et al. "A model for the simulation of the SHARON process: pH as a key factor". In: *Environmental technology* 28.3 (2007), pp. 255–265.

[201] S Sözen, D Orhon, and HA San. "A new approach for the evaluation of the maximum specific growth rate in nitrification". In: *Water Research* 30.7 (1996), pp. 1661–1669.

[202] MS Jetten et al. "The SHARON-Anammox process for treatment of ammonium rich wastewater." In: *Water science and technology: a journal of the International Association on Water Pollution Research* 44.1 (2001), pp. 153–160.

[203] Jun Wu et al. "Selection of ammonium oxidizing bacteria (AOB) over nitrite oxidizing bacteria (NOB) based on conversion rates". In: *Chemical Engineering Journal* 304 (2016), pp. 953–961.

[204] Qi Zhang et al. "Supernatant organics from anaerobic digestion after thermal hydrolysis cause direct and/or diffusional activity loss for nitritation and anammox". In: *Water Research* (2018).

[205] Adriano Joss et al. "Combined nitritation–anammox: advances in understanding process stability". In: *Environmental science & technology* 45.22 (2011), pp. 9735–9742.

[206] Chunyan Li et al. "Quantification of particulate matter attached to the bulk-biofilm interface and its influence on local mass transfer". In: *Separation and Purification Technology* 197 (2018), pp. 86–94.

[207] Luyara de Almeida Fernandes et al. "Effect of temperature on microbial diversity and nitrogen removal performance of an anammox reactor treating anaerobically pretreated municipal wastewater". In: *Bioresource technology* 258 (2018), pp. 208–219.

[208] Hongkeun Park et al. "Impact of inocula and growth mode on the molecular microbial ecology of anaerobic ammonia oxidation (anammox) bioreactor communities". In: *Water Research* 44.17 (2010), pp. 5005–5013.

[209] Y Xiao et al. "Coexistence of nitrifiers, denitrifiers and Anammox bacteria in a sequencing batch biofilm reactor as revealed by PCR-DGGE". In: *Journal of applied microbiology* 106.2 (2009), pp. 496–505.

[210] Eduardo Isanta et al. "Microbial community shifts on an anammox reactor after a temperature shock using 454-pyrosequencing analysis". In: *Bioresource technology* 181 (2015), pp. 207–213.

[211] Daniel Aird et al. "Analyzing and minimizing PCR amplification bias in Illumina sequencing libraries". In: *Genome biology* 12.2 (2011), R18.

[212] Ping Han et al. "A comparison of two 16S rRNA gene-based PCR primer sets in unraveling anammox bacteria from different environmental samples". In: *Applied microbiology and biotechnology* 97.24 (2013), pp. 10521–10529.

[213] Julián Carrera et al. "Inhibition of nitrification by fluoride in high-strength ammonium wastewater in activated sludge". In: *Process Biochemistry* 39.1 (2003), pp. 73–79.

[214] JHT Luong. "Kinetics of ethanol inhibition in alcohol fermentation". In: *Biotechnology and bioengineering* 27.3 (1985), pp. 280–285.

[215] Shou-Qing Ni et al. "Substrate removal evaluation of granular anammox process in a pilot-scale upflow anaerobic sludge blanket reactor". In: *Ecological Engineering* 38.1 (2012), pp. 30–36.

[216] Cíntia Dutra Leal et al. "Anammox for nitrogen removal from anaerobically pre-treated municipal wastewater: effect of COD/N ratios on process performance and bacterial community structure". In: *Bioresource technology* 211 (2016), pp. 257–266.

[217] Hongkeun Park et al. "Linking community profiles, gene expression and N-removal in anammox bioreactors treating municipal anaerobic digestion reject water". In: *Environmental science & technology* 44.16 (2010), pp. 6110–6116.

[218] Daan R Speth et al. "Genome-based microbial ecology of anammox granules in a full-scale wastewater treatment system". In: *Nature communications* 7 (2016), p. 11172.

[219] M-KH Winkler, R Kleerebezem, and MCM Van Loosdrecht. "Integration of anammox into the aerobic granular sludge process for main stream wastewater treatment at ambient temperatures". In: *Water research* 46.1 (2012), pp. 136–144.

[220] Sarina Jenni et al. "Successful application of nitritation/anammox to wastewater with elevated organic carbon to ammonia ratios". In: *Water Research* 49 (2014), pp. 316–326.

[221] Martin I Krzywinski et al. "Circos: an information aesthetic for comparative genomics". In: *Genome research* (2009).

[222] Xiaoming Li et al. "Granulation of simultaneous partial nitrification and anammox biomass in one single SBR system". In: *Applied biochemistry and biotechnology* 163.8 (2011), pp. 1053–1065.

[223] Zaoli Gu et al. "Inhibition of anammox by sludge thermal hydrolysis and metagenomic insights". In: *Bioresource technology* 270 (2018), pp. 46–54.

[224] Thomas Seviour et al. "Gel-forming exopolysaccharides explain basic differences between structures of aerobic sludge granules and floccular sludges". In: *Water research* 43.18 (2009), pp. 4469–4478.

[225] Xiaolin Hou, Sitong Liu, and Zuotao Zhang. "Role of extracellular polymeric substance in determining the high aggregation ability of anammox sludge". In: *Water research* 75 (2015), pp. 51–62.

[226] Julia K Goodrich et al. "Conducting a microbiome study". In: *Cell* 158.2 (2014), pp. 250–262.

[227] Larissa Quartaroli et al. "Ammonium removal from high-salinity oilfield-produced water: assessing the microbial community dynamics at increasing salt concentrations". In: *Applied microbiology and biotechnology* 101.2 (2017), pp. 859–870.

[228] Alejandro Gonzalez-Martinez et al. "Microbial community analysis of a full-scale DEMON bioreactor". In: *Bioprocess and biosystems engineering* 38.3 (2015), pp. 499–508.

[229] Tomonori Kindaichi, Tsukasa Ito, and Satoshi Okabe. "Ecophysiological interaction between nitrifying bacteria and heterotrophic bacteria in autotrophic nitrifying biofilms as determined by microautoradiography-fluorescence in situ hybridization". In: *Applied and Environmental Microbiology* 70.3 (2004), pp. 1641–1650.

[230] Margarete Bauer et al. "Whole genome analysis of the marine Bacteroidetes ?Gramella forsetii?reveals adaptations to degradation of polymeric organic matter". In: *Environmental Microbiology* 8.12 (2006), pp. 2201–2213.

[231] Bing Tian and Yuejin Hua. "Carotenoid biosynthesis in extremophilic Deinococcus–Thermus bacteria". In: *Trends in microbiology* 18.11 (2010), pp. 512–520.

[232] Olga Sánchez et al. "Assessing bacterial diversity in a seawater-processing wastewater treatment plant by 454-pyrosequencing of the 16 S rRNA and amoA genes". In: *Microbial biotechnology* 6.4 (2013), pp. 435–442.

[233] Heng Yu et al. "Understanding bacterial communities of partial nitritation and nitratation reactors at ambient and low temperature". In: *Chemical Engineering Journal* 337 (2018), pp. 755–763.

[234] Wenru Liu et al. "High-throughput sequencing-based microbial characterization of size fractionated biomass in an anoxic anammox reactor for low-strength wastewater at low temperatures". In: *Bioresource technology* 231 (2017), pp. 45–52.

[235] Mirna Mrkonjic Fuka, Sara Hallin Gesche Braker, and Laurent Philippot. "Molecular tools to assess the diversity and density of denitrifying bacteria in their habitats". In: *Biology of the Nitrogen Cycle*. Elsevier, 2007, pp. 313–330.

[236] Peter F Dunfield et al. "Methane oxidation by an extremely acidophilic bacterium of the phylum Verrucomicrobia". In: *Nature* 450.7171 (2007), p. 879.

[237] Xiao-Hui Yi et al. "Structure and succession of bacterial communities of the granular sludge during the initial stage of the simultaneous denitrification and methanogenesis process". In: *Water, Air, & Soil Pollution* 228.3 (2017), p. 121.

[238] Bo Wang et al. "Long-term partial nitritation and microbial characteristics in treating low C/N ratio domestic wastewater". In: *Environmental Science: Water Research & Technology* 4.6 (2018), pp. 820–827.

[239] Ren-Gang Zhang et al. "Moheibacter sediminis gen. nov., sp. nov., a member of the family Flavobacteriaceae isolated from sediment, and emended descriptions of Empedobacter brevis, Wautersiella falsenii and Weeksella virosa". In: *International journal of systematic and evolutionary microbiology* 64.5 (2014), pp. 1481–1487.

[240] Yingmu Wang et al. "Robustness and microbial consortia succession of simultaneous partial nitrification, ANAMMOX and denitrification (SNAD) process for mature landfill leachate treatment under low temperature". In: *Biochemical Engineering Journal* 132 (2018), pp. 112–121.

[241] Peter Kämpfer et al. "Castellaniella gen. nov., to accommodate the phylogenetic lineage of Alcaligenes defragrans, and proposal of Castellaniella defragrans gen. nov., comb. nov. and Castellaniella denitrificans sp. nov." In: *International journal of systematic and evolutionary microbiology* 56.4 (2006), pp. 815–819.

[242] María J Pujalte et al. "The family Rhodobacteraceae". In: *The Prokaryotes*. Springer, 2014, pp. 439–512.

[243] Eddie Cytryn et al. "Identification of bacteria potentially responsible for oxic and anoxic sulfide oxidation in biofilters of a recirculating mariculture system". In: *Applied and environmental microbiology* 71.10 (2005), pp. 6134–6141.

[244] Stephanie A Eichorst et al. "Community dynamics of cellulose-adapted thermophilic bacterial consortia". In: *Environmental microbiology* 15.9 (2013), pp. 2573–2587.

[245] Danyang Zheng et al. "Multistage AO activated sludge process for paraformaldehyde wastewater treatment and microbial community structure analysis". In: *Journal of Chemistry* 2016 (2016).

[246] Colin M Fitzgerald et al. "Ammonia-oxidizing microbial communities in reactors with efficient nitrification at low-dissolved oxygen". In: *Water research* 70 (2015), pp. 38–51.

[247] Sara Borin et al. "Sulfur cycling and methanogenesis primarily drive microbial colonization of the highly sulfidic Urania deep hypersaline basin". In: *Proceedings of the National Academy of Sciences* 106.23 (2009), pp. 9151–9156.

[248] Kwang Kyu Kim et al. "Pontibaca methylaminivorans gen. nov., sp. nov., a member of the family Rhodobacteraceae". In: *International journal of systematic and evolutionary microbiology* 60.9 (2010), pp. 2170–2175.

[249] Zhao Wang et al. "Nonylphenol biodegradation in river sediment and associated shifts in community structures of bacteria and ammonia-oxidizing microorganisms". In: *Ecotoxicology and environmental safety* 106 (2014), pp. 1–5.

[250] Andrey V Mardanov et al. "Metagenome of the Microbial Community of Anammox Granules in a Nitritation/Anammox Wastewater Treatment System". In: *Genome announcements* 5.42 (2017), e01115–17.

[251] Huijie Lu, Kartik Chandran, and David Stensel. "Microbial ecology of denitrification in biological wastewater treatment". In: *Water Research* 64 (2014), pp. 237–254.

[252] Alyne Duarte Pereira et al. "Microbial communities in anammox reactors: a review". In: *Environmental Technology Reviews* 6.1 (2017), pp. 74–93.

[253] AV Mardanov et al. "Dynamics of the composition of a microbial consortium during start-up of a single-stage constant flow laboratory nitritation/anammox setup". In: *Microbiology* 85.6 (2016), pp. 681–692.

[254] Maria Cristina Monteiro S Costa et al. "Impact of inocula and operating conditions on the microbial community structure of two anammox reactors". In: *Environmental technology* 35.14 (2014), pp. 1811–1822.

[255] A Olav Sliekers et al. "CANON and Anammox in a gas-lift reactor". In: *FEMS microbiology letters* 218.2 (2003), pp. 339–344.

[256] David M Graham and Domenec Jolis. "Pilot-Scale Evaluation of pH-Based Control of Single Stage Deammonification Processes for Sidestream Treatment". In: *Water Environment Research* 89.2 (2017), pp. 99–104.

[257] Samik Bagchi, Rima Biswas, and Tapas Nandy. "Alkalinity and dissolved oxygen as controlling parameters for ammonia removal through partial nitritation and ANAMMOX in a single-stage bioreactor". In: *Journal of industrial microbiology & biotechnology* 37.8 (2010), pp. 871–876.

[258] Shenbin Cao et al. "High-throughput profiling of microbial community structures in an ANAMMOX-UASB reactor treating high-strength wastewater". In: *Applied microbiology and biotechnology* 100.14 (2016), pp. 6457–6467.

[259] Bingyu Zheng et al. "Suspended sludge and biofilm shaped different anammox communities in two pilot-scale one-stage anammox reactors". In: *Bioresource technology* 211 (2016), pp. 273–279.

[260] Chao Wang et al. "Achieving mainstream nitrogen removal through simultaneous partial nitrification, anammox and denitrification process in an integrated fixed film activated sludge reactor". In: *Chemosphere* 203 (2018), pp. 457–466.

[261] MD Asadur Rahoman, Chai Tianyu, and Zhu Tong. "Study on Sludge Characteristics and Nitrogen Removal Mechanism of Hybrid Partial Nitrification Anammox Reactor (HPNA)". In: *American Scientific Research Journal for Engineering, Technology, and Sciences (ASRJETS)* 29.1 (2017), pp. 80–115.

[262] Qiulai He et al. "Hydrodynamic shear force shaped the microbial community and function in the aerobic granular sequencing batch reactors for low carbon to nitrogen (C/N) municipal wastewater treatment". In: *Bioresource technology* (2018).

[263] Jie Xu et al. "Cultivation and stable operation of aerobic granular sludge at low temperature by sieving out the batt-like sludge". In: *Chemosphere* 211 (2018), pp. 1219–1227.

[264] Cuiqin Yin, Fangang Meng, and Guang-Hao Chen. "Spectroscopic characterization of extracellular polymeric substances from a mixed culture dominated by ammonia-oxidizing bacteria". In: *Water research* 68 (2015), pp. 740–749.

[265] Zhao-rui Chu et al. "Microbial characterization of aggregates within a one-stage nitritation–anammox system using high-throughput amplicon sequencing". In: *Chemical Engineering Journal* 262 (2015), pp. 41–48.

[266] Petra J Reeve et al. "Effect of feed starvation on side-stream anammox activity and key microbial populations". In: *Journal of environmental management* 171 (2016), pp. 121–127.

[267] Alyne Duarte Pereira et al. "Effect of phenol on the nitrogen removal performance and microbial community structure and composition of an anammox reactor". In: *Bioresource technology* 166 (2014), pp. 103–111.

[268] Sebastian Lücker et al. "A Nitrospira metagenome illuminates the physiology and evolution of globally important nitrite-oxidizing bacteria". In: *Proceedings of the National Academy of Sciences* 107.30 (2010), pp. 13479–13484.

[269] Libin Zhang et al. "Enhanced bioelectrochemical reduction of p-nitrophenols in the cathode of self-driven microbial fuel cells". In: *Rsc Advances* 6.35 (2016), pp. 29072–29079.

[270] Dawen Gao et al. "Aerobic granular sludge: characterization, mechanism of granulation and application to wastewater treatment". In: *Critical reviews in biotechnology* 31.2 (2011), pp. 137–152.

[271] Tomonori Kindaichi et al. "Ecophysiological role and function of uncultured Chloroflexi in an anammox reactor". In: *Water Science and Technology* 66.12 (2012), pp. 2556–2561.

[272] Hongsheng Lu et al. "Limnobacter litoralis sp. nov., a thiosulfate-oxidizing, heterotrophic bacterium isolated from a volcanic deposit, and emended description of the genus Limnobacter". In: *International journal of systematic and evolutionary microbiology* 61.2 (2011), pp. 404–407.

[273] Duntao Shu et al. "Effects of Fe (II) on microbial communities, nitrogen transformation pathways and iron cycling in the anammox process: kinetics, quantitative molecular mechanism and metagenomic analysis". In: *RSC Advances* 6.72 (2016), pp. 68005–68016.

[274] Huosheng Li et al. "Long-term performance and microbial ecology of a two-stage PN–ANAMMOX process treating mature landfill leachate". In: *Bioresource technology* 159 (2014), pp. 404–411.

[275] Marcus Vinicius Freire Andrade et al. "Effects of hydraulic retention time, co-substrate and nitrogen source on laundry wastewater anionic surfactant degradation in fluidized bed reactors". In: *Bioresource technology* 224 (2017), pp. 246–254.

[276] Sille Bendix Larsen et al. "Ex-situ bioremediation of polycyclic aromatic hydrocarbons in sewage sludge". In: *Journal of Hazardous Materials* 164.2-3 (2009), pp. 1568–1572.